EXPLORATION OF BIOMATERIALS DESIGN SPACE THROUGH COMBINATORIAL AND HIGH-THROUGHPUT APPROACHES: TYROSINE-DERIVED POLYCARBONATES AS A CASE STUDY

by

RAMIRO ROJAS ESCONTRILLAS

A dissertation submitted to the

Graduate School-New Brunswick

Rutgers, The State University of New Jersey

In partial fulfillment of the requirements

For the degree of

Doctor of Philosophy

Graduate Program in Chemistry and Chemical Biology

Written under the direction of

Joachim Kohn

And approved by

_____

_____

_____

_____

New Brunswick, New Jersey

October, 2009

ABSTRACT OF THE DISSERTATION

Exploration of biomaterials design space through combinatorial and high-throughput approaches: Tyrosine-derived polycarbonates as a case study

By RAMIRO ROJAS ESCONTRILLAS

Dissertation Director:

Joachim Kohn

The use of combinatorial and high-throughput approaches in the design and exploration of materials space has been gaining increasing acceptance in recent years. While these methods have been successfully employed in the development of materials for the fields of electronics and optics, only a few examples exist within the field of biomaterials science. While there is a clear need for complex polymer structures that can be tailored for specific applications, most current research is being done on the basis of "trial and error" approaches that simply cannot keep up with the demand for novel technologies.

As part of the work involved in this thesis, the number of viable biomaterial candidates was increased by varying the chemical composition of tyrosine-derived monomers in two positions, namely the backbone and pendent chain. The resulting monomers proved to have different physical and chemical properties, derived from small modifications to their chemical structure.

In order to effectively synthesize several compositions of tailored tyrosine-derived polycarbonates, automated synthetic procedures were created and evaluated in a modern robotic platform. The challenges involved in the automation of polycondensation reactions, such as liquid handling, dropwise addition, and toxic chemical handling, were addressed successfully. A considerable amount of time was saved in comparison to manual methods when generating large polymer libraries.

In order to study structure-property relationships, the mass-per-flexible-bond principle was used to quantitatively explain the large range of glass transitions observed in a library of polymers containing homo-, co-, and terpolymers. Within this context, the information gathered in this thesis is expected to be used as a guideline for the rational design of polymers for specific applications.

The information derived from this work made it possible to ascertain that future research can certainly benefit from the automated parallel synthesis methods developed during it, as well as from the linear relationships found. It is expected for the research done in this thesis to have a definite impact not only on the use of combinatorial and high-throughput approaches in polymer science, but also on the informatics aspect involved.

DEDICATION

To Nelly and Ramiro,

For giving me your trust and endless support.

For your unconditional love.

To Sara,

For waiting patiently (and not so patiently) for me.

For your unique self which I utterly love.

To Daniel,

I love you with all my heart my dear nephew.

This thesis is for you too.

ACKNOWLEDGMENTS

First of all, I would like to thank my advisor, Prof. Joachim Kohn, for giving me the opportunity of working in his non-traditional chemistry laboratory, which in turn gave me the possibility to collaborate with an excellent interdisciplinary group. For me, working within the Kohn Lab was an exploratory journey in which I was surrounded, at all times, by incredibly smart colleagues that allowed me to acquire great knowledge in various different areas, as well as to broaden my vision of the (polymeric) biomaterials field.

I would also like to thank my thesis committee: Prof. Kathryn Uhrich, who always had the time to listen to my updates and to any other academic and non-academic matters, and who also provided useful suggestions and observations regarding my projects. I appreciate the few weeks I spent in the Uhrich Lab, during which I was able to get a good perspective of applied polymer science, engage in fruitful conversations, and develop good friendships. Prof. Ralf Warmuth, whom I first met several years ago during a very interesting talk that he gave at the ITESM in Monterrey, México. I am grateful for his assistance whenever I have needed it, whether it was a simple question or getting him on board for my thesis committee despite his busy schedule. Finally, Prof. Matthew Becker, who has collaborated with the Kohn Lab for several years now. It is an honor to have such an insightful and helpful committee member on board.

My appreciation goes to the Kohn Lab, past and present, with very sincere gratitude to certain specific people: Dr. Durgadas Bolikal (Das), for his trust and always-cheerful way of managing life inside and outside the laboratory. I appreciate all the help

he provided others and me through the very important stage that graduate school represents. I thank him for considering me to be one of his friends, and would like to remind him that I consider him one of mine as well. I am also indebted to members of Lab 210 (the self-proclaimed "210ers") for many things: friendship, lunches, laughs, politically correct (and incorrect) points of view, perspective, help, constructive criticism, and the overall unique and pleasant (and sometimes crazy) atmosphere that each one of them helped to create within those four walls: Larisa Sheihet, Abraham Joy, Karolina Piotrowska, Paul Holmes, Marius Costache, Yi Zhang, Aarti Rege, Dan Lewitus, and Aaron Pesnell. My apologies for skipping their respective titles, but I would like to clarify that this does not affect the respect I have for any of them in any way whatsoever. Members of the "Biology Box" in Kohn's group: Dr. Hak-Joon Sung, Dr. Prafulla Chandra, and Dr. Robert Dubin. I am grateful for their teaching and for the fact that they shared their time to help me learn further about the biological aspects of biomaterials science. I would be very pleased to collaborate with them again at some later point in my life. Particular recognition goes to the brilliant Ph. D. students belonging to Kohn's group, especially Charles Florek, Arnold Luk, Dan Lewitus, and Loreto Valenzuela. Graduate school has its hurdles, and each one of these Ph.D. students helped ameliorate the tribulations of "grad-school life" by merely listening to the struggles with which I was dealing, by providing excellent suggestions and ideas related to work, etc. I am extremely grateful for their camaraderie and for the support that each one of them provided during every single part of my time at Rutgers. I am also grateful to other past group members, like Jaap Schut and Nicole Harris, for their help, teaching, and genuine interest in my work and welfare (JS: "You will make it work, you will figure it out, you are a smart

guy"). My appreciation goes out to other research faculty and office staff from the New Jersey Center for Biomaterials and the Chemistry Department at Rutgers: Dave Devore, Narayan Pallassana, Barry Cunningham, Carole Kantor, Ann Doeffinger, Melissa Grunwerg, Melissa Aranzamendez, Shirley Maimone, Don Lindorfer, Kathy Piano, and Debra Fenton. Their efforts in making the lives of graduate students run smoothly deserve special recognition.

I also appreciate the friendship of many Ph. D. students at Rutgers (not only in the Chemistry Department). Special thanks go to Mauricio Esguerra, who is a real chemist, even if he has not worn gloves, safety glasses, or a lab coat in a long time, and to Jeremy Pronchik, Kristina Paris, Mohannad Abdo, Mike Wininger, Ron Pérez, Rebecca Baerga, James Bennett, Lisa Veliath, Ahalya Ramanathan, Roberto Delgado, and Benjamin Lee. I would like to express my appreciation for all their support and trust during graduate school.

I also would like to acknowledge several Chemistry Faculty members: Professors Larry Romsted, Edward Castner, Alan Goldman, Jing Li, Yves Chabal (now at UT Dallas), Eddy Arnold, and Lawrence Williams ("Principles of Organic Synthesis": best class for me in graduate school, excellent instructor): In many ways, their teaching, conversations, and suggestions have shaped my development in order to help me become a better scientist and person.

From a teaching perspective, I appreciate the time spent and efforts made by Donald Siegel and Patrick O'Connor in order to help my development as a teacher and my education as a scientist in a liberal arts college like Rutgers. Without their help, my teaching experience while in graduate school would have been rather rough. My students

can testify that this was not the case, and I am grateful for that. My chemistry students when I worked as a laboratory instructor and as a recitation instructor, as well as those from the Kohn Lab (Scott Barbolt, Opeyemi Awe, Rabieh Saad, Zach Brill, and Krishna Shah), deserve my recognition for their great work. They learnt from me as much as I learnt from them.

Life in New Jersey would have been rather complicated without the support and friendship of many people, including Cyril Coumarbatch and everyone else at Rutgers Graduate Residence Life. I am tremendously grateful for the opportunity they gave me by allowing me to become a Graduate Residence Life Assistant, as well as for their authentic friendship. Dave Thompson and Peter Talley were the best housemates ever. I would like to acknowledge their help and friendship over these years on behalf of both Sara and me. All the "after-work" friendships with many Rutgers graduate students is deeply appreciated, and I will make sure that these friendships are kept going for many years to come.

This thesis would not have been possible without the help of many others outside Rutgers. I am indebted to many people that "were always there for me": Marcelo Silveyra for his help with proofreading, editing, and translation. Professors Cecilia Rojas de Gante, Mario Álvarez, and Marcelo Videa for their support and teaching in many aspects that have covered my undergraduate education, graduate school, and beyond. My dear friends in Monterrey, "Los Ojas", for their moral support and true friendship of over 15 years now. My dear family for all their love and encouragement: Ramiro and Nelly, as well as Nelia, Ricardo, and Daniel. I appreciate their unwavering support throughout my years at Rutgers, my upcoming experience in Sweden, and wherever else I end up

living/working in the future. My deepest gratitude goes to my girlfriend, Sara Dover, whose love and support throughout these years has been absolutely invaluable. Sara has been an inspiration for many things, and her encouragement and strength have helped me out tremendously. Her daily joy and cheerfulness just made every single one of my days better.

Finally, I would like to acknowledge you, the reader, for the time you are taking to read this thesis. Hopefully, reading it provides you with some insight and useful information on the application of combinatorial and high-throughput approaches to polymer chemistry and biomaterials science.

TABLE OF CONTENTS

LIST OF TABLES

LIST OF FIGURES

LIST OF ACRONYMS, ABBREVIATIONS, AND SYMBOLS

4-NH	4-needle head
6-hH	6-hydroxyhexanoic acid
ANOVA	analysis of variance
ATRP	atom-transfer radical polymerization
CC	combinatorial chemistry
CMR	Combinatorial Materials Research
CPH	1,6-bis(p-carboxyphenoxy)hexane
DAPI	4',6-diamidino-2-phenylindole
DIPEA	*N,N*-diisopropylethylamine
DMF	*N,N*-dimethylformamide
DoE	design of experiments
DP	degree of polymerization
DSC	differential scanning calorimetry
DTE	desaminotyrosyl-tyrosine ethyl ester
DTR	desaminotyrosyl-tyrosine alkyl ester
EAFUS	Everything Added to Food in the United States
EDC•HCl	ethyl-3-(3-dimethylamino)propyl carbodiimide hydrochloride salt
FDA	Food and Drug Association, American
FT-mIR	Fourier transform infrared microspectroscopy
GA	glycolic acid

GFP	green fluorescence protein
GPC	gel permeation chromatography
GRAS	Generally Recognized As Aafe
GSE	General Solubility Equation
hMSC	human Mesenchymal Stem Cell
HOBt	1-hydroxybenzotriazole hydrate
HPLC	high performance liquid chromatography
IPA	isopropanol
LA	lactic acid
LSD	least significant difference
MADIX	macromolecular design via the interchange of xanthates
MCGS	mesenchymal cell growth supplement
MSCBM	mesenchymal stem cell basal medium
N-EtMo	*N*-ethylmorpholine
NIST	National Institute of Standards and Technology
NMP	*N*-methylpyrrolidone
NMR	nuclear magnetic resonance
PAFA	Priority-based Assessment of Food Additives
PBS	phosphate buffer saline
PCL	poly(ε-caprolactone)
PDi	polydispersity index(es)
PDMS	poly(dimethylsiloxane)
PEG	poly(ethylene glycol)

PEG_{1k}	poly(ethylene glycol) MW = 1,000 $gmol^{-1}$
PTFE	polytetrafluoroethylene
PU	polyurethane
R&D	research and development
RAFT	reversible addition-fragmentation chain transfer
RH	relative humidity
RP	reversed-phase
RT	room temperature
SA	sebacic acid
SEM	scanning electron microscopy
TBA	tri-*N*-butylamine
TCPS	tissue culture polystyrene
TE•HCl	tyrosine ethyl ester hydrochloride
TEA	triethylamine
TFA	trifluoroacetic acid
THF	tetrahydrofuran
TP	triphosgene or bis(trichloromethyl)carbonate
TR	tyrosine alkyl ester
T*t*Bu	tyrosine *tert*-butyl ester
Tukey HSD	Tukey's honestly significant difference
PLLA	poly(L-lactide)

$(Boc)_2O$	*tert*-butyl dicarbonate
°C	degrees Celsius
^1H	proton
B acid	4-hydroxybenzoic acid
C acid	4-hydroxycinnamic acid
Cbz-Cl	benzyl chloroformate
$CDCl_3$ or chloroform-*d*	chloroform, deuterated
CH_2Cl_2	dichloromethane
CH_3CN	acetonitrile
cLogP	calculated partition coefficient, water/octanol
D-acid or DAT	3-(4-hydroxyphenyl)propionic acid
DMSO-d_6 or (methyl sulfoxide)-d_6	dimethylsulfoxide, deuterated
eq	molar equivalents
EtOAc	ethyl acetate
EtOH	ethanol
Fmoc-Cl	9-fluorenylmethyl chloroformate
G acid	*N*-(4-hydroxyphenyl)glycine
H acid	4-hydroxyphenylacetic acid
H_2O	water
H_2O_c	water, cell culture grade
H_2O_d	water, distilled
HCl	hydrochloric acid 37%

K	degrees Kelvin
L	liter
LogS	natural logarithm of the molar solubility
Macro	macro task
MeOH	methanol
$MgSO_4$	magnesium sulfate
min	minute(s)
μL	microliter
mL	milliliter
Mn	number average molecular weight
NaCl	sodium chloride
$NaHCO_3$	sodium bicarbonate
NH_4OH	ammonium hydroxide
P acid	(4-hydroxyphenoxy)acetic acid
rpm	revolutions per minute
T_g	temperature, glass transition
T_m	temperature, melting point
T_p	temperature, peak max

ΔG_{iwi}	free energy of interaction between surface molecules *i* immersed in water
f	flexibility index or number of flexible bonds

M/f	mass-per-flexible-bond
M_i	molecular weight of repeating unit "i"
R^2	square of the correlation coefficient in a linear regression
W_{sl}	work of adhesion between a solid substrate and a probe liquid
x_i	mass fraction of repeating unit "i"
γ^-	electron donor component of γ^{AB}
γ^+	electron acceptor component of γ^{AB}
γ^d *or* γ^{LW}	dispersive component of the surface energy/Lifshitz-Van der Waals components
γ_{iw}	interfacial tension between the surface and water
γ_l	surface energy of a liquid
γ^p *or* γ^{AB}	polar component of the surface energy/ acid-base components
γ_s	surface energy of a solid
γ_{sl}	surface energy of a solid-liquid interface
θ	contact angle of a liquid on a solid surface

1. INTRODUCTION

1.1 CURRENT PROGRESS IN SYNTHETIC & DEGRADABLE POLYMERIC BIOMATERIALS DISCOVERY

The field of synthetic and degradable polymeric biomaterials is relatively new, and its ultimate goal is to provide a number of different industries and disciplines, such as tissue engineering, drug delivery, and the medical device industry, with materials featuring a high degree of versatility.[1] Specifically speaking, the use of synthetic and degradable polymeric biomaterials in the aforementioned disciplines and industries is aimed at the development and use of temporary medical implants designed to replace their permanent equivalents. In tissue engineering, the main goal is to implant a temporary reconstructive or regenerative scaffold into a diseased or injured site, allowing the body to heal itself in a faster and directed way. Once implanted, the temporary scaffold must be safely resorbed inside the body while leaving healthy and functional tissue behind.[2] The concept of using this type of minimally invasive medical procedure in order to promote and accelerate the body's natural healing process is well known, but its execution is still rather limited. This can be partly attributed to the lack of adequate biomaterials, which is a direct result of the wide variety of organs found inside the human body. The fact that each one of these organs has different characteristics translates into an inherently high level of complexity in the design and synthesis of polymers for specific applications.[3] As a consequence, the number of polymeric biomaterials featuring the

characteristics (e.g., mechanical properties, enabling molecular interactions with cells, biocompatibility, non-cytotoxic degradation products) required for their appropriate use in tissue engineering or medical device applications is very limited.[2, 4] An example can be seen in Table 1.1, which lists the major polymer classes of degradable synthetic polymers applied to the manufacture of medical devices during the last four decades. The table includes the corresponding medical device that was approved by the Food and Drug Administration (FDA) and the primary chemical component or starting material for the relevant polymer.[2] This table does not include copolymers or other structural modifications (e.g., the use of D-lactic acid, L-lactic acid or DL-lactic acid).

Table 1.1 Classes of synthetic degradable polymers and their primary starting material(s) as used in FDA-approved medical devices

Polymer class	Major component(s)	Type of device(s)	Year of device(s) approval by FDA
Polyester	Glycolic acid	Suture	1969
Polyester	Lactic acid	Suture	1971
Polycarbonate	1,3-trimethylene carbonate	Suture	1974
Polyester	1,4-dioxan-2-one	Suture and bone fixation	1981
Polyanhydride	Sebacic acid	Drug delivery system	1996
Polyester	ε-caprolactone	Coating for suture	1997
Photocrosslinkable polyester	Lactid acid and poly(ethylene glycol)	Lung and tissue sealant	1998
Polyarylate	Tyrosine-derived bisphenol and diacid	Hernia repair device	2006
Polyarylate	Tyrosine-derived bisphenol and diacid	Anti-bacterial envelope for pacemakers	2008

While the table confirms the fact that there is a lack of diversity in material properties among these classes of polymers, it fails to show a much more important limitation: the fact that research efforts do not normally go beyond the use of the corresponding poly(α-hydroxy acids) and copolymers thereof. Moreover, most research is done on a "trial and error" basis that simply cannot keep up with the demand for complex structures that can be tailored to the needs of several medical applications.[1, 2, 5]

While most of these polymers perform adequately when used in relatively simple medical device applications such as sutures, coatings, and pins, they are still subject to certain limitations (e.g., autocatalytic degradation, accumulation of acidic degradation products, poor mechanical stability).[1] Moreover, and although tissue engineers and clinicians have shown great interest in expanding the range of available synthetic biodegradable polymeric biomaterials in order to find optimum compositions for specific applications and for applications for which the corresponding requirements still cannot be met, the design and synthesis of new degradable polymeric biomaterials still constitutes a challenge.[3, 6, 7] As a result, the number of medical applications that can be addressed with "off-the-shelf" polymeric biomaterials is very limited. This leads to the conclusion that the discovery of synthetic degradable polymeric biomaterials has not advanced significantly in the last three decades and therefore has failed to meet the demands of the tissue engineering and medical device industries.

In order to promote the development of new and useful polymeric biomaterials, a new paradigm is needed in terms of how to discover them.[2] A few attempts at rationalizing the design of polymeric biomaterials for function-specific applications have been made,[6, 7] but the resulting conclusions have inevitably led back to the use of

"traditional" biomaterials, e.g., poly(lactic acid) and poly(glycolic acid) and their corresponding copolymers. In order to overcome this situation, Kohn proposed the adoption of combinatorial, high-throughput, and computational approaches when designing biomaterials in order to (i) accelerate the discovery of new biomaterials and (ii) increase the diversity of promising polymer structures.[2, 4, 8, 9]

Holder and colleagues have applied similar concepts by designing dental materials (albeit non-degradable) with computational chemistry approaches,[10] and ever since the development of the first combinatorially designed library of biomaterials,[11, 12] more researchers have adopted combinatorial and high-throughput approaches in order to rationally design and synthesize suitable biomaterials for specific applications.[13-17] While these techniques are linked to the development and use of rapid characterization and screening techniques in general,[18-21] the next sub-chapter will not focus on them, and will instead concentrate specifically on the use of combinatorial and high-throughput methods in polymeric materials (not necessarily biomaterials) discovery processes, as well as on the impact that this approaches might have on new advances in polymer science.

1.2 COMBINATORIAL AND HIGH-THROUGHPUT METHODS IN THE DISCOVERY OF POLYMERIC MATERIALS

1.2.1 Combinatorial and High-Throughput Approaches

The work of Schultz and colleagues, published under the title of "A Combinatorial Approach to Materials Discovery", marked the beginning of combinatorial materials research (CMR) as a discipline by applying combinatorial techniques to the search for superconductors from a large library of materials.[22] Although combinatorial and high-throughput experiments have a long history in materials science, even going as far back as Thomas Alva Edison's experiments in the late 1800's, it was not until 1970 that Hanak developed his "Multiple Sample Concept" for the development of electronic materials at RCA Corporation, thus establishing what researchers consider a forerunner to CMR.[23-28] Despite these efforts, the application of combinatorial to materials science went unnoticed until Schultz's work in 1995. Since then, the CMR concept has been applied to various different kinds of materials, including catalysts, electronic, optical, and magnetic materials, and is currently emerging in the fields of polymers, resin supports, biomaterials, paints, coatings, drug formulations, detergents, cosmetics, and others.[24, 29-32] Combinatorial experiments (i.e., experiments in which elements of a composition or synthesis are combined) are often linked to high-throughput methods (i.e., the rapid systematic variation of given parameters to explore a wide parameter space), and both techniques are incorporated as part of CMR.[24] In order to review the potential of CMR in polymer applications, it is first necessary to compare and contrast certain variables as

they are affected by traditional synthetic methods and combinatorial chemistry (CC) when applied to the drug discovery process. The fact that the identification of lead or active compounds is possible within a complex mixture (e.g., split-pool synthesis) when CC is applied to the drug discovery process is crucial.[2, 33] In materials research (specifically polymer science) performing characterizations on a mixture of polymers is impossible, as deconvolution of the mixture is rarely possible and it is not feasible to trace back properties to a unique polymer composition.[34] Another difference is that, in the case of combinatorially-created drug candidate libraries, biological activity, determined by its chemical structure, is the ultimate test, leading to a "Yes" or "No" answer when performing a screening assay.[35, 36] In the case of polymers, chemical structure is one of the many parameters (e.g., molecular weight, molecular weight distribution) that can affect the final properties of a material.[32] The goals and strategies of CMR and CC applied to the drug discovery process are summarized in Table 1.2, shown below.[29]

Table 1.2 Differences between drug discovery and materials development

Drug discovery	Materials Development
Focused on the chemical synthesis that can lead to the identification of a single compound that is effective as a drug	Focused on the discovery of systems that can meet a number of physical, chemical, and structural properties
Synthesis of thousands of compounds within a complex mixture	Synthesis of several discrete material compositions
Emphasis on diversity within known metrics (i.e., target disease or active site)	Emphasis on broad coverage and synergy in physical and chemical properties
Easy sample evaluation at the nanogram level (i.e., rapid screening plus deconvolution of mixture)	Sample evaluation is difficult, and has to be individualized for each system in many cases

Applying the CMR approach is not a straightforward process, and doing so presents both advantages and challenges when implemented for the first time in a traditional laboratory setting. Table 1.3 summarizes the advantages and challenges resulting from the application of the CMR approach, regardless of the corresponding setting (i.e., industry or academia).

Table 1.3 Advantages and challenges resulting from the application of the Combinatorial Materials Research approach

Advantages	Challenges
Systematic and accelerated optimization of synthetic procedures	Amount of time needed to translate manual protocols to automated ones
Acceleration of throughput	Inherent limitations of the instrumentation used
Effective exploration of materials design space	Universal screening tools for materials science are scarce
Rapid identification of new material compositions	Need to overcome the current materials discovery paradigm
Can lead to the discovery and development of new technologies	

The fact that researchers need to overcome the current paradigms that pervade materials discovery processes is of special significance. The association of materials discovery and combinatorial and high-throughput approaches generates a sense of risk in regard to the potential success of implementing these strategies, a hesitant reaction brought about by the fact that scientists are trying to find the same level of success that is achieved in the discovery of drugs when using the CMR approach. As previously mentioned, however, this comparison cannot be made straightforward due to the significant differences between small molecules and materials. Therefore, the required paradigm change can be summarized by looking at the “Classical” vision of

combinatorial and high-throughput approaches as used for research and the “Emerging” vision, as outlined in Table 1.4 below.

Table 1.4 Expectations of success for the Combinatorial Materials Research approach

"Classical" Vision	"Emerging" Vision
Follows the mantra of "Screen in a day what you synthesize in a day; and analyze in a day what you screen in that day"	Focuses on the individual components of a workflow rather than on the workflow as a whole (e.g., Design of Experiments by itself)
Assumes no bottlenecks in the process	Immediate benefits from any aspect of the workflow applied to research (e.g., improved output)
Assumes the application of comprehensive workflows from concept to synthesis to analysis, highly associated with an informatics component	Applying the CMR approach leads to fast discovery and technology development
Outcome: Skepticism and sense of risk on behalf of researchers	**Outcome:** Immediate acquisition of multiple benefits beyond the "single-sample paradigm"

There are several examples of researchers applying elements of the CMR approach and still obtaining multiple benefits as a result. One common example is the optimization of polymerization conditions for different polymer systems.[37-41] The work by Li and colleagues, who used the concepts of CMR without any automation or high-throughput approaches, is of particular interest.[39] The Li Group reported on combinatorial optimization for the synthesis of a soluble polyfuran and poly(furan-*co*-aniline)s with variable conductivity levels. The polymerizations were optimized by modifying various parameters, such as the furan concentration, the nature of the oxidant species, the oxidant/monomer ratio, and the furan/aniline ratio, as well as processing variables. Although the study was not performed with high-throughput methods, this is a clear example of research performed with the use of CMR principles as a way to extend the knowledge acquired past the one-reaction system by systematically modifying the parameters involved in a given synthetic procedure.

The idea behind CMR is to effectively and efficiently explore a large compositional space.[42-44] This is done with the purpose of speeding up both the discovery of materials and the development processes in a determined field. CMR often combines rapid synthesis and reaction optimization, high-throughput testing or screening, and adequate information processing with the purpose of preparing, analyzing, and interpreting the individual members of libraries.[38, 45] When automated processes can be coupled to one or more of these steps (e.g., automated parallel synthesis, automated processing of characterization data), time-consuming manual steps are minimized. Moreover, when computational tools are used in order to evaluate certain members of a library, trends can be determined, and correlations (and even predictions) can be found for similar members of a family of materials.[8, 46, 47]

Most of the time, combinatorial and high-throughput experiments in materials research are defined only by the relevant type of material, but the tendency is for experiments to be defined based on the material's application.[4, 10] CMR typically requires preparing an array of materials, referred to as libraries, that normally hold structurally related materials. It also requires a fast or adequate method for screening for properties, as well as a set of computational tools that make it possible to store and analyze data and to design subsequent experiments.[24-26] CMR results in two major benefits, namely the discovery of a new material (e.g., polymer, resin, coating) with unique properties and an increased knowledge of the corresponding structure-property relationships. By surveying a broad compositional design space and using adequate screening and characterization methods, the compounds featuring those unique characteristics can become apparent to the researcher. At the same time, structure-

property relationships can be drawn for the examined compositions, which make it possible to predict or approximate the physical or chemical properties of unknown compounds.

In conclusion, and when talking specifically about polymers in materials science, a polymer's performance properties can be obtained through a careful design that can include chain size, uniformity, topology, microstructure, composition, etc. Therefore, the application of combinatorial and high-throughput approaches in the design and exploration of polymer space is expected to lead to important new discoveries and innovations not feasible with traditional experimental methods. Recently, several new innovations concerning the high-throughput synthesis of polymers, both automated and non-automated, have been reported, and will be surveyed next, as they are inherently important to the application of the CMR approach to polymer science.

1.2.2 High-Throughput Polymer Synthesis

The use of combinatorial and high-throughput approaches in macromolecular materials research can facilitate the discovery of complex, highly specific polymer compositions that would be impractical, if not impossible, to discover with traditional (i.e., one-by-one) experimental methods.[32] The extensive collection of currently available monomers and synthetic techniques makes it very difficult for polymer chemists to find appropriate chemical compositions for specific applications. This presents an important challenge in the field of polymer science, since synthesized polymer systems have to meet certain criteria in order to perform adequately. One of the

features of high-throughput polymer synthesis that makes it possible to address this issue is the fact that this method not only allows for the optimization of reaction conditions (especially with new monomers and reagents), but also permits the simultaneous exploration of structurally related polymer libraries, enabling the quick discovery of innovative polymers.

The concept of CMR has been applied to the synthesis of polymer libraries in order to better handle the current diversity of compounds and the process involved in optimizing reaction conditions.[48-51] This is made possible through the systematic variation of reaction parameters, e.g., reaction temperatures, stirring or vortexing speeds, types of catalysts, types of monomers or co-monomers, etc. There are several reaction methods available for polymer synthesis, with step-growth (e.g., condensation polymerization) and addition polymerization (i.e., e.g., radical and ionic polymerization) being the ones most frequently used. The variety of relatively simple synthetic approaches available, combined with the large variety of monomers available, makes the use of CMR in polymer synthesis particularly convenient. Indeed, developing a method for a single polymer type in such a way that it can be extrapolated for use with similar reagents makes it possible to easily create entire libraries of materials. This, in turn, allows for the rapid exploration of polymer design space more effectively than with the use of traditional methods.

The last six years have been particularly prolific for Schubert's group (Friedrich Schiller University of Jena in Germany and Eindhoven University of Technology in the Netherlands) in terms of its application of CMR to polymers. Schubert and colleagues have been very active in the exploration of polymer synthesis methods, especially radical

and ionic polymerization.[26, 28, 52-54] They have synthesized several poly(2-oxazoline)s through automated parallel synthesis, creating high-molecular-weight materials both with traditional heating sources and with microwave radiation.[28, 53, 55-57] The ring-opening polymerization of 2-oxazolines performed by Schubert's group demonstrated the potential that the use of high-throughput approaches holds for the development of new poly(2-oxazoline)s; a potential that had gone largely unexplored since their discovery in 1966.[53] The Schubert group has also pursued the synthesis of polymers through emulsion polymerization and more demanding procedures, such as anionic polymerization, both which represent moisture–sensitive and oxygen-sensitive non-trivial reactions.[52, 54] In the case of anionic polymerizations, these require several steps for the cleaning and the rendering of reactors inert prior to any reaction. These steps would be highly impractical with manual procedures, but do not take any additional time (from the operator) during automated synthesis, and have yielded several types of homopolymers and copolymers with different morphologies, such as random, block, and gradient, with a high degree of consistency.[52, 53] Most recently, Schubert's group evaluated several polymerizations with controlled radical polymerization methods such as reversible addition-fragmentation chain transfer (RAFT), atom-transfer radical polymerization (ATRP), and nitroxide-mediated polymerization.[28, 37, 58-62] The use of automated parallel synthesis coupled with combinatorial approaches has allowed the group to overcome several synthetic hurdles and explore several reaction types that are important for the synthesis of industrial-relevant materials. In addition, Schubert's group has applied CMR concepts to the synthesis of polymers with various topologies (e.g., star, brushes, dendritic), compositions, and microstructures (e.g., periodic, blocks, grafts),

based on the principles involved in controlled radical polymerization when applied to macromolecular engineering.[37, 56, 63-65]

Other polymer systems have been synthesized with non-automated and automated parallel methods. Webster's group at North Dakota State University has been particularly active with research on polymer coatings for various applications (mainly antifouling underwater coatings). They have provided reports on the synthesis of libraries and on the characterization of 3-aminopropyl terminated poly(dimethylsiloxane) (PDMS) and poly(ε-caprolactone)-*block*-poly(dimethyl siloxane)s, as well as on hydroxyalkyl and dihydroxyalkyl carbamate-terminated PDMS oligomers and their block copolymers with poly(ε -caprolactone) (PCL).[51, 66-68] Together with Chisholm, Webster has reported on the development of coatings with the use of CMR, going from the design of experiments to the automated synthesis, characterization, formulation, and specific screening tests involved in producing coatings.[42, 69] Webster's group has provided reports on the synthesis of aqueous polyurethane dispersions, using automated parallel synthesis systems, for various different applications, including flame retardant materials.[70] Most recently, they have begun to explore different polymerization methods, such as ATRP, by using automated parallel synthesis in order to obtain specific molecular weights and compositions of polystyrene-based polymers.[71]

Another leader in the field of CMR is Radislav Potyrailo, who has studied the result of applying a number of elements inherent to the CMR approach to various applications at General Electric in respect to the synthesis of polymers. Potyrailo and his colleagues have undertaken the task of exploring several new coating compositions on a small scale, but have gone a step further and explored the scale-up of combinatorial leads

using CMR principles.[72, 73] Another active area of research for Potyrailo's group consists of the optimization of process conditions in combinatorial microreactors. This is mainly done to establish optimal combinatorial process conditions and translate them to conventional synthetic scales or larger scale-ups. In conventional reactions, the optimization of synthesis processes often represents a trade-off between adequate performance (e.g., yield, purity, molecular weight) and "least experimental investment".[74] Because of this, Potyrailo has explored optimization procedures for the synthesis of poly(bisphenol-A carbonate) in the melt from bisphenyl carbonate, bisphenol-A, and sodium hydroxide (NaOH) as a catalyst. Using fluorescence spectroscopy, he and his group obtained chemical data that could be correlated to other parameters such as molecular weight and the formation of side-products, all dependent on the conditions involved in the synthesis process.[74] Another area of interest for Potyrailo's group is the development of matrix polymer-based vapor and liquid sensors.[30, 31, 75] His work has comprised an enormous variety of sensor materials, including sensing polymers and copolymers, formulated polymeric compositions, polymeric structures with engineered morphologies, and molecular-shape recognition polymeric materials.[31] The main benefits of CMR in Potyrailo's research with sensor materials can be found in the exploration of synthesis and processing parameters and in multi-dimensional chemical composition analysis at a detailed level, yet across a broad area of chemical space that was previously unavailable with one-at-a-time experimentation in this area.[74, 75]

Other researchers have targeted the largely unexplored application of CMR to condensation polymerizations.[40, 50, 76] In one instance, Lavastre and colleagues

combinatorially synthesized polymeric organic light-emitting diodes (Polymeric OLED) for the first time by condensing various aromatic dibromides with aromatic diacetylenes in the presence of palladium-based catalysts in order to obtain 96 poly(arylene ethynylene)s, in a very similar fashion to Kohn and colleagues when obtaining their library of 112 tyrosine-derived polyarylates.[12, 76] In another example, Hodge and colleagues explored the high-throughput synthesis of polyesters using entropically-driven ring-opening polymerizations.[50] The fact that this was the first time ever that these types of reactions were obtained using CMR resulted in a promising avenue for the investigation of poly(alkylene terephtalate)s. The synthetic procedure reported by Hodge involved mixing the corresponding macrocyclic oligoesters and subsequent heating at high temperatures (i.e., 200–300 °C) for two hours in the presence of di-*n*-butyltin oxide or tetra-*n*-butylammonium tetrafluoroborate as a catalyst.[50] As an example, the authors compared the results obtained with the typical synthesis of poly(ethylene terephthalate) from dimethyl terephthalate and ethylene glycol, which requires a reaction time of several hours (i.e., 3 or more), high temperatures, constant stirring, and the continuous removal of methanol and/or excess glycol under reduced pressure. Six families of copolymers were reported on a 100 mg scale with an average polydispersity of 2.0 (typical for these types of polymers) and with purities that were high enough as to make it possible to follow-up with the synthesis of more compositions for their characterization and an eventual structure-property relationship analysis.

More recently, the application of the CMR approach to polymer membranes (i.e., polyimide-based) has been reported on by Vankelecom and colleagues.[41, 77] Instead of using a traditional factorial design for their design of experiments (DoE), they used

"evolutionary strategies", similar to a simplex type of DoE in that an outer array or parameters is explored in order to get closer to an optimized composition or process by varying the best performers of each generation.[41] The outcome of using the CMR approach in their research was the fact that Vankelecom and colleagues were able to identify specific membrane compositions that ranked higher than commercially available polyimide-based membranes when tested in a benchmark comparison.[77]

Another example comes from a team of researchers, led by Petro, who are working at Symyx Technologies, Inc. and who have provided reports on the creation of polymer delivery systems for bioactives derived from several acrylates or methacrylates through free-radical polymerization. They have developed automated and high-throughput methods for the synthesis and characterization of their substrates and expect to extend these methods to innovative materials in pharmaceutics (i.e., excipients), personal care, and other biotechnology-related areas.[78] In their report, they mentioned further advantages and benefits of combinatorial and high-throughput approaches when applied to polymer research and development (R&D):

- Speed, resulting from debottlenecking the idea-to-product process. This can also lead to earlier opportunities for materials development (i.e., turnover is reduced).
- Opportunity of comparing like experiments within the same set of experiments. This makes it much easier to derive qualitative trends regarding synthetic methods and/or characterization.
- Significant reduction of costs per experiment, as well as a reduction of

physical labor on behalf of the researcher.

- Lower amount of material needed for the screening process.
- Greater protection in terms of intellectual property thanks to the broad range of materials explored.

A quick comparison between conventional and automated polymer syntheses in academia is shown below (in connection with the third point, i.e., cost reduction, made by Petro and colleagues), The figures in Table 1.5 are based on one Ph. D. student, one post-doctoral associate, and one laboratory technician with an operational cost basis of $10,000/month:

Table 1.5 Cost of traditional (one-at-a-time) methods *vs.* combinatorial approaches for polymer synthesis

Synthesis platform	**Polymers synthesized/month**	**Cost of compound, $**	**Yield, mg**	**Application**
Single synthesis	10-20	500-1000	500-20,000	Specific studies
Small-scale parallel reactors	100-200	50-100	100-2,500	Screening & development
Microtiter plate	500-1000	10-20	5-50	Screening

In relation to the last synthesis platform addressed on the table (i.e., microtiter plate), a remarkable example was recently reported by Mallapragada, Narasimhan, and colleagues. Their work addressed the parallel synthesis and high-throughput dissolution testing of biodegradable polyanhydrides intended for drug delivery systems.[48] During the corresponding work, the team synthesized a combinatorial discrete library from anhydride pre-polymers of 1,6-bis(*p*-carboxyphenoxy)hexane (CPH) and sebacic acid

(SA) in order to synthesize poly[1,6-bis(*p*-carboxyphenoxy)hexane-*co*-sebacic acid] with varying composition forms (0 to 100 mol% SA). Their synthesis platform was a contact lithography-built multi-well glass slide that consisted of a 10×10 grid with a capacity of 2-μL per microwell. After automated dispensing of the reagents in solution, the multi-well glass slides were placed in a preheated vacuum oven at 180 °C for one hour. The group mapped the compositions with Fourier Transform Infrared Microspectroscopy in reflectance mode (FT-mIR RM). Although Mallapragada and his colleagues synthesized a hundred compositions in a high-throughput manner coupled with a rapid characterization method, no information was obtained for the entire library in terms of molecular weight, polydispersity, and other physical data – hence its limited use for other researchers. As mentioned earlier, physical and chemical properties are very important for polymers, since their behavior is highly dictated by these characteristics (e.g., the free volume of a low molecular weight polymer is likely to affect how a bioactive molecule diffuses from its matrix in comparison to the same event occurring with a higher molecular weight polymer).

Continuing with examples of polymer systems intended for biomaterials-related applications, the work of Kohn and colleagues is presented as the first combinatorially designed library of biomaterials, which was produced through several parallel polymerization reactions, albeit manually.[11, 12] This library allowed a start-up company in New Jersey, TyRx Pharma, to use one of the polymers for the design of a hernia repair device that received FDA clearance in 2006.[2] Langer and Anderson have reported on the synthesis of poly(β-amino ester)s as potential gene delivery systems. The Michael addition-type reaction of amines to diacrylates was conducted in multi-well

plates at high temperatures (56 °C) for 5 days. Although this kind of reaction was not performed with automated instrumentation, it is highly suited to automated parallel synthesis, even with the high solution viscosities reported by Langer and colleagues.[13, 79] A team of researchers from the University of Edinburgh, led by Bradley, reported on the use of CMR for the creation of polymer microarrays intended for the study of cellular adhesion.[80, 81] A library of poly(urethane)s was synthesized in parallel for this purpose and was fully characterized before its use in the creation of the microarrays.[49] Although Bradley's research did not include the use of high-throughput polymer synthesis, the repercussions of the CMR approach for the evaluation of large polymer libraries is obvious, as screening of several polymers could be performed much faster compared to the one-at-a-time investigation of each polymer.[49, 81]

This sub-chapter has covered the major work that has been done on the synthesis of polymers (in the form of libraries) intended for diverse applications, including research done in parallel (although manually), in automated parallel fashion, and combinatorially (using multi-wells for the creation of libraries and the exploration of reaction conditions). However, it did not include one additional approach to the combinatorial study of polymers, which is the formation of gradient libraries (e.g., thickness-, composition-, temperature-, and surface energy-gradient libraries). These efforts have been undertaken largely by the National Institute of Standards and Technology (NIST), and have been reviewed elsewhere.[82, 83] In short, when referring to the gradient approach, the library consists of a physical sample in which different properties are spatially varied across the sample.[32, 42] A couple of advantages of using the gradient library approach are the fabrication of the library (i.e., micro-scale) and its use to characterize fundamental

polymer properties, including blend behavior, wetting, surface morphology, and mechanical properties.[84-87] Although some research on the synthesis of polymers *in situ* during the creation of the gradient library has been done, most synthetic methods available for polymer chemistry are incompatible with the creation of this kind of samples. The use of gradient libraries is much more suitable when specific polymers must be explored or when a surface modification must be made, rather than when synthesizing polymer libraries, and thus was not reviewed in this sub-chapter.

In conclusion, this chapter has reviewed the application of high-throughput approaches to the development of new polymers. The parallel synthesis of polymers allows for the preparation of a large number of individual compounds at a fast rate. Compared to traditional combinatorial chemistry approaches, the parallel synthesis of polymers allows for the individual preparation of polymers – in sufficient amounts for their characterization. In contrast to small molecules, multiple parameters must be fine-tuned for polymers, particularly in the case of biomedical applications. Therefore, the use of parallel synthesis for the rapid exploration of polymer design space and synthetic conditions may be the only possible way of efficiently increasing the discovery rate of polymeric biomaterials. While many successful cases have been mentioned in this overview, there are still limitations regarding the application of parallel synthesis on specific reaction systems, including switching from manual methods to automated and/or combinatorial methods, using more efficient catalyst systems, and controlling the corresponding reactions with an automated instrument, all of which must be addressed before CMR can be of practical utilization in polymeric biomaterials research.

1.3 HYPOTHESES AND RATIONALE

It is evident that the use of combinatorial and high-throughput approaches in the development of polymer systems can help develop optimal biomaterials in an efficient and cost-effective manner. The hypotheses presented in this thesis are based on the application of these approaches, as outlined below:

- Small structural changes to a library of monomers, accomplished by modification of their backbone, can influence the performance of the final biomaterial.
- The creation of automated parallel synthesis procedures for the polymerization of tyrosine-derived polycarbonates can be used to optimize reaction conditions systematically and to explore polymer design space effectively.
- A physical characterization of the synthesized polymers can be used to determine structure-property relationships of homo-, co-, and terpolymers.
- The incorporation of combinatorial and high-throughput approaches in the design and synthesis of biomaterials can lead to a new biomaterials discovery paradigm.

The goal behind the work presented in this thesis is to outline a materials design strategy that can be used for the creation of biomaterials based on specific clinical needs (i.e., rational design), rather than on the basis of conventional “trial and error” strategies. In line with this objective, the thesis shows how the synthesis of new monomers can expand directly on the diversity of materials based on natural metabolites, and how the creation of suitable automated synthesis protocols for polycarbonates can allow for the

systematic and accelerated exploration of compositional polymer space. Using physical and chemical properties from libraries of polymeric materials together with systematic variations can be used as a way to provide feedback for the design approach, making it possible to support future research by expanding the knowledge base available for the prediction or estimation of the performance of new (i.e., not yet synthesized) biomaterials. Overall, the rationale behind this work is to further support the application of high-throughput approaches (i.e., automated parallel synthesis) to the creation of customized biomaterials that can satisfy the needs of specific tissue engineering applications.

1.4 THESIS OUTLINE

The thesis is organized into six chapters, without including the introduction. The "Materials and Methods", or "Experimental Procedures", are collected in Chapter 2, with some very specific details being found throughout the subsequent chapters as needed. Chapters 3 to 5 contain the main part of the thesis, going from the monomers used, to the synthesis of polymers, to the characterization of the latter. These chapters include an introduction that is intended to support the ideas behind the work and results presented. Chapter 6 summarizes the efforts made as part of this thesis and identifies the most important achievements of the latter.

2. EXPERIMENTAL

2.1 MATERIALS

All chemicals and solvents were high purity (98% or better), reagent, or HPLC-grade, and were used as received unless otherwise specified. Cell culture grade water (H_2O_c), ammonium hydroxide (NH_4OH), dichloromethane (CH_2Cl_2), 1,4-dioxane, ethyl acetate (EtOAc), and isopropanol (IPA) were obtained either from Fisher Scientific or from its fine chemicals division, Acros Organics (Pittsburgh, PA). 1,2-dichloroethane, acetonitrile (CH_3CN), *N*-methylpyrrolidone (NMP), toluene, pyridine, *N*-ethylmorpholine (*N*-EtMo), triethylamine (TEA), tri-*N*-butylamine (TBA), *N,N*-diisopropylethylamine (DIPEA), hydrochloric acid 37% (HCl), trifluoroacetic acid (TFA), 1-hydroxybenzotriazole hydrate (HOBt), poly(ethylene glycol) MW = 1,000 $gmol^{-1}$ (PEG_{1k}), 3-(4-hydroxyphenyl)propionic acid (D acid *or* DAT), 4-hydroxyphenylacetic acid (H acid), 4-hydroxybenzoic acid (B acid), 4-hydroxycinnamic acid (C acid), (4-hydroxyphenoxy)acetic acid (P acid), *N*-(4-hydroxyphenyl)glycine (G acid), and benzyl chloroformate (Cbz-Cl) were obtained from Sigma-Aldrich (St. Louis, MO). Tetrahydrofuran (THF) and *N,N*-dimethylformamide (DMF) were obtained from VWR (West Chester, PA). Ethylene glycol and chlorobenzene were obtained from MP Biomedicals (Solon, Ohio). Some solvents and reagents were dried under molecular sieves overnight before their use: CH_2Cl_2, pyridine, toluene, 1,2-dichloroethane and PEG_{1k} in CH_2Cl_2 (4A sieves), and THF and 1,4-dioxane (5A sieves). Tyrosine ethyl ester hydrochloride (TE•HCl) was obtained from Tanabe USA (Marlboro, NJ). Tyrosine *tert*-

butyl ester (T*t*Bu) was obtained from Bachem Bioscience (King of Prussia, PA). Ethyl-3-(3-dimethylamino)propyl carbodiimide hydrochloride salt (EDC•HCl) was obtained from Kawaguchi Chemical (Tokyo, Japan). Bis(trichloromethyl)carbonate or triphosgene (TP) was obtained from Fluka Chemicals (St. Louis, MO).

Warning: Triphosgene is extremely toxic and should be handled with care and only in suitable fume hoods.

2.2 INSTRUMENTATION

2.2.1 Nuclear Magnetic Resonance (NMR)

Proton NMR spectroscopy (^{1}H-NMR) was performed with a Varian VNMR spectrometer at 300, 400, or 500 MHz. Deuterated solvents, either chloroform-*d* ($CDCl_3$) or (methylsulfoxide)-d_6 (DMSO-d_6), were purchased from Acros Organics (Pittsburgh, PA) or from Sigma-Aldrich (St. Louis, MO), and were used as received. The concentration used for small molecules was 7.5-15 mg/mL, while the concentration used for macromolecules was 15-30 mg/mL. The number of scans per molecule ranged from 16 to 256, with an average of 64 for all the compounds that were analyzed by this method. All runs were performed at room temperature (RT).

2.2.2 Gel Permeation Chromatography (GPC)

Gel Permeation Chromatography (GPC) was performed with a 5 μm gel pre-column and two PL Columns with a pore size of 10^3-10^5 Å (Polymer Labs) on a Waters 510 HPLC unit equipped with a Waters 410 Differential Refractometer. Samples were prepared by dissolving 5-10 mg of the polymer sample in 0.75-1.0 mL of *N,N*-dimethylformamide (DMF) containing 0.1% trifluoroacetic acid (TFA). The column temperature for all runs was kept at 35 °C. The mobile phase and flow rate were DMF/0.1% TFA at 0.8 mL/min. Molecular weights (number and weight average) and polydispersity indices (PDi) were determined relative to polystyrene calibration standards.

2.2.3 Differential Scanning Calorimetry (DSC)

Thermal analyses were performed either on a TA Instruments DSC 2920 or on a Mettler Toledo DSC823^e unit equipped with a TSO801RO sample robot. A typical run used to determine glass transition temperatures (T_g) is described in Table 2.1. The second heating cycle was used to calculate T_g. Sample preparation involved 2-5 mg of polymer crimped between an aluminum pan and an aluminum lid.

Table 2.1 Typical DSC experiment used to determine the T_g of a polymer sample

Step	Description
1	Equilibrate to −20 °C
2	Ramp from −20 °C to 160 °C at 10 °C/min
3	Equilibrate at 160 °C
4	Jump to −20 °C
5	Equilibrate at −20 °C
6	Ramp from −20 °C to 200 °C at 10 °C/min

Two runs were needed in order to determine purity by means of melting point depression. The first one was a standard ramp from RT to 200 °C at 10 or 15 °C/min used in order to determine the peak max temperature, T_p, of the curve, which is very close to the actual melting point, T_m, of the sample. The typical sample used consisted of 0.5-1.5 mg crimped between an aluminum pan and an aluminum lid. The second run is described in Table 2.2:

Table 2.2 Typical DSC experiment used to determine the purity of a monomer sample by means of melting point depression

Step	Description
1	Equilibrate to −20 °C
2	Ramp from −20 °C to T_p−20 °C at 10 °C/min
3	Equilibrate at T_p −20 °C
4	Ramp from T_p −20 °C to T_p +20 °C at 1 °C/min
5	Equilibrate at T_p +20 °C
6	Ramp from T_p +20 °C to 250 °C at 10 °C/min

2.2.4 High Performance Liquid Chromatography (HPLC)

High Performance Liquid Chromatography (HPLC) analysis was performed at 25 °C with a reversed-phase (RP) C18 column (33 mm × 4.6 mm, Perkin-Elmer Brownlee Analytical) on a Waters 2695 HPLC unit equipped with a dual absorbance UV/VIS detector at 220 nm (Waters 2487). A gradient of H_2O:CH_3CN (both with 0.1% TFA) was used as a mobile phase at a flow rate of 1.0 mL/min, as explained in Table 2.3. Samples were prepared by dissolving 3.0 mg of the monomer in 2.5 mL of CH_3CN/0.1% TFA and then adding 7.5 mL of H_2O/0.1% TFA to that solution. Approximately 2 mL of the prepared solution were filtered through a 0.45 μm PTFE syringe filter (Whatman, Florham Park, NJ) before injection.

Table 2.3 HPLC gradient flow used for monomer characterization

Time, min	H_2O, %	CH_3CN, %
0-15	95	5
15-20	20	80
20-21	0	100
21-25	95	5

2.2.5 Analysis of Monomer Solubility in Phosphate Buffer Saline with HPLC

Monomer solubility was assessed with a chromatographic/spectroscopic method at 25 °C, using the instrument described in Section 2.2.4. As a first step, saturated solutions were prepared by weighing 20 mg of the monomer and adding 2 mL of Phosphate Buffer Saline (PBS). Each monomer solution was vortexed for two hours, after which 1 mL was filtered through a 0.45 µm PTFE syringe filter before injecting 5 µL into the HPLC. As a second step, 5 mg of the monomer to be analyzed were dissolved in 2 mL of HPLC-Grade methanol, and were then filtered. Three solutions from this stock were prepared by diluting 200, 100, and 50 µL to 1 mL with methanol. These standards were analyzed in duplicate by injecting 5 µL of each solution into the HPLC, and a calibration curve was built from this data (for each monomer) for the calculation of the monomer's solubility.

2.2.6 Mechanical Testing

For mechanical testing, 200 µm compression molded films pressed at 70 °C above T_g and cut into a "mini" dog-bone shape were used. The dimensions of the "mini" dog bone are shown in Figure 2.1. The benefits of using this shape consisted of limiting material use and of focusing the load on the center of the film. A Sintech 5/D mechanical tester (MTS Systems Corp.) was used for all mechanical tests. Testing was performed at a rate of 7 mm/min, with a pre-load of 10 mm/min, using a 100 N load cell. The tensile modulus, yield, and failure point were reported for an average of at least 3 samples at ambient conditions and after an incubation period of 24 h in PBS 37 °C.

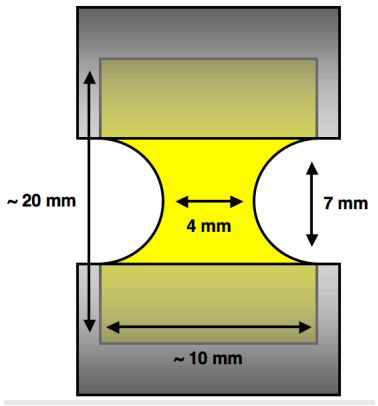

Figure 2.1. Dimensions of "mini" dog bone used for tensile testing.

2.2.7 Spin Coating of Polymer Solutions

Glass cover slips (with a 15 mm diameter) from Fisher Scientific were cleaned using a process that involved a sequence of solvents (EtOAc, Acetone, 99% EtOH, and

CH_2Cl_2) and sonication in a water bath for 15 minutes per solvent. The glass cover slips were kept in CH_2Cl_2 for storage purposes and were dried with nitrogen before use. The polymer solutions used (2% w/v) were prepared with one of the following solvents, in the order of preference indicated: THF > CH_2Cl_2 > $CHCl_3$ > Dioxane > 5% MeOH in CH_2Cl_2. All solvents were dried with 4A or 5A molecular sieves before use. The polymer solutions were filtered with a 0.45 μm PTFE membrane filter with a syringe before use. The cover slips were spin coated with a spin coater (Headway Research, Inc. TX) placed inside a humidity control chamber at a RH of 15% or less. For the spin coating process, 80-100 μL of solution were placed in the center of the cover slip and then spun for 30 seconds at 4,000 rpm. All coated cover slips were placed in a heated vacuum oven at 40 °C for at least 12 hours before use.

2.2.8 Goniometry

Air-water static contact angles were measured at RT and 40-50% relative humidity (RH) on an NRL contact angle goniometer, model 250 (Ramé-Hart Instruments), equipped with a camera and a computer interface. For each experiment, a drop (5-10 μL) of the liquid probe (e.g., H_2O_d, ethylene glycol or chlorobenzene) was placed on the substrate (i.e., spin-coated polymer on glass) and an image was captured after 30 seconds. The left and right contact angles were measured for each drop by using DROPimage Advanced software. At least three drops of each probe liquid were used for each polymer substrate that was analyzed.

2.2.9 Scanning Electron Microscopy (SEM)

Surface analysis was conducted with an Amray 1830-I Scanning Electron Microscopy (SEM) unit with an acceleration potential of 10kV at various magnifications. Samples (i.e., spin-coated on glass or pressed films) were mounted on aluminum studs with adhesive and then coated with gold and palladium using a Blazers SCD004 sputter-coater at 0.05 mbar and 30 mA for 120 seconds before imaging.

2.2.10 Human Mesenchymal Stem Cell (hMSC) Culture

Poietics® human mesenchymal stem cells (hMSCs) were acquired from Lonza Walkersville, Inc. (Walkersville, MD) at passage number two. Following the manufacturer's instructions, the hMSCs were subcultured to no more than five passages in Mesenchymal Stem Cell Basal Medium (MSCBM), from Lonza Walkersville, Inc., supplemented with L-Glutamine, Pen/Strep, and hMSC SingleQuots® media supplements. Before the cell seeding process, a 24-tissue culture polystyrene (TCPS) well plate from Corning Inc. (Corning, NY) was prepared by placing a UV-sterilized spin-coated cover slip on each well and subsequently securing each coated cover slip with a Class VI Silicone O-ring from Molding Solutions (Lexington, KY). Four wells were used for each substrate, and empty wells with just the O-rings were used as controls. The hMSCs cell density was normalized to 5,000/cm^2. Cells were cultured in direct contact with the substrates for 3, 7, and 14 days in either basal or osteogenic-inducing media from Lonza (i.e., supplemented basal medium plus dexamethasone, L-Glutamine,

ascorbate, Pen/Strep, MCGS, and β-Glycerolphosphate). Cells were fed every 3 days as part of a standard protocol.

2.2.11 Cell Fixing and Staining

The cell culture supernatant was removed from the wells at pre-designated time points, and the corresponding cells were washed twice with PBS solution containing calcium and magnesium from Hyclone Laboratories, Inc. (Logan Utah). After the washing supernatant was removed, the cells were fixed with formalin for 10 minutes. Following the fixing step, the cells were washed twice with PBS without calcium or magnesium and then Hoechst 33258, pentahydrate (bis-benzimide)- and Phalloidin-stained (1:500 and 1:200 respectively) for 10 minutes in the dark in order to image the nucleus and the F-actin filaments. Before imaging, the cells were washed twice with PBS without calcium or magnesium and stored with 200 μL of PBS for each well.

2.2.12 Fluorescence Microscopy

A Zeiss Observer D1 Fluorescence microscope from Carl Zeiss Imaging Solutions (Munich, Germany) was used to image the cells' nuclei and F-actin filaments. The microscope was equipped with 4',6-diamidino-2-phenylindole (DAPI) and Green Fluorescence Protein (GFP) filters. All images obtained were taken at 20X and were captured with AxioVision Software, Version 4.6.3.0 (Carl Zeiss Imaging Solutions). The

nuclei count was obtained through image analysis with Image J, Version 1.37 (National Institutes of Health). For each substrate n = 4. The values used for the nuclei count were among the 35th to the 65th percentile (i.e., three values above and below median and the median itself) in order to account for outliers.

2.3 SPECIAL EQUIPMENT

2.3.1 Automated Parallel Synthesizer

For the synthesis of polycarbonates, an Accelerator SLT-100 parallel synthesizer from Chemspeed Technologies AG (Augst, Switzerland) was used. A schematic overview of the platform configuration is illustrated in Figure 2.2. The synthesizer's platform was equipped with various (1-6) reactor blocks, each holding 16 jacketed reactors (16 to 96 effective reaction vessels of 13 mL each) or 4 non-jacketed reactors of 100-mL each. The reactor blocks were connected to an argon line and a vacuum pump. The jackets of the reactors were in turn connected to a Huber Unistat Tango (Offenburg, Germany) unit: a hydraulically-sealed circulator capable of cooling or heating the reactors within a temperature range of -45 to 250 °C. The reactor platform was equipped with a stock solution rack, in which the monomer solutions or solvents that were dried over molecular sieves were contained under inert conditions. Agitation was performed by means of vortex mixing at a rate of 800 rpm. An 8-mL vial holder was used to support the vials with solutions used in smaller-scale amounts (PEG_{1k} and DT*t*B), as well as the

triphosgene and the triphosgene quencher (10% triethylamine in ethanol). All 8-mL vials, with the exception of the vials containing the triphosgene quencher, were equipped with pre-cut Teflon-lined septa to allow volatiles exchange during solution transfers; the triphosgene quencher vials, in the meantime, had regular septa. Liquid transfers were handled by using a 4-needle head (4-NH). The 4-NH was equipped with four fluorosilane-coated needles and was supplied via Teflon tubing by a 4-dilutor/syringe-pump system: 25-mL, 10-mL, and 2×1-mL. The dilutors were connected to different reservoir solvent bottles in order to rinse the needles and the tubing after each liquid transfer: 1,2-dichloroethane; 10% pyridine in 1,2-dichloroethane and a separate line for acetone; and toluene, respectively. Table 2.4 shows common dispensing and aspirating rates for each dilutor. Two rinsing stations were used within the synthesizer hood in order to segregate waste and to prevent any contamination or quenching of reagents.

Table 2.4 Common aspiration and dispensing rates for dilutors

Step	25-mL	10-mL	1-mL
Aspirate (mL/min)	10	5	2
Dispense (mL/min)	5	5	2

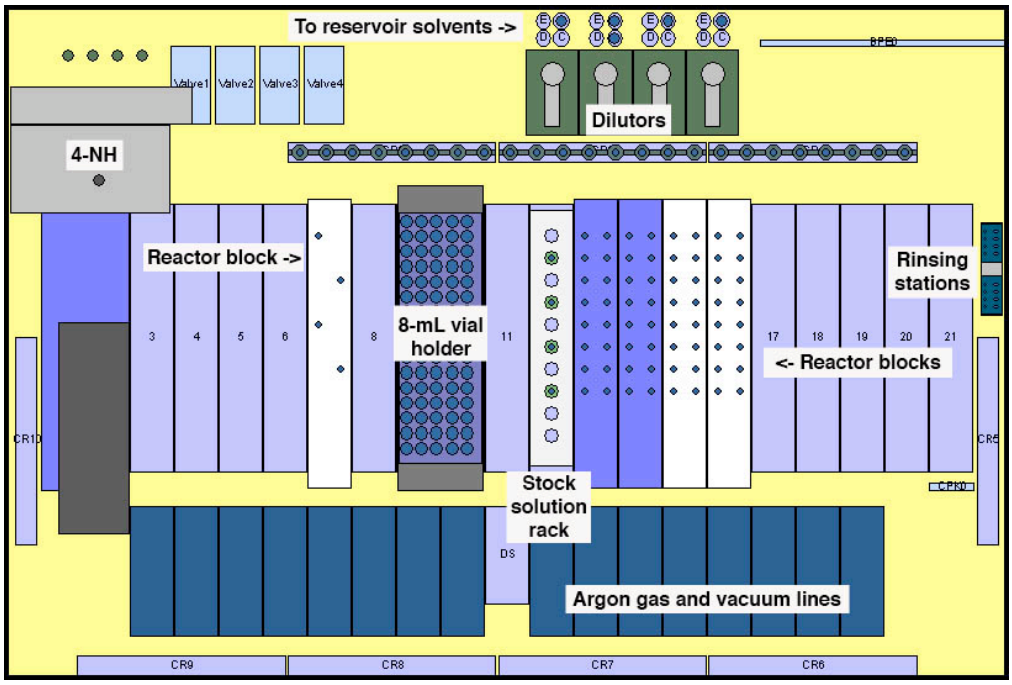

Figure 2.2 Layout used in the automated parallel synthesizer

2.4 PROCEDURES

A note on the nomenclature used: All tyrosine-derived monomers are diphenols derived from a phenolic acid (see 2.1 Materials for synthesis) and a tyrosine alkyl ester (TR). The nomenclature used for the diphenol comes from the specific phenolic acid used and the pendent ester R group of the tyrosine unit. For example: **DTE** monomer is desaminotyrosyl-tyrosine ethyl ester (**D** for desaminotyrosine, **T** for tyrosine and **E** for the ethyl ester). There are three pendent ester R groups used in this thesis: **E**thyl (short pendent chain), **H**exyl (medium pendent chain) and **D**odecyl (long pendent chain).

2.4.1 Generic Monomer Synthesis

The monomers were synthesized using a previously published procedure[88] with some modifications. However, the monomers derived from *N*-(4-hydroxyphenyl)glycine were an exception and were synthesized with a different procedure, since they required the amine to be protected before the peptide coupling as explained below. The reagents' molecular weights and molar equivalents for the reactions described in this section are shown in Table 2.5. Following is a representative monomer synthesis procedure that in this case uses a scale starting with 25 g of the phenolic acid:

The tyrosine alkyl ester (1.05 eq), the phenolic acid (1.0 eq), the HOBt (0.10 eq), and 150 mL of THF were placed in a 1 L round-bottom flask equipped with overhead stirring and cooled to 5 °C with an ice-water bath. After the contents of the flask were mixed homogeneously (15-45 minutes), the EDC•HCl was added together with 50 mL of THF, and the mixture was stirred for one hour at 5 °C and then at room temperature until completion (2-4 hours). The reaction was quenched with 600 mL of distilled water (H_2O_d) when a single peak was detected by HPLC. The reaction was stirred until the product separated as oil. The aqueous phase containing THF, unreacted base, and urea formed from the peptide coupling was decanted and the corresponding work-up followed.

Table 2.5 Molecular weights and molar equivalents for reagents

Reagents	**MW ($gmol^{-1}$)**	**Equivalents used**
Tyr-Ethyl ester•HCl	245.70	1.05
Tyr-Hexyl ester	265.35	1.05
Tyr-Dodecyl ester	349.51	1.05
Tyr-*tert*-Butyl ester	237.30	1.05
D acid / DAT	166.17	1.00
H acid	152.14	1.00
B acid	138.12	1.00
C acid	164.16	1.00
P acid	168.14	1.00
Cbz-G or Z-G acid	301.29	1.00
HOBt	135.12	0.10
EDC•HCl	191.70	1.05
TEA	101.19	1.05
TEA density	$\rho = 0.726\ gmL^{-1}$	

2.4.2 Extra Steps for the Synthesis of Tyrosine-Ethyl Ester Diphenols

Since TE•HCl was used for the synthesis of diphenols containing an ethyl ester pendent chain instead of the free base, the synthesis required deprotection of the amine from the hydrochloride salt *in situ*. For the deprotection stage, triethylamine (1.05 eq) was added, drop-wise, and stirred for 15 minutes before the addition of the EDC•HCl. No further modifications were made to the generic synthesis method.

2.4.3 Monomers Containing *N*-(4-Hydroxyphenyl)glycine

Before peptide coupling, the amine from the *N*-(4-hydroxyphenyl)glycine (G acid) was protected with a Cbz group. The G acid (55 g, 0.329 mol) was added to a 3 L round-bottom flask equipped with an overhead stirrer, and was then dissolved with 275 mL of NMP. Cbz-Cl (50.1 mL, 0.352 mol) was added, drop-wise, to this solution while stirring over a period of 40 min. The solution was stirred overnight and quenched with 100 mL H_2O_d. Precipitation was carried out by the addition of water until the cloud point was reached, which was followed by storage at 4 °C for 24 hours. Recrystallization was done in warm ethanol, followed by drying under vacuum at 40 °C overnight. No further purification was needed.

2.4.4 Work-Up after Peptide Coupling

The oil was dissolved in 500 mL ethyl acetate and then washed sequentially with 2×200 mL 0.4 M HCl, 2×200 mL 0.5 M sodium bicarbonate ($NaHCO_3$) and 2×100 mL saturated sodium chloride (NaCl), ~20% w/v solutions. The organic layer was then mixed with 2.5 g magnesium sulfate ($MgSO_4$) in order to remove all water, and with 2.5 g of powdered activated charcoal to remove any color. The mixture was filtered through fluted filter paper. The filtrate was then roto-evaporated to a viscous oil and then dried overnight under vacuum. In the event that a solid was not formed after roto-evaporation or after vacuum drying, crystallization was induced through mechanical stirring of the oil

in hexane or in H_2O_d. The precipitate was further dried under vacuum and characterized by ^{1}H-NMR, HPLC, and DSC (purity by melting point depression).

2.4.5 Manual Polymer Synthesis

Warning: Triphosgene is extremely toxic and should be handled with care and only in suitable fume hoods.

The monomer(s) were solubilized in pyridine/CH_2Cl_2 (3.45 equivalents of pyridine/equivalent of monomer) to a final concentration of 10% (w/v) in a 50-mL round bottom flask equipped with a magnetic stir bar. The approximate surface area for the type of flask used was around 9,000 mm^2, while for the reactors used for automated synthesis it was around 5,000 mm^2. The flask was closed with rubber septa and connected to a dual-syringe infusion pump through a Teflon tube. The triphosgene solution in CH_2Cl_2 (20% w/v, 1.15 phosgene equivalents/equivalent of monomer) was delivered, drop-wise, to the reaction with the syringe pump over 45 - 60 min. The reactions were stirred an additional 45 minutes prior to quenching with 25% of the total reaction volume of a THF:H_2O_d (7:3) solution. Two polymers could be synthesized in parallel by this method.

2.4.6 Automated Polymer Synthesis

Warning: Triphosgene is extremely toxic and should be handled with care.

A phosgene detector (TLD-1 Toxic Gas Detector, Zellweger Analytics) was installed in the hood of the automated synthesizer so that the absence of phosgene could be verified at the end of the reaction (prior to opening the robot's hood to the laboratory). Additionally, a vial (8-mL) containing NH_4OH and sealed with septa, and an empty and uncapped vial (8-mL) for transferring the ammonia, were placed in the instrument in the event that any residual phosgene in the air space of the hood (from the triphosgene breakdown) needed to be quenched. The remaining, unused triphosgene solution was quenched with 3X the volume of 10% triethylamine in ethanol, as explained below.

A 0.45 M stock solution of main diphenol monomer in pyridine/CH_2Cl_2 (3.45 equivalents of pyridine/equivalent of monomer) was prepared. For copolymers with *tert*-butyl containing monomers, a 0.15 M stock solution was prepared with DT*t*B in pyridine/CH_2Cl_2 similar to that in the principal monomer solution. For copolymers with PEG_{1k}, a 0.02 M stock solution was prepared in CH_2Cl_2. The automated steps for the polymerization are described in Table 2.6. In summary, the monomer(s) stock solution is transferred to jacketed reactors equipped with septa and diluted to a total volume of 3.6 mL using fresh CH_2Cl_2. The reactors were vortexed at 800 rpm at RT. A stock solution of triphosgene in toluene (10 wt%, 0.9 mL, 90 mg, 0.33 M equivalents of phosgene) was dispensed to each reactor, with (2) 1-mL syringes equipped with ceramic-coated needles, at a flow rate of 50 µL/min. After the addition, the reactions were vortexed for 45-60 min

at RT and quenched with 1.5 mL of a THF/H_2O_d (7:3) solution. Up to 96 polycarbonate reactions could be synthesized in about 48 hours using this method.

Table 2.6 Protocol for diphenol polycondensation with triphosgene in SLT-100 automated parallel synthesizer

Step	Task	Description
1	Inertization	Macro task
2	Primelines (25 mL syringe)	Macro task
3	Primelines (10 mL syringe)	Macro task
4	Primelines (1 mL syringes)	Macro task
5	Transfer liquid	From monomer 'n' stock to zone reactors
6	Transfer liquid	From monomer 'n_i+1' stock to zone reactors
7	Transfer liquid	From CH_2Cl_2 stock to zone reactors
8	Vortex	Agitation ON (800 rpm) on zone reactors
9	Waiting	Mixing solutions for 5 minutes
10	Polycondensation n	Macro task
11	Polycondensation n_i+1	Macro task
12	Primelines	Primelines of 1-mL dilutors every five Polycondensation tasks
13	Transfer liquid	From triphosgene quencher to triphosgene vials
14	Primelines	Macro task (all syringes)
15	Shut down	Shut down thermostat, vortex and park 4-NH

An important aspect of the program is the macro task, or Macro, which embeds a set of instructions in an abbreviated format. Different macro tasks can be programmed in

order to create a robust workflow with minimum error. The macro tasks used for this workflow are described in Tables 2.7 – 2.9, shown below.

Table 2.7 Steps for the Inertization macro task

Step	Sub-step	Task	Description
1		Set drawer on reaction block	Close zone reactors under vacuum
2		Set vacuum	Vacuum ON on zone reactors (0 mbar)
3		Macro task (Cycle of inertization)	Loop 3 times
	3.1	Heating/Cooling	Thermostat ON (140 °C) on zone reactors
	3.2	Vacuum/Waiting	System under vacuum for 15 minutes
	3.3	Set drawer on reaction block	Close zone reactors under inert gas (argon)
	3.4	Waiting	Purge zone reactors with inert gas for 1 minute
	3.5	Set drawer on reaction block	Close zone reactors under inert gas
4		Cooling	Thermostat ON (25 °C) on zone reactors
5		Vacuum/Waiting	System under vacuum for 10 minutes
6		Vacuum	Vacuum OFF on zone reactors
7		Set drawer on reaction block	Close zone reactors under inert gas
8		Heating/Cooling	Thermostat OFF on zone reactors

Table 2.8 Steps for the Polycondensation macro task

Step	Task	Description
1	Transfer liquid	From triphosgene solution to reactions x and y
2	Waiting time	Set reaction time for 45 minutes
3	Transfer liquid	From reaction quencher to reactions x and y

Table 2.9 Steps for the Primelines macro task

Step	Task	Description
1	Transfer liquid	Transfer liquid to waste ports at programmed volumes and aspiration/dispensing rates. Loops at least twice.

Each macro task features a series of variables that have to be specified when adding the macro task as a step, making macro tasks a very flexible tool for the overall workflow. An example of the variables that can be specified, and their corresponding units (if applicable), is shown in Table 2.10 for the Polycondensation macro task.

Table 2.10 Variables in Polycondensation macro task

Variable	Unit
Triphosgene location	Zone
Reaction location	Zone
Quencher location	Zone
Volume of triphosgene	mL
Volume of reaction quencher	mL
Aspiration rate of triphosgene	mL/min
Dispensing rate of triphosgene	mL/min
Aspiration rate of quencher	mL/min
Dispensing rate of quencher	mL/min
Cycles of triphosgene addition	N/A
Timer set	min

2.4.7 Work-Up after Polycondensation

For automated parallel synthesis, the work-up procedure involved the following steps:

a) Transfer quenched polymer solution by disposable polyethylene transfer pipet (Fisher Scientific) from reactor to 20-mL scintillation vial (Wheaton).
b) Add ~14 mL of IPA in order to induce polymer precipitation.
c) Shake gently for 1-2 min on a Gyratory Shaker, Model G2 (New Brunswick Scientific Co., Inc).
d) Decant solvent mixture containing pyridine hydrochloride salt and low-MW fractions (i.e., pseudo-fractionation and purification).
e) Redissolve polymer by adding 2-3 mL of THF (or CH_2Cl_2 if polymer not soluble in THF).
f) Reprecipitate polymer with H_2O_d (or IPA if polymer was dissolved in CH_2Cl_2).
g) Shake gently for 5-10 minutes.
h) Decant solvent and vent-dry overnight inside the hood.
i) Dry under vacuum at 30-40 °C for 24 hours.

A second precipitation allows for further purification of the polymer and, in the case of water-based work-ups, offers the possibility of using lyophilization instead of regular drying under vacuum. This is especially important for polymers with a low T_g

that can become rubbery at the temperature used in the vacuum oven and as a result become difficult to handle physically.

2.4.8 Acid-Based Cleavage of *tert*-Butyl Ester Side Chain in Polycarbonates

Acid-based ester cleavage or acidolysis is used for the removal of the *tert*-butyl ester side chain in order to obtain a free-carboxylate. The dry polymer is dissolved in 4X (w/w) CH_2Cl_2, and 2X of neat TFA is added. The solution is then stirred for 4-8 h, after which precipitation is effected in IPA. After precipitation, the solution is decanted and the polymer is redissolved in 6X THF (w/w) and precipitated in H_2O_d in order to remove any excessive TFA. After this second precipitation, the solution is decanted and the polymer is lyophilized after freezing. For selected polymers, *tert*-butyl ester cleavage was confirmed by ^{1}H-NMR.

2.4.9 Statistical Analysis

Statistical significance was calculated using the one-way analysis of variance (One-way ANOVA), with a *post-hoc* Tukey's Honestly Significant Difference analysis (Tukey HSD) when needed (KaleidaGraph Software, Synergy Software, Reading PA). To indicate statistically significant differences in the data, P values < 0.05 were used.

3. NOVEL DIPHENOLIC MONOMERS DERIVED FROM NATURAL METABOLITES OR METABOLITE-ANALOGS

3.1 INTRODUCTION

All synthetic and degradable polymeric biomaterials have specific requirements for specific applications. In principle, and seen from a design perspective, some of a biomaterial's properties are more relevant to certain applications (e.g., high strength for vascular stent devices), while others have a universal degree of importance (e.g., biocompatibility). At the same time, it is true that, while a single material might be suitable for many applications, several other materials might also be suitable for the same application. Therefore, a proper "design" will identify the material that is best suited to a given application. Most of the biomaterial's properties will come from the final polymer and its processing, but, in the case of temporal therapeutic devices, the design has to take degradation products into consideration, since their effect on the human body will be different from that of their polymeric matrix. Michel Vert, from the Montpellier 1 University (Montpellier, France), has described "artificial biopolymers" as biocompatible, degradable (and/or biodegradable) polymers that are composed of non-toxic pro-metabolite repeating units that, upon degradation, can be inserted into biochemical pathways and/or eliminated via the kidney route.[89] The most representative example of this type of artificial biopolymer is poly(glycolic acid), the simplest of the poly(α-hydroxy acid)s, which was the first synthetic degradable polymer to be developed as a suture in the 1960s.[2, 90] The basic principle behind creating

artificial biopolymers is to take bifunctional or multifunctional metabolites or metabolite-analogs (such as hydroxy acids, vitamins, or amino acids) present in biochemical pathways and to use them to synthesize polymers with non-natural, chemically degradable backbones.[91, 92] The objective is to promote engineered/controlled degradation and resorption of temporary medical devices without any cytotoxic effects. A few researchers have already used this principle in order to use natural metabolites to synthesize polymeric biomaterial candidates. A couple of examples from two groups will be discussed next.

Vert and colleagues reported on the creation of a monomer composed of a glycolyl and a D-gluconyl unit derived form gluconic acid, namely 3-(1,2,3,4-tetraoxobutyl-diisopropylidene).[93] This monomer allowed the researchers to create copolymers with lactide and glycolide with aliphatic hydroxyl groups in the side chains and, as a result, to increase the chemical variability of traditional degradable polymers used in medical devices. The presence of these aliphatic hydroxyl functional groups allowed them to bind different compounds, such as dyes and poly(ethylene glycol), to the main polymer chain. Also, they were able to crosslink these compounds by using difunctional metabolites such as succinic and maleic acids. Vert's group has also synthesized aminated aliphatic polyesters derived from L-serine, L-lysine, and citric acid as polyelectrolytes for drug solubilization and delivery applications.[94]

As an alternative to industrial diphenols such as Bisphenol-A, Kohn's group developed monomers derived from L-tyrosine, one of the 21 essential amino acids.[95] The most studied monomers belonging to this type of compounds are desaminotyrosyl-tyrosine alkyl esters (DTRs) consisting of a unit of L-tyrosine alkyl ester and its

metabolite, desaminotyrosine, i.e., 3-(4'-hydroxyphenyl)propionic acid.[88] This type of synthetic monomer is similar to a dipeptide of L-tyrosine, but with two important modifications: The C-terminus is replaced/protected by an alkyl ester pendent chain, and the N-terminus is replaced with hydrogen.[88, 95] DTR monomers have been polymerized into polycarbonates, polyarylates, and polyethers for multiple potential applications.[96] The reasoning behind the synthesis of these types of polymers is partially related to the hydrolysable bonds in the backbone of these materials (i.e., carbonate, ester, ether) and the ester pendent chains. After degradation to the corresponding monomeric unit, it is expected for the diphenol (or dimers, trimers, etc.) to be excreted through the kidney or enzymatically degraded into the starting materials inside the body.[95] After performing different studies on these compounds, it was observed that small changes in the chemical composition of the polymers (i.e., pendent chain, mol% of PEG in copolymers, type of diacid in polyarylates) can have a significant impact on tissue-implant interactions *in vivo* and also on cell-material interactions *in vitro*.[11, 96-101] While the changes in the backbone of these polymers have been explored in a library of polyarylates,[11, 12] mostly by changing the type of diacid used for the corresponding syntheses, they have been largely unexplored in polycarbonates.

This chapter will discuss the design and synthesis of novel diphenolic monomers and will describe the corresponding sources as part of a design strategy based on the concept of artificial biopolymers (as reported by Vert). The characterization of these structurally related monomers will also be described and discussed in detail.

3.2 RESULTS AND DISCUSSION

3.2.1 Selection Criteria for Phenolic Acids Intended for the Synthesis of New Monomers

Kohn's group has reported on the synthesis and subsequent polymerization of several diphenolic monomers.[11, 88, 96, 101] This process has included the modification of the ester pendent chain to incorporate linear alkyls (e.g., methyl, ethyl, butyl, hexyl, octyl, and dodecyl), branched alkyls (e.g., isopropyl, isobutyl, *sec*-butyl), an aromatic ester pendent chain (i.e., benzyl), and an ester pendent chain containing oxygen, i.e., 2-(2-ethoxyethoxy)ethyl.[11, 12] Kohn's group has also reported on minor modifications to the backbone, namely the peptide coupling of a tyrosine alkyl ester with either 3-(4-hydroxyphenyl)propionic acid (D acid *or* DAT) or 4-hydroxyphenylacetic acid (H acid).[12] The difference between these two compounds is the number of methylene units (two for DAT and one for H acid) between the phenyl ring and the carboxylic acid. Although this small change can have an effect on the physical and chemical properties of the material (e.g., tensile modulus, solubility), the difference between the polymers derived from these two diphenol monomers has not been studied in detail. While several reports on the effect of changing the alkyl length as part of the pendent chain in polycarbonates have been made, including *in vivo* studies (such as the canine bone chamber model[99] and the implantation of pins in the proximal tibia and distal femur of rabbits[97]), the effect of structural changes in the backbone of tyrosine-derived polycarbonates has not been addressed. This, however, can add another dimension to the design and development of novel biomaterials and is thus of importance

to this thesis.

In order to extend the family of tyrosine-derived diphenols by modifying its backbone, the following criteria were used in order to select the diphenols to be synthesized:

- Commercially available phenolic acids were selected where economically feasible.
- These phenolic acids had to be natural metabolites, metabolite-analogs, and/or had to be included in any or all of the following listings: the American Food and Drug Association's Generally Recognized As Safe (FDA's GRAS) listing; food additives approved by the FDA; Priority-Based Assessment of Food Additives (PAFA) listing, also known as the "Everything" Added to Food in the United States (EAFUS) listing, maintained by the FDA.[102-105]
- The chemical structures selected had to be chemically adaptable for both the peptide coupling reaction with a tyrosine-alkyl ester and the subsequent condensation reaction with phosgene or a phosgene equivalent (i.e., triphosgene), as well as for the deprotection reaction of the *tert*-butyl ester pendent chain (i.e., acidolysis).
- It was extremely important for the final tyrosine-derived diphenols to be structurally related in order to make it possible to obtain structure-property relationships for the derived polycarbonates, therefore making it possible to successfully assess the polymer design space.

A range of phenolic acids was chosen on the basis of these selection criteria, and a summary of the corresponding properties and sources is provided next. Most phenolic acids that are analogs to the aromatic amino acids (i.e., tyrosine, phenylalanine, and tryptophan) are synthesized through the "shikimate pathway" in plants.[106, 107] The shikimate pathway links the carbohydrate metabolism in plants, and some bacteria, to the synthesis of aromatic compounds through seven metabolic steps, starting from the condensation of phosphoenlopyruvate and erythrose 4-phosphate, in order to obtain chorismate, which is a precursor of the three aromatic amino acids and other aromatic secondary metabolites.[106, 108] These other aromatic secondary metabolites include the cinnamates, which in turn are precursors to the biosynthesis of lignin, i.e., the structural material of a cell's walls in plants.[108-110] Recently, several phenols and phenolic acids derived from plants and herbs have attracted public and scientific interest because of their potential antioxidant properties and the associated health benefits.[111] These compounds include 3-(4-hydroxyphenyl)propionic acid, 4-hydroxybenzoic acid, and 4-hydroxycinnamic acid, which are relevant compounds in terms of the peptide coupling with L-tyrosine derivatives studied in this thesis. These compounds have been identified in several plants and fruits, and their antioxidant effect has been analyzed in some cases.[108, 112-116] Of the potential candidates that were commercially available, six phenolic acids, shown in Figure 3.1, were selected for synthesizing the monomers.

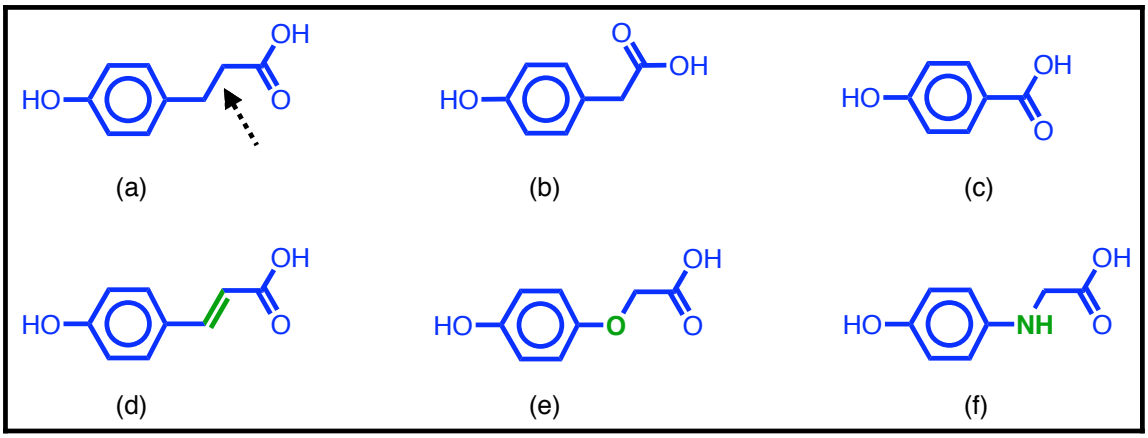

Figure 3.1 Phenolic acids used for the synthesis of tyrosine-derived diphenols; (a) 3-(4-hydroxyphenyl)propionic acid, (b) 4-hydroxyphenylacetic acid, (c) 4-hydroxybenzoic acid, (d) 4-hydroxycinnamic acid, (e) (4-hydroxyphenoxy)acetic acid, (f) *N*-(4-hydroxyphenyl)glycine; the arrow points at the point of the structural change modification

The non-hydroxylated forms of compounds (a), (b), (d), and (e) are listed in the FDA's EAFUS listing, while (c) appears as is. Compound (f) has not been reported as a food ingredient or a derivative of plants, but its use could potentially lead to polymeric compounds with reactive functional groups.

The fact that some of these compounds are not only present in the walls of cells in plants, but have also been used for therapeutic applications, is of particular relevance.[112, 117-120] 3-(4-hydroxyphenyl)propionic acid, or D acid, was found in the product obtained from the digestion of maize with rumen fluid, indicating its presence as part of the cell wall's lignin-carbohydrate complexes.[121, 122] It also has been identified as a potential anti-inflammatory phenolic compound in blueberries.[118] Meanwhile, 4-hydroxyphenylacetic acid, or H acid, has been found to be one of ten phenolic compounds in mangosteen fruit, *Garcinia Mangostana*, as reported by Naczk and colleagues.[123] 4-hydroxybenzoic acid, or B acid, has also been identified as a

fermentation product of maize,[122] and has been found in high amounts in the seed peels of mangosteen fruit.[123] It also has been studied as a potential antioxidant that finger millet (*Eleusine coracana*, a legume native to different regions in Africa and Asia) naturally contains.[112] On the other hand, 4-hydroxycinnamic acid, or C acid, has been widely studied as part of the cinnamates found in several plants and fruits.[108, 124] Just to include a few lines regarding the research done on this phenolic acid and its derivatives and complexes: Clifford has published various reviews concerning the nature, occurrence, dietary burden, absorption, and metabolism of chlorogenic acids and other cinnamates.[125, 126] Clifford reports that C acid and its derivatives are present in significant amounts in coffee, apples, cider, blueberries, spinach, sugar beet fiber, and various cereals and brans. He also estimates that an average British citizen can have a daily cinnamate intake of 500 to 800 mg.[126] Sankawa and colleagues have identified different cinnamic acids, including C acid, in the phenolic compounds isolated from the root of *Dalbergia odorifera*, a legume that is native to China.[117] This root is used to treat "stagnant blood" syndrome. Sankawa has studied the isolated phenolic compounds *in vitro* through the inhibition of prostaglandin biosynthesis and platelet aggregation by fatty acids, with cinnamoyl-phenols and benzoic acid being among the best performers.[127] On a similar note, Liu and colleagues have studied different hydroxycinnamic acid derivatives *in vitro*, including 4-hydroxycinnamic acid as an anti-oxidant, by studying their protective effect against low density lipoprotein (LDL) peroxidation.[128] Michel Baltas and colleagues, from the Université Paul Sabatier (Toulouse, France), have used 4-hydroxycinnamic acid in order to combinatorially synthesize a series of antituberculous drugs that are effective against *Mycobacterium*

tuberculosis, and studied these compounds *in vitro*.[129] Meanwhile, in terms of therapeutic potential, Yamaguchi's group, from the University of Shizuoka in Japan, has recently made several reports on the use of 4-hydroxycinnamic acid as a phytochemical with the potential to inhibit osteoclast cell formation and stimulate bone mineralization *in vitro*, as well as to stimulate bone formation and inhibit bone resorption in rat femoral tissue *in vitro.* They have also reported on *in vivo* studies with two rat models, namely ovariectomized and streptozotocin-induced diabetic rats, obtaining similar effects in regard to the prevention of bone loss.[119, 120, 130-133] Finally, (4-hydroxyphenoxy)acetic acid, or P acid, has been found as a constituent element of cell walls in both maize and soy beans, and has been found to be incorporated into soil as a degradation product of different pesticides as well.[121, 122, 134, 135] As mentioned before, *N*-(4-hydroxyphenyl)glycine, or G acid, has not been reported as a plant metabolite, but has been utilized in order to synthesize derivatives intended for use as tyrosinase-targeted compounds due to the latter's potential as antitumor agents against malignant melanoma.[136] However, these reports have been sparse and inconclusive.

The previous information regarding the properties and origin of the selected phenolic acids makes it possible to visualize the required monomer synthesis procedure. Using the 3-(4-hydroxyphenyl)propionic acid as the "parent" phenolic acid, it is possible to hypothesize that the decrease in methylene units in the backbone, as well as the addition of a double bond, could lead to an increase of backbone stiffness, which in turn would likely affect the physical properties of the resulting diphenol and of the eventual polycarbonate synthesized from these materials. The addition of a double bond would also provide a plausible crosslinking site that can be used before or after the

polymerization of the diphenol obtained.

The addition of an oxygen atom to the backbone should increase the chain flexibility of the resulting polymer.[137] At the same time, it might increase its hydrophilicity and function as a complexation site in relation to metal ions present in the body. The aforementioned incorporation of a secondary amino group into the backbone should provide a reactive functional group or bioactive site. The decision of synthesizing tyrosine-derived monomers with these six phenolic acids was made on the basis of the preceding information, and the corresponding synthesis is discussed next.

3.2.2 Synthesis and Characterization of Monomers

The generic synthesis of diphenol monomers was described in Chapter 2, and is shown schematically in Figure 3.2, below.

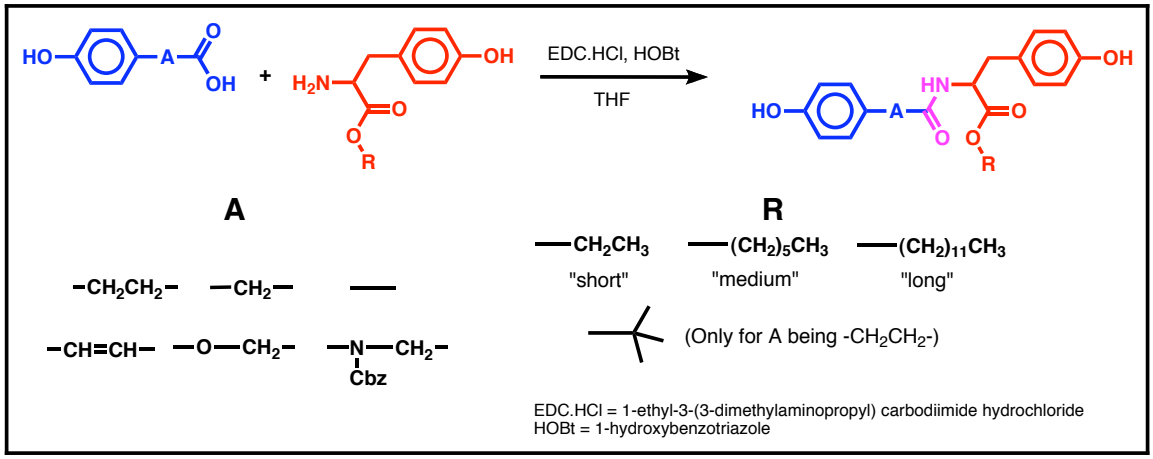

Figure 3.2 Synthesis of tyrosine-derived diphenol via carbodiimide peptide coupling

Basically, each tyrosine alkyl ester that was selected (i.e., ethyl, hexyl, dodecyl, and *tert*-butyl) was coupled with each one of the six phenolic acids (as received, except the G acid, which had to be protected prior to its use) with EDC•HCl (1.05 equivalents) and HOBt (0.10 equivalents) in THF. After aqueous work-up, rotoevaporation, and trituration in either water or hexane, the diphenolic monomers shown in Figure 3.2 were obtained with purity higher than 98% (as measured by means of melting point depression and confirmed with HPLC). For the synthesis of tyrosine-ethyl ester derivatives, the TE•HCl was used in the presence of triethylamine to allow for the *in situ* deprotection of the salt. This simultaneous reaction did not affect the performance of the reaction, and high purities and yields were obtained for these monomers.[88, 138]

Although it was proven that peptide coupling with tyrosine hexyl ester was possible without protecting the secondary amine in the *N*-(4-hydroxyphenyl)glycine (as evidenced in the ^{1}H-NMR shifts and in the HPLC analysis), the need for capped amine was essential before any polymerization reactions. This requirement resulted from the higher basicity of the secondary amine in relation to the phenol, as evidenced in the pKa's of [Ar][NH_2+][R] and [Ar][OH_2+] (25-30 and ~20 respectively).[139, 140] This difference in pKa would make the phosgene react preferentially with the secondary amine, regardless of any steric hindrance provided by the benzene ring. In order to attempt to prevent this, the aniline analog was protected. Two methods were attempted at first, namely protection with *tert*-butyl dicarbonate, i.e., $(Boc)_2O$,[141-143] and protection with 9-fluorenylmethyl chloroformate, i.e., Fmoc-Cl,[141, 144-147] without high conversion. The reason for selecting these deprotection groups was their high reactivity, as well as their subsequent relatively mild deprotection after the

polymerization reaction, the latter of which was needed in order to remove the protecting group without affecting the polymer's molecular weight (i.e., through carbonate bond cleavage). In the specific case of protection with $(Boc)_2O$, obtaining these protected monomers was highly desirable, since cleavage could have been accomplished in tandem with *tert*-butyl ester deprotection. However, after trying different bases for proton abstraction (sodium bicarbonate, *N,N*-diisopropylethylamine, triethylamine, and lithium perchlorate), the results were not encouraging. In the case of Fmoc-Cl as a protecting group, the reactions attempted were more encouraging, but featured low yields, and the purification process for the protected compound was not straightforward. Since these reactions did not work out as expected, another protecting group, in the form of benzyl chloroformate (Cbz-Cl), was considered.[146] Although no mild deprotection conditions have been reported for this protecting group (that would have been compatible with the other bonds in the polymer backbone), the reaction was performed as a proof of principle experiment. The protection reaction was effected in *N*-methylpyrrolidone at room temperature,[148] and precipitation was induced in the product by adding water to the reaction mixture until the cloud point was reached. As a side note, this reaction did not work when using Fmoc-Cl, probably due to the steric hindrance of the reagent and the protecting precursor. After filtration, the isolated product was recrystallized in warm ethanol and dried under vacuum. The light pink powder obtained was used for the subsequent monomer synthesis of Z-GTR diphenols.

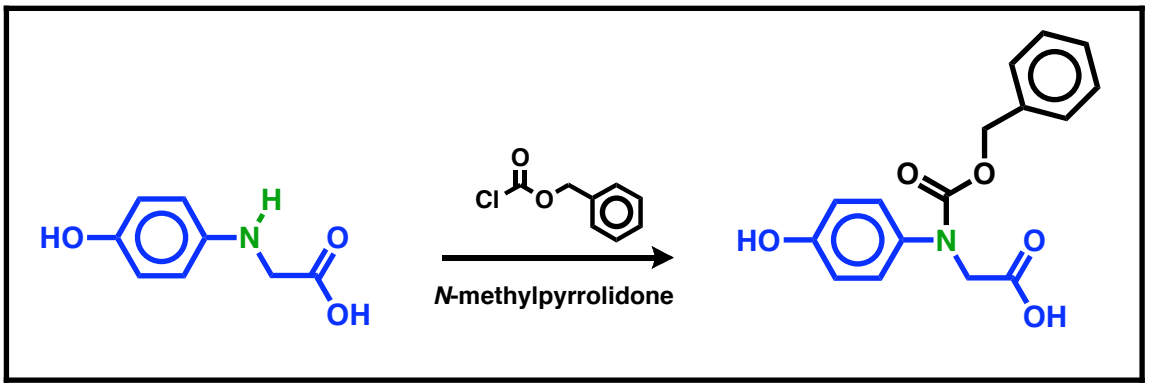

Figure 3.3 Cbz-protection reaction of *N*-(4-hydroxyphenyl)glycine

After all the precursors and diphenols were synthesized, a 1H-NMR analysis was performed, as was additional physical characterization (as summarized below):

Characterization data of tyrosine-derived diphenols and phenol intermediates synthesized for this thesis. All monomers containing 3-(4-hydroxyphenyl)propionic acid, except for DT*t*B, were synthesized by Bolikal and colleagues at the Kohn Laboratory and were used as received.

Note: Compounds with their chemical name in bold have not been described previously in the literature.

L-Tyrosine-N-[3-(4-hydroxyphenyl)-1-oxopropyl]-*tert*-Butyl Ester, DT*t*B

$C_{22}H_{27}NO_5$, MW = 385.45, Yield: 85 mol%, MP = 138-141 °C.

^{1}H-NMR (500 MHz, DMSO-d_6) δ 9.24 – 9.18 (m, 1H, phenol), 9.16 – 9.10 (m, 1H, phenol), 8.13 (dd, J = 7.4, 4.0, 1H, amide), 6.95 (ddd, J = 9.5, 6.6, 2.5, 4H, aryl), 6.75 – 6.57 (m, 4H, aryl), 4.34 – 4.15 (m, 1H, α-proton), 2.87 – 2.68 (m, 2H, -CH_2-), 2.68 – 2.56

(m, 2H, -CH_2-), 2.31 (td, *J* = 7.6, 4.4, 2H, -CH_2-), 1.39 – 1.25 (m, 9H, -CH_3).

L-Tyrosine-N-[2-(4-hydroxyphenyl)-1-oxoethyl]-Ethyl Ester, HTE

$C_{19}H_{21}NO_5$, MW = 343.37, Yield: 85 mol%, MP = 116-119 °C.

^{1}H-NMR (300 MHz, DMSO-d_6) δ 9.20 (s, 2H, phenol), 8.31 (d, *J* = 7.8, 1H, amide), 6.95 (t, *J* = 8.2, 4H, aryl), 6.64 (dd, *J* = 8.2, 1.4, 4H, aryl), 4.35 (dt, *J* = 8.3, 6.1, 1H, α-proton), 4.10 – 3.92 (m, 2H, -O-CH_2-), 3.29 (s, 2H, -CH_2-), 2.83 (ddd, *J* = 22.6, 13.8, 7.4, 2H, -CH_2-), 1.10 (t, *J* = 7.1, 3H, -CH_3).

L-Tyrosine-N-[2-(4-hydroxyphenyl)-1-oxoethyl]-Hexyl Ester, HTH

$C_{23}H_{29}NO_5$, MW = 399.48, Yield: 92 mol%, MP = 94-97 °C.

^{1}H-NMR (300 MHz, DMSO-d_6) δ 9.20 (d, *J* = 7.8, 2H, phenol), 8.31 (d, *J* = 7.7, 1H, amide), 6.95 (t, *J* = 7.8, 4H, aryl), 6.64 (dd, *J* = 8.3, 1.4, 4H, aryl), 4.35 (d, *J* = 6.2, 1H, α-proton), 4.05 – 3.88 (m, 2H, -O-CH_2-), 3.28 (s, 2H, -CH_2-), 2.83 (dd, *J* = 15.9, 7.4, 2H, -CH_2-), 1.54 – 1.38 (m, 2H, -CH_2-), 1.24 (d, *J* = 14.9, 6H, - CH_2-), 0.86 (t, *J* = 6.7, 3H, -CH_3).

L-Tyrosine-N-[2-(4-hydroxyphenyl)-1-oxoethyl]-Dodecyl Ester, HTD

$C_{29}H_{41}NO_5$, MW = 483.64, Yield: 94 mol%, MP = 100-103 °C.

^{1}H-NMR (300 MHz, DMSO-d_6) δ 9.20 (d, *J* = 7.3, 2H, phenol), 8.31 (d, *J* = 7.8, 1H, amide), 6.95 (t, *J* = 7.9, 4H, aryl), 6.79 – 6.53 (m, 4H, aryl), 4.35 (d, *J* = 5.7, 1H, α-proton), 4.09 – 3.88 (m, 2H, -O-CH_2-), 3.28 (s, 2H, -CH_2-), 2.83 (dd, *J* = 17.6, 7.3, 2H, -CH_2-), 1.48 (d, *J* = 6.0, 2H, -CH_2-), 1.24 (s, 18H, -CH_2-), 0.85 (t, *J* = 6.6, 3H, -CH_3).

L-Tyrosine-N-[(4-hydroxyphenyl)-1-oxomethyl]-Ethyl Ester, BTE

$C_{18}H_{19}NO_5$, MW = 329.35, Yield: 74 mol%, MP = 148-151 °C.

^{1}H-NMR (300 MHz, DMSO-d_6) δ 9.99 (s, 1H, phenol), 9.19 (s, 1H, phenol), 8.45 (d, J = 7.7, 1H, amide), 7.81 – 7.60 (m, 2H, aryl), 7.07 (d, J = 8.5, 2H, aryl), 6.86 – 6.73 (m, 2H, aryl), 6.71 – 6.54 (m, 2H, aryl), 4.50 (dd, J = 15.2, 7.6, 1H, α-proton), 4.15 – 3.97 (m, 2H, -O-CH_2-), 2.98 (dd, J = 11.7, 6.0, 2H, -CH_2-), 1.13 (t, J = 7.1, 3H, -CH_3).

L-Tyrosine-N-[(4-hydroxyphenyl)-1-oxomethyl]-Hexyl Ester, BTH

$C_{22}H_{27}NO_5$, MW = 385.45, Yield: 85 mol%, MP = 116-119 °C.

^{1}H-NMR (300 MHz, DMSO-d_6) δ 9.98 (s, 1H, phenol), 9.18 (s, 1H, phenol), 8.45 (d, J = 7.7, 1H, amide), 7.69 (d, J = 8.6, 2H, aryl), 7.06 (d, J = 8.4, 2H, aryl), 6.78 (d, J = 8.6, 2H, aryl), 6.64 (d, J = 8.3, 2H, aryl), 4.49 (dd, J = 15.2, 7.7, 1H, α-proton), 4.10 – 3.90 (m, 2H, -O-CH_2-), 3.07 – 2.91 (m, 2H, -CH_2-), 1.60 – 1.39 (m, 2H, -CH_2-), 1.31 – 1.13 (m, 6H, -CH_2-), 0.83 (t, J = 6.7, 3H, -CH_3).

L-Tyrosine-N-[(4-hydroxyphenyl)-1-oxomethyl]-Dodecyl Ester, BTD

$C_{28}H_{39}NO_5$, MW = 469.61, Yield: 87 mol%, MP = 111-114 °C.

^{1}H-NMR (300 MHz, DMSO-d_6) δ 9.97 (s, 1H, phenol), 9.17 (s, 1H, phenol), 8.45 (d, J = 7.7, 1H, amide), 7.76 – 7.61 (m, 2H, aryl), 7.06 (d, J = 8.5, 2H, aryl), 6.83 – 6.72 (m, 2H, aryl), 6.64 (d, J = 8.5, 2H, aryl), 4.49 (dd, J = 15.2, 7.6, 1H, α-proton), 4.10 – 3.85 (m, 2H, -O-CH_2-), 3.07 – 2.87 (m, 2H, -CH_2-), 1.48 (d, J = 5.8, 2H, -CH_2-), 1.25 (dd, J = 18.8, 5.5, 18H, -CH_2-), 0.85 (t, J = 6.7, 3H, -CH_3).

L-Tyrosine-N-[3-(4-hydroxyphenyl)-1-oxopropenyl]-Ethyl Ester, CTE

$C_{20}H_{21}NO_5$, MW = 355.38, Yield: 85 mol%, MP = 154-157 °C.

^{1}H-NMR (300 MHz, DMSO-d_6) δ 9.85 (s, 1H, phenol), 9.22 (s, 1H, phenol), 8.33 (d, J = 7.7, 1H, amide), 7.38 (t, J = 5.6, 2H, aryl), 7.31 (d, J = 15.8, 1H, alkene), 7.06 – 6.97 (m, 2H, aryl), 6.84 – 6.74 (m, 2H, aryl), 6.71 – 6.62 (m, 2H, aryl), 6.48 (d, J = 15.8, 1H, alkene), 4.49 (dt, J = 8.2, 6.1, 1H, α-proton), 4.05 (q, J = 7.1, 2H, -O-CH_2-), 2.89 (ddd, J = 22.5, 13.8, 7.4, 2H, -CH_2-), 1.12 (t, J = 7.1, 3H, -CH_3).

L-Tyrosine-N-[3-(4-hydroxyphenyl)-1-oxopropenyl]-Hexyl Ester, CTH

$C_{24}H_{29}NO_5$, MW = 411.49, Yield: 80 mol%, MP = 145-148 °C.

^{1}H-NMR (300 MHz, DMSO-d_6) δ 9.82 (d, J = 35.5, 1H, phenol), 9.18 (d, J = 36.2, 1H, phenol), 8.32 (t, J = 11.4, 1H, amide), 7.38 (d, J = 8.6, 2H, aryl), 7.28 (dd, J = 16.4, 7.0, 1H, alkene), 7.01 (d, J = 8.5, 2H, aryl), 6.79 (d, J = 8.6, 2H, aryl), 6.65 (d, J = 8.5, 2H, aryl), 6.46 (dd, J = 15.9, 6.7, 1H, alkene), 4.56 – 4.41 (m, 1H, α-proton), 3.99 (s, 2H, -O-CH_2-), 3.02 – 2.73 (m, 2H, -CH_2-), 1.61 – 1.37 (m, 2H, -CH_2-), 1.22 (s, 6H, -CH_2-), 0.83 (d, J = 1.8, 3H, -CH_3).

L-Tyrosine-N-[3-(4-hydroxyphenyl)-1-oxopropenyl]-Dodecyl Ester, CTD

$C_{30}H_{41}NO_5$, MW = 495.65, Yield: 87 mol%, MP = 134-137 °C.

^{1}H-NMR (300 MHz, DMSO-d_6) δ 9.84 (s, 1H, phenol), 9.20 (s, 1H, phenol), 8.33 (d, J = 7.7, 1H, amide), 7.38 (d, J = 8.7, 2H, aryl), 7.30 (d, J = 15.7, 1H, alkene), 7.05 – 6.97 (m, 2H, aryl), 6.78 (d, J = 8.6, 2H, aryl), 6.68 – 6.61 (m, 2H, aryl), 6.47 (d, J = 15.7, 1H, alkene), 4.57 – 4.41 (m, 1H, α-proton), 3.99 (t, J = 6.4, 2H, -O-CH_2-), 2.88 (dd, J = 14.6,

7.4, 2H, -CH_2-), 1.55 – 1.41 (m, 2H, -CH_2-), 1.29 – 1.14 (m, 18H, -CH_2-), 0.90 – 0.79 (m, 3H, -CH_3).

L-Tyrosine-N-[2-(4-hydroxyphenoxy)-1-oxoethyl]-Ethyl Ester, PTE

$C_{19}H_{21}NO_6$, MW = 359.37, Yield: 87 mol%, MP = 132-135 °C.

^{1}H-NMR (300 MHz, DMSO-d_6) δ 9.23 (s, 1H, phenol), 8.98 (s, 1H, phenol), 8.19 (d, *J* = 7.9, 1H, amide), 6.98 (d, *J* = 8.4, 2H, aryl), 6.77 – 6.59 (m, 6H, aryl), 4.46 (d, J = 5.8, 1H, α-proton), 4.35 (s, 2H, -CH_2-), 4.06 (q, *J* = 7.1, 2H, -O-CH_2-), 2.92 (t, *J* = 6.7, 2H, -CH_2-), 1.24 – 1.05 (m, 3H, -CH_3).

L-Tyrosine-N-[2-(4-hydroxyphenoxy)-1-oxoethyl]-Hexyl Ester, PTH

$C_{23}H_{29}NO_6$, MW = 415.48, Yield: 79 mol%, MP = 94-97 °C.

^{1}H-NMR (300 MHz, DMSO-d_6) δ 9.23 (s, 1H, phenol), 8.97 (s, 1H, phenol), 8.19 (d, *J* = 7.9, 1H, amide), 6.97 (d, *J* = 8.4, 2H, aryl), 6.76 – 6.60 (m, 6H, aryl), 4.54 – 4.40 (m, 1H, α-proton), 4.34 (s, 2H, -CH_2-), 4.08 – 3.94 (m, 2H, -O-CH_2-), 3.01 – 2.83 (m, 2H, -CH_2-), 1.49 (dd, *J* = 13.2, 6.5, 2H, -CH_2-), 1.35 – 1.14 (m, 6H, -CH_2-), 0.85 (t, *J* = 6.7, 3H, -CH_3).

L-Tyrosine-N-[2-(4-hydroxyphenoxy)-1-oxoethyl]-Dodecyl Ester, PTD

$C_{29}H_{41}NO_6$, MW = 499.64, Yield: 81 mol%, MP = 77-80 °C.

^{1}H-NMR (300 MHz, DMSO-d_6) δ 9.22 (s, 1H, phenol), 8.97 (s, 1H, phenol), 8.19 (d, *J* = 7.9, 1H, amide), 6.97 (d, *J* = 8.4, 2H, aryl), 6.81 – 6.58 (m, 6H, aryl), 4.47 (d, *J* = 6.1, 1H, α-proton), 4.34 (s, 2H, -CH_2-), 4.01 (t, *J* = 6.4, 2H, -O-CH_2-), 3.01 – 2.83 (m, 2H, -CH_2-),

1.50 (s, 2H, -CH_2-), 1.22 (d, J = 10.3, 18H, -CH_2-), 0.85 (t, J = 6.6, 3H, -CH_3).

2-((benzyloxycarbonyl)(4-hydroxyphenyl)amino)acetic acid, Cbz-G Acid

$C_{16}H_{15}NO_5$, MW = 301.29, Yield: 75 mol%, MP = 196-198 °C.

^{1}H-NMR (500 MHz, DMSO-d_6) δ 12.80 (s, 1H, phenol), 9.50 (s, 1H, phenol), 7.58 – 6.95 (m, 7H, aryl), 6.74 (s, 2H, aryl), 5.10 (d, J = 21.9, 2H, -CH_2-), 4.22 (d, J = 21.7, 2H, -CH_2-).

L-Tyrosine-N-[2-((benzyloxycarbonyl)(4-hydroxyphenyl)amino)-1-oxoethyl]-Ethyl Ester, Z-GTE

$C_{27}H_{28}N_2O_7$, MW = 492.52, Yield: 80 mol%, MP = 50-55 °C.

^{1}H-NMR (500 MHz, DMSO-d_6) δ 9.45 (s, 1H, phenol), 9.23 (s, 1H, phenol), 8.32 (s, 1H, amide), 7.28 (d, J = 48.2, 5H, aryl), 7.05 (ddd, J = 8.7, 6.5, 2.3, 2H, aryl), 6.95 (s, 2H, aryl), 6.77 – 6.56 (m, 4H, aryl), 5.06 (d, J = 5.7, 2H, Ph-CH_2-), 4.43 (s, 1H, α-proton), 4.12 (d, J = 23.6, 2H, -CH_2-), 4.08 – 3.96 (m, 2H, -CH_2-), 2.97 – 2.71 (m, 2H, -CH_2-), 1.10 (d, J = 4.8, 3H, -CH_3).

L-Tyrosine-N-[2-((benzyloxycarbonyl)(4-hydroxyphenyl)amino)-1-oxoethyl]-Hexyl Ester, Z-GTH

$C_{31}H_{36}N_2O_7$, MW = 548.63, Yield: 85 mol%, MP = 65-70 °C.

^{1}H-NMR (500 MHz, DMSO-d_6) δ 9.45 (s, 1H, phenol), 9.23 (s, 1H, phenol), 8.33 (s, 1H, amide), 7.28 (d, J = 48.6, 5H, aryl), 7.11 – 7.01 (m, 2H, aryl), 6.95 (s, 2H, aryl), 6.67 (dd, J = 13.5, 11.8, 4H, aryl), 5.05 (s, 2H, Ph-CH_2-), 4.43 (s, 1H, α-proton), 4.13 (s, 2H, -CH_2-

), 3.97 (d, J = 2.9, 2H, -CH_2-), 2.99 – 2.70 (m, 2H, -CH_2-), 1.46 (s, 2H, -CH_2-), 1.21 (d, J = 1.8, 6H, -CH_2-), 0.95 – 0.78 (m, 3H, -CH_3).

L-Tyrosine-N-[2-((benzyloxycarbonyl)(4-hydroxyphenyl)amino)-1-oxoethyl]-Dodecyl Ester, Z-GTD

$C_{37}H_{48}N_2O_7$, MW = 632.79, Yield: 76 mol%, MP = 87-95 °C.

^{1}H-NMR (500 MHz, DMSO-d_6) δ 9.46 (s, 1H, phenol), 9.23 (s, 1H, phenol), 8.33 (s, 1H, amide), 7.28 (d, J = 45.9, 5H, aryl), 7.11 – 7.01 (m, 2H, aryl), 6.94 (d, J = 5.1, 2H, aryl), 6.78 – 6.59 (m, 4H, aryl), 5.06 (d, J = 6.9, 2H, Ph-CH_2-), 4.44 (s, 1H, α-proton), 4.13 (s, 2H, -CH_2-), 3.98 (d, J = 5.5, 2H, -CH_2-), 2.97 – 2.70 (m, 2H, -CH_2-), 1.47 (s, 2H, -CH_2-), 1.24 (s, 18H, -CH_2-), 0.95 – 0.78 (m, 3H, -CH_3).

L-Tyrosine-N-[2-(4-hydroxyphenylamino)-1-oxoethyl]-Hexyl Ester, GTH

$C_{23}H_{30}N_2O_5$, MW = 414.49, Yield: 38 mol%, MP = 144-147 °C.

^{1}H-NMR (300 MHz, DMSO-d_6) δ 9.21 (s, 1H, phenol), 8.47 (s, 1H, phenol), 8.01 (d, J = 8.1, 1H, amide), 6.89 (t, J = 7.0, 2H, aryl), 6.62 (t, J = 6.5, 2H, aryl), 6.54 (t, J = 6.0, 2H, aryl), 6.37 (t, J = 6.0, 2H, aryl), 5.36 (t, J = 5.8, 1H, amine), 4.47 (q, J = 7.0, 1H, α-proton), 3.97 (t, J = 6.5, 2H, -CH_2-), 3.51 (d, J = 5.7, 2H, -CH_2-), 2.93 – 2.74 (m, 2H, -CH_2-), 1.57 – 1.38 (m, 2H, -CH_2-), 1.33 – 1.11 (m, 6H, -CH_2-), 0.86 (t, J = 6.7, 3H, -CH_3).

3.2.3 Effect of Backbone Modification on the Properties of Monomers

In addition to the chemical structure properties confirmed through ^{1}H-NMR, the monomers were further analyzed in an attempt to find any existing structure-property relationships. The melting points were first compared to see if the stated hypothesis (*vide supra*, end of sub-chapter 3.2.1) held true. The melting points for all 18 monomers used in this project are shown in Figure 3.4; the "free amine" counterparts of Z-GTH and Z-GTD are also included.

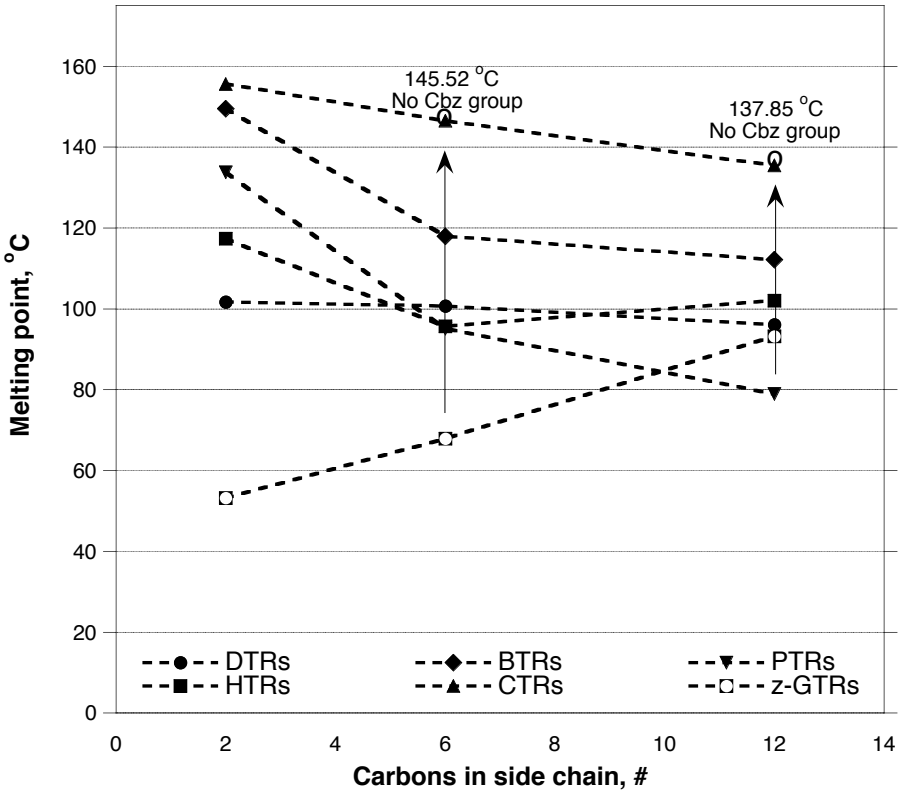

Figure 3.4 Melting points of structurally related tyrosine-derived diphenols

The highest melting points were those corresponding to the CTR monomers, a characteristic due to the stiffness caused by the double bond in the backbone. The expected trend was as follows: CTR, GTR > BTR > HTR > DTR > PTR. However, the PTE monomer featured a higher melting point was than DTE and BTE, which suggests some additional intermolecular hydrogen bonding, made possible by the extra oxygen in the backbone (similar to eugenol).[149] As the number of carbons in the pendent chain increased, the trend became more similar to that predicted above, meaning that the alkyl chain had more influence over the conformation of the molecule, making it more amorphous-like (as could be noted with the similar melting points found for DTH, HTH, and PTH monomers). Meanwhile, the expected trend was confirmed for the dodecyl ester monomers, possibly due to the long alkyl chains preventing the backbones from interacting with each other and effectively showing the real effect of the modifying the backbone in the monomers. An interesting observation is that of the difference in melting points between DTR and CTR monomers, as the difference in chemical composition consists of only two hydrogens. As for the Z-GTR monomers, the effect of the Cbz protecting group was that of a melting point increase, rather than a decrease, perhaps due to the increased occurrence of π- π interactions. Finally, regarding the "free amine" GTR monomers, the melting points were very close to those of the 4-hydroxycinnamic-acid-containing molecules, possibly due to increased intramolecular and intermolecular hydrogen bonding.

Another feature that is worth examining is the monomers' solubility. Various *in vivo* results and *in vitro* studies have revealed that the mass loss in tyrosine-derived polycarbonates is very low over time.[96, 150] This is caused by the highly hydrophobic

structure of these polycarbonates and the poor solubility of the corresponding degradation products, or even their monomers, in water or PBS with pH = 7.4. While tyrosine-derived polycarbonates have suitable degradation profiles for different biomedical applications, ensuring the resorption of materials over a timeframe suitable for tissue engineering applications still remains a challenge. Solubility in PBS with pH = 7.4 for the desaminotyrosyl-tyrosine ethyl ester (DTE) and its free acid counter part (DT) has been reported at 1.4 mg/mL and 9.3 mg/mL respectively.[150, 151] The de-esterified product of the DTE is six times more soluble than its esterified counterpart. This allows for the design of biomaterials with potentially versatile levels of degradation, as well as for the enhancement of the solubility of degradation products. To put this information into perspective, the water/octanol partition coefficient (cLogP) of several monomers was calculated using Biobyte's algorithm, as defined in the CS Chembiodraw Ultra software program (Cambridge, MA). A monomer's water/octanol partition coefficient is the logarithm of the ratio between water and octanol in a compound's concentration. It is a measure of molecular hydrophobicity, and therefore accounts for the compatibility of a compound in water. A large cLogP means that the molecule is hydrophobic, while a smaller cLogP means that that the molecule is hydrophilic.

Hansch and colleagues have reported on the linear free-energy relationship between partition coefficients and the aqueous solubility of organic compounds. This was done by establishing an analogy between the dissolution of a compound in water (partition with itself and water) and a partition between two solvents, like the octanol-water system.[152] For molecules with negative values, it can be said that their solubility in water is very high. The cLogP values of some monomers, their de-esterified

counterparts, and other relevant molecules (i.e., degradation products of traditional biomaterials) are presented in Figure 3.5. The bars for GA, LA, and 6-hH represent glycolic acid, lactic acid, and 6-hydroxyhexanoic acid (ultimate degradation product of PCL) respectively. A degradation product of poly(L-lactic acid), L-lactic acid has a solubility of 100 mg/mL in water, as approximated from the work reported by Lockwood and colleagues.[153] This high solubility in water makes the resorption of medical devices created from this material (e.g., sutures) possible (after degradation to a certain extent).

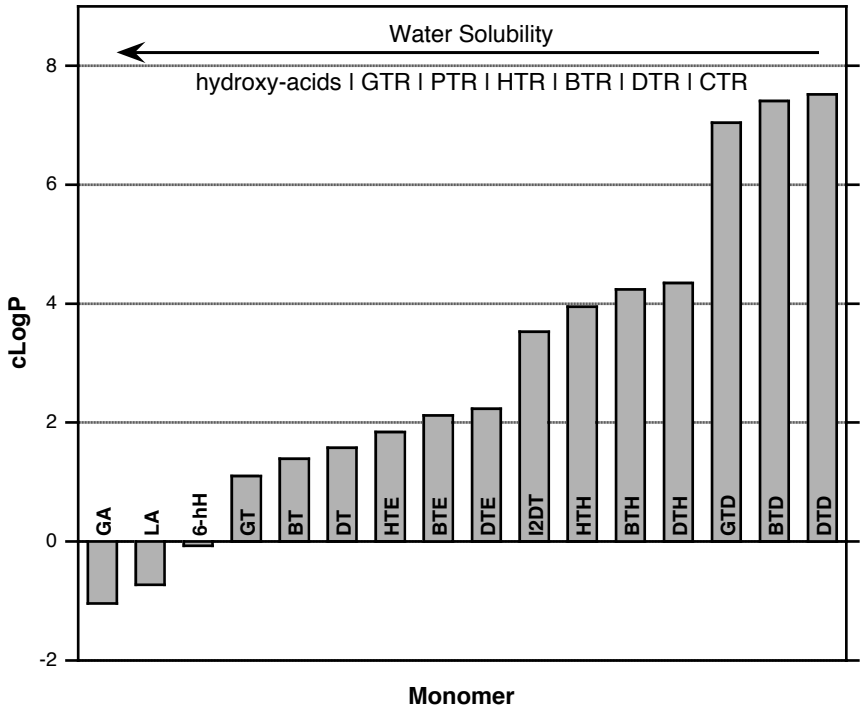

Figure 3.5 Calculated partition coefficients for different monomers

The solubility of the monomers synthesized for this thesis was obtained by using an HPLC method developed by Das Bolikal at the New Jersey Center for Biomaterials. In

short, a saturated solution of the monomer in PBS was filtered and analyzed through HPLC, after which a calibration curve of the same monomer in methanol was used to calculate solubility. This way, the relationship between the cLogP and the solubility of the synthesized diphenols was studied. It is worth noting that, although the dissolution of a compound in a solvent is a complex process that involves a variety of forces such as hydrogen bonding, dipole-dipole interactions, and dispersion forces, a cLogP (an additive-constitutive property of organic molecules) and solubility can be related to each other.[152] Table 3.1 shows the different solubility parameters obtained for the synthesized tyrosine-derived diphenols, both in μg/mL and as a logarithm of molar solubility ($LogS_{PBS}$). The solubility of compounds with dodecyl ester pendent chains was very low (>5 μg/mL), and therefore could not be assessed in a straightforward manner with the aforementioned HPLC protocol.

Table 3.1 Solubility of monomers in PBS

Compound	Solubility, μg/mL	$LogS_{PBS}$
DTE	651	-2.74
DTH	18	-4.37
HTE	1533	-2.35
HTH	36	-4.05
BTE	1154	-2.46
BTH	14	-4.43
CTE	83	-3.63
CTH	4	-5.02
PTE	414	-2.94
PTH	15	-4.43
Z-GTE	55	-3.95
Z-GTH	13	-4.63
GTH	52	-3.90
DT	6600	-1.70

The difference between the solubility values obtained for DTE and DT monomers and those already reported in the literature is worth noting.[150, 151] This can only mean an overestimation regarding the previously reported solubility values, as the HPLC method is more sensitive than weighing methods. In the field of drug discovery, it is estimated that 85% of drugs have a LogS value between -1 and -5, while very few have values below -6 and those with values above -1 are associated with highly polar molecules such as sugars or small peptides.[154] Once these solubility values in PBS were obtained, it was possible to see their linear relationship with the cLogP previously mentioned. The linear relationship between cLogP and $LogS_{PBS}$ is shown in Figure 3.6 below.

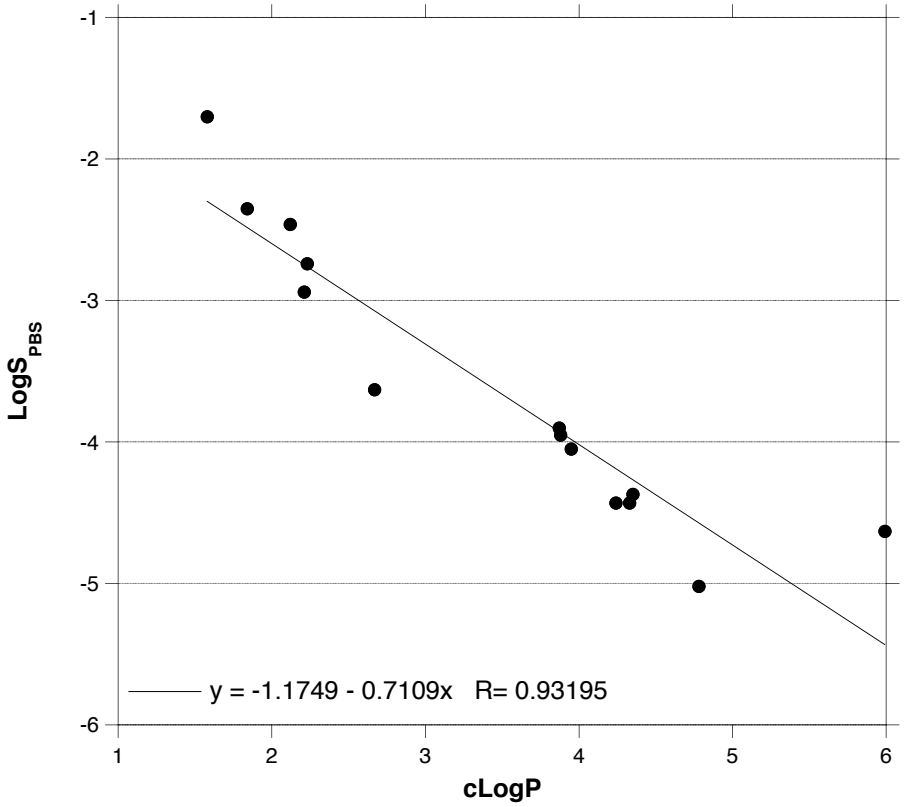

Figure 3.6 Linear relationship between cLogP and $LogS_{PBS}$

This information is important from a design perspective, since it means that calculating the solubility of other tyrosine-derived diphenols is a very easy procedure that simply requires the corresponding cLogP values. Moreover, Jain and Yalkowsky have proposed a General Solubility Equation (GSE) used to obtain an estimate of the aqueous solubility of organic non-electrolytes.[155] The GSE presented in Equation 3.1 is derived from a thermodynamic standpoint, where the equilibrium between a compound's solid phase and saturated aqueous solution can be seen as a two-step process: First, the melting of the crystal to neat liquid and, second, the transfer of that neat liquid to water.[154] The full derivation of this equation has been reviewed elsewhere.[155]

$$\log S_w^{solid} = 0.5 - 0.01(T_m - 25) - \log P_{o/w} \quad (3.1)$$

The calculated solubility values expressed in $LogS_{PBS}$, the $cLogS_{PBS}$ calculated from the linear equation shown in Figure 3.6, and the $cLogS_w$ from Yalkowsky's equation (Eq. 3.1) are all shown on Table 3.2. The experimental data obtained with the HPLC method is comparable to these calculated values, and it can be said that the results are within experimental error.

Table 3.2 Experimental solubility values in PBS compared to calculated values

Compound	MP, °C	$LogS_{PBS}$	$cLogS_{PBS}$[a]	$clogS_w$[b]
DTE	102	-2.74	-2.76	-2.50
DTH	101	-4.37	-4.27	-4.61
HTE	117	-2.35	-2.48	-2.26
HTH	96	-4.05	-3.98	-4.16
BTE	150	-2.46	-2.68	-2.87
BTH	118	-4.43	-4.19	-4.67
CTE	156	-3.63	-3.07	-3.48
CTH	147	-5.02	-4.57	-5.50
PTE	134	-2.94	-2.75	-2.80
PTH	95	-4.43	-4.25	-4.53
Z-GTE	53	-3.95	-3.93	-3.66
Z-GTH	68	-4.63	-5.43	-5.92
GTH	146	-3.90	-3.93	-4.58
DT	168	-1.70	-2.30	N/A[c]

[a]Calculated on the basis of the linear relationship between solubility and partition coefficient data.
[b]Calculated with Jain and Yalkowsky's equation using melting points and partition coefficient data.
[c]Equation deviates from linearity with weak electrolytes.

There are other, more sophisticated methods of calculating the solubility of compounds on the basis of their molecular structure and without the need for experimental data.[154, 156-158] Although these methods are adequate for pre-screening

synthetic candidates, the data generated in this sub-chapter will make it possible to predict solubility values for structurally related monomers, and therefore can help in the design of polymeric biomaterials.

3.3 CONCLUSIONS

The rationale used in selecting materials for the synthesis of a series of tyrosine-derived diphenols was presented. After said synthesis was performed with traditional peptide coupling methods, the corresponding monomers were characterized satisfactorily with a variety of methods. The melting point analysis of the compounds revealed a trend that was correlated not only to the pendent chain, but also to the backbone characteristics of the diphenols. The fact that the analysis of the compounds' melting point proved to be of importance in calculating the solubility of the diphenols *a priori* is of special significance. Also, the linear relationship between molar solubility in PBS (expressed as $LogS_{PBS}$) and the cLogP value was described. This is important for future research, as this information could be used as a selection tool for polymerization reagents based on the application or environment to be used.

4. AUTOMATED PARALLEL SYNTHESIS OF TYROSINE-DERIVED POLYCARBONATES

4.1 INTRODUCTION

The automated parallel synthesis of polymers is an emerging strategy in modern polymeric materials research.[40, 54, 159] The use of advanced robotic platforms can help accelerate the creation of structurally-related polymer libraries and provide ample assistance in optimizing reaction conditions.[32, 40, 58, 160] By performing simultaneous exploration of reaction conditions (i.e., type of monomer, initiator, solvent, temperature, stirring speed, reaction time), scientists have been able to accelerate their throughput and efficiently explore polymer design space.[26, 48, 57, 64, 67, 70, 159] In contrast to classical "trial-and-error" approaches, which only provide a narrow window for studying the effect of certain parameters on a reaction, combinatorial and automated procedures allow for a better understanding of reaction conditions based on multiple experiments performed under the same exact conditions and having minimal or no errors during reagent handling and reaction control (e.g., measuring masses or volumes, temperature control).[40, 61]

The fact that they allow for faster, unattended experiments in a reliable manner has made it possible for scientists to successfully use automated parallel synthesizers with different polymer systems, in line with the example set by work in other research areas (including drug and catalyst research).[25, 59, 60, 70] Ultimately, the expected result is to be able to identify new and useful material compositions for diverse applications and

even promote the discovery and development of new or improved technologies in significantly shorter periods of time, without the burden that manual synthetic procedures represent.[15, 26, 38, 58, 161]

It is important to notice that only a handful of publications have described successful cases of switching from manual polymer synthesis methods to automated procedures. Examples include the synthesis of polycarbonates and polyarylates, polyurethane dispersions, nitroxide-mediated polymerizations, ABA triblock copolymers, anionic polymerizations, star-shaped copolymers, and MADIX copolymers (Macromolecular Design via the Interchange of Xanthates), among a few others.[37, 40, 51, 64, 70, 71, 159] Although the research done so far has covered many reactions that are relevant to industrial applications, automated synthetic procedures are just starting to "take off", in a manner of speech, and it is important to perform additional research on new reactions and to revisit manual synthetic procedures in order to improve them, especially if this can result in cost and time savings for researchers.[40]

This chapter describes the automated parallel synthesis of tyrosine-derived polycarbonates, going from the concept behind the procedure to its actual validation, and comparing it to the corresponding manual synthesis method. Some of the challenges involved are: handling toxic chemicals, the accuracy of liquid dispensing, and the levels of reproducibility that can be achieved in regard to degrees of polymerization and specific copolymer compositions. Specifically, the condensation of triphosgene with a diphenol involves challenges both in terms of safety and of dispensing, such as ensuring adequate isolation of a toxic chemical –triphosgene– inside the automated parallel

synthesizer, and finding a suitable automated process for its drop-wise addition to reactions in parallel.

Additionally, this chapter focuses on acquiring a general perspective of the advantages and challenges involved in operating automated synthesizers for solution polycondensation reactions. Some of the advantages described include the rapid optimization of reaction conditions, accelerated throughput levels, the standardization of methods, and the retention of expertise.

4.2 RESULTS AND DISCUSSION

4.2.1 Initial Screening of Reaction Conditions and Comparison to Manual Procedures

An initial screening of reaction conditions in the SLT-100 was performed in order to verify the feasibility of automating a polycondensation reaction in order to obtain a high molecular weight polycarbonate. The selected model reaction was the polycondensation of a DTE monomer, as shown in Figure 4.1. Due to the fact that manual polymer synthesis procedures using triphosgene solutions call for a slow and drop-wise addition to the reaction mixture, the development of an automated protocol mimicking the “drop-wise” addition of a triphosgene solution while vortexing of reactions would be beneficial in a wide range of synthetic procedures, and not just in polycarbonate synthesis.

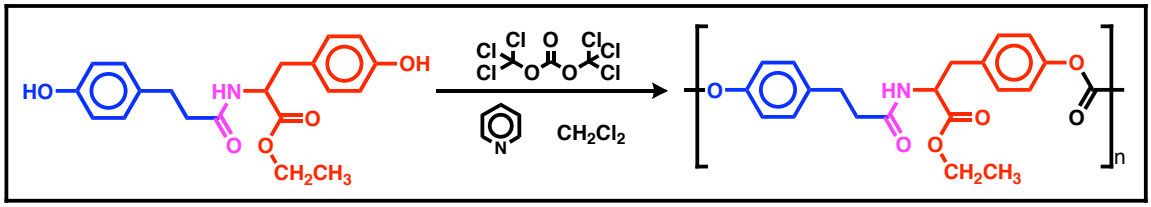

Figure 4.1 Polycondensation of DTE monomer and triphosgene

The greatest challenge involved in automating the phosgenation reaction was to define a series of dispensing parameters that could mimic the drop-wise addition of triphosgene solution over 45 minutes to 1 hour in the manual protocol and allow for multiple reactions to be run in parallel. The slowest possible flow rate when using a 1-mL syringe in the automated synthesizer is 50 µL/min, i.e., the time required for every mL of triphosgene solution transferred is only 20 minutes – a rate that is more than twice as fast as the corresponding manual protocols. To include a delay in the triphosgene addition, the same 1.0 mL of triphosgene solution was dispensed in aliquots of 50, 100, and 1000 µL. At the same time, a manual reaction was performed in parallel in order to compare the molecular weights obtained when dispensing the triphosgene across a period of 20 minutes, as shown in Figure 4.2.

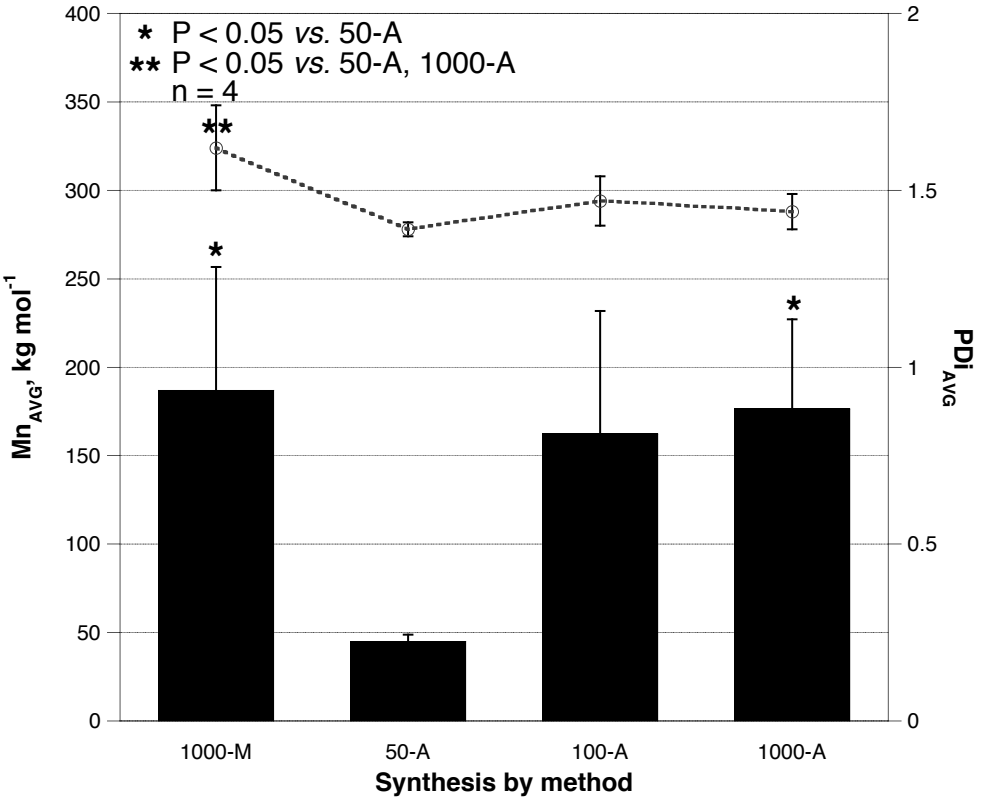

Figure 4.2 Synthesis of poly(DTE carbonate) by (M)anual and (A)utomated protocols, # = aliquot size used to dispense 1000 µL of triphosgene solution

Although the manual syntheses registered higher molecular weights in comparison to their automated equivalents, the difference is not significant, save for the molecular weight achieved with the 50-A method. This is possibly due to triphosgene solution quenching, caused by moisture inside the hood of the automated synthesizer. Since more aliquot transfers are required (i.e., 20 times) for the 50-A method, the probability of triphosgene quenching over time is greater. By using a larger aliquot of 100 µL, the molecular weights achieved were similar to those obtained through manual synthesis, but with higher standard deviations. The methods that yielded the highest molecular weight materials in this particular comparison were the 1000-M and 1000-A

methods. However, there was a significant difference in the PDi of the polymers obtained via manual synthesis when compared to the corresponding automated procedures. This indicates the fact that automated synthesis results in more homogeneous reactions when compared to manual protocols. Based on these results, the feasibility of synthesizing polycarbonates in an automated manner with the use of automated parallel synthesizers is confirmed, as is the reproducibility achieved with said method. The expectation is that, with two needles working at the same time, a maximum of eight reactions can be performed in parallel. Since the total reaction time is only 1 h, it would be possible to perform 48 reactions overnight. Comparatively speaking, manually synthesizing 48 polycarbonates would be possible, at best, in two to three weeks, which would require running four reactions a day, or 20 reactions per week; thus, the automated synthesis of polycarbonates is a preferable approach for accelerating output and exploring polymer design space.

4.2.2 The Use of Different Bases in Order to Catalyze Polycarbonate Synthesis

A major advantage of using automated procedures is the fact that the approach makes it possible to explore different reaction conditions in parallel, e.g., using different catalysts in a reaction. In the synthesis of tyrosine-derived polycarbonates, pyridine is used both as an acid scavenger and as a catalyst. The acid released from the diphenol condensation with the triphosgene is HCl, and the reaction is illustrated in Figure 4.3 with its phosgene equivalent.

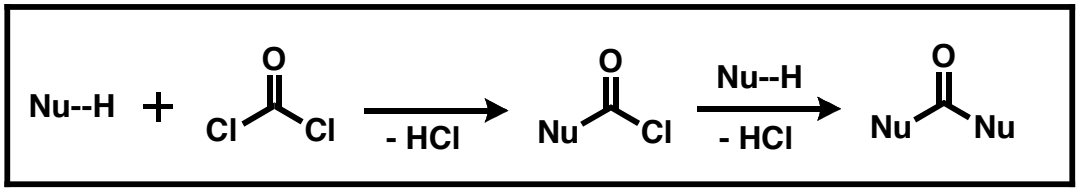

Figure 4.3 Generic reaction of a phosgene molecule and two nucleophiles

The removal of this HCl is important in order to be able to push the reaction forward and obtain high molecular weight polymers. The catalytic effect of pyridine is illustrated in Figure 4.4. During a solution polycondensation reaction, there are four chemical species at all times: the diphenol (monomer), the chloroformate, a phenoxide formed between the phenol and the pyridine, and a pyridinium chloroformate formed between a chloroformate and the pyridine.

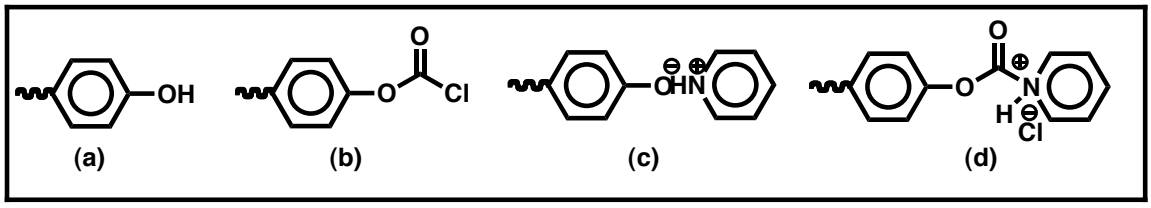

Figure 4.4 Chemical species present during a diphenol phosgenation (a) (di)phenol, (b) benzyl chloroformate, (c) phenoxide (d) pyridinium chloroformate

Kricheldorf and colleagues have observed a side reaction occurring during the interfacial polycondensation of bisphenol-A when using pyridine as a catalyst.[162-164] The reaction in Figure 4.5 shows how pyridine efficiently catalyzes the hydrolysis of chloroformate groups first by forming a pyridinium chloroformate species and then reacting with trace amounts of water.

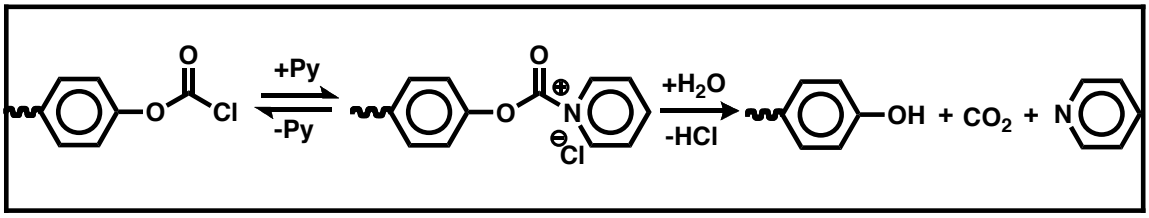

Figure 4.5 Hydrolysis of chloroformate catalyzed by pyridine

This reaction is of particular importance for the phosgenation reaction of tyrosine-derived diphenols, as shown in the initial screening. Trace amounts of water in our system would make it very difficult to obtain consistently high molecular weight polymers, and would result in high batch-to-batch variability. In turn, the fact that the phenoxyacylium ion is highly hydrophilic makes it possible to hypothesize that the introduction of more hydrophobic bases as catalysts would help towards our goal of reproducible reactions in the automated synthesizer.

An experiment was performed with the different bases shown in Figure 4.6. For all bases, except pyridine, a solvent mixture of CH_2Cl_2:dioxane was used to solubilize the DTE monomer, which is not soluble in neat CH_2Cl_2. Reactions catalyzed with pyridine, but using the aforementioned solvent mixture, were performed as a control.

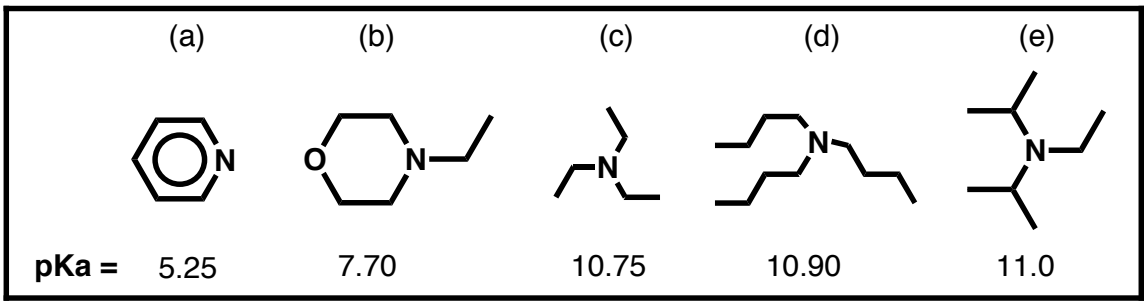

Figure 4.6 Different bases used as catalyst (a) pyridine, (b) *N*-ethylmorpholine, (c) triethylamine, (d) tri-*N*-butylamine, and (e) diisopropylethylamine

The basicity of the catalysts is also different, with pyridine being the least basic catalyst and diisopropylethylamine the most basic catalyst. The experiments were achieved by performing an "inertization" step for the reactors prior to the dispensing of the reagents as in the screening reactions in Chapter 4.2.1. This way, a dry environment was ensured. The results in Figure 4.7 show that obtaining high molecular weight polymers with low polydispersities is only possible by rendering the reactors inert before dispensing the corresponding solutions.

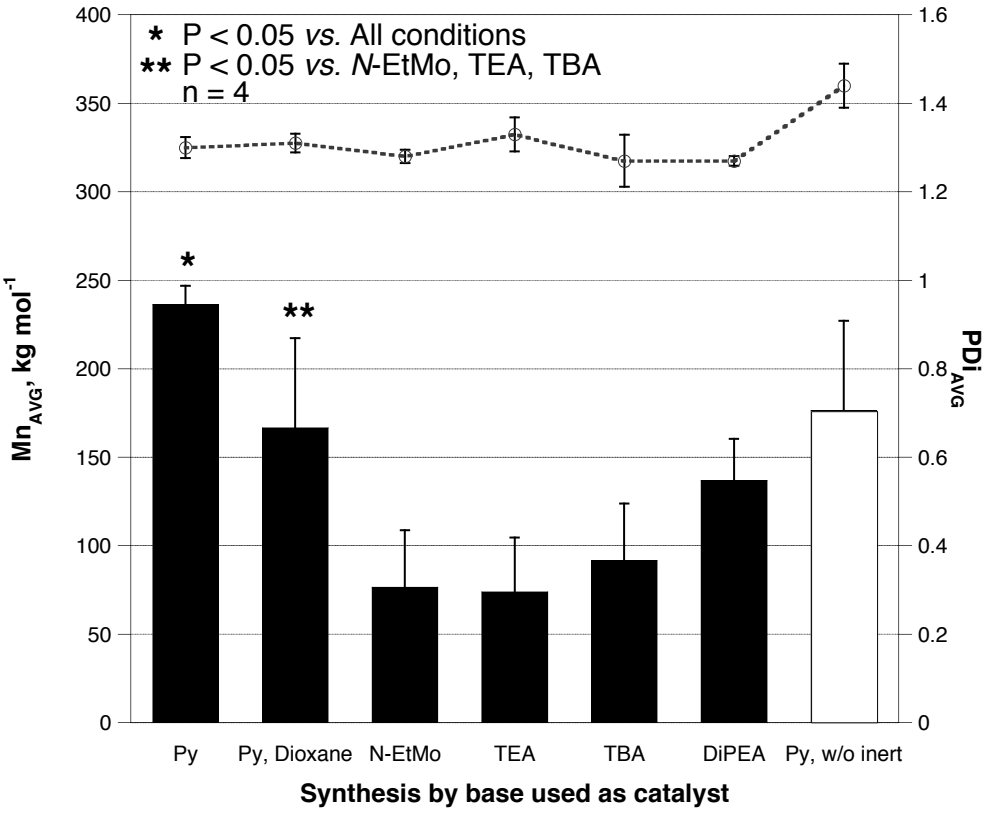

Figure 4.7 Results of the polycarbonates synthesis using different catalysts

The results of this automated synthesis show the effect of the different bases on the synthesis of polycarbonates, and, more specifically, their effect on the corresponding molecular weight. The reactions that used pyridine (without dioxane) as a catalyst yielded the highest molecular weights. The addition of dioxane as a co-solvent of the monomer yielded results that were very similar to the reactions from the initial screening. Even though the dioxane was dried with 5A molecular sieves prior to its use, the end result was practically the same as that achieved when humidity is present in the system. The use of all other bases resulted in polymers with lower, yet consistent, molecular weights and polydispersities. The molecular weights increased in line with the increasing basicity and

nucleophilicity of the bases used; however, the different colors obtained for the polymers indicated side reactions, as shown in Figure 4.8.

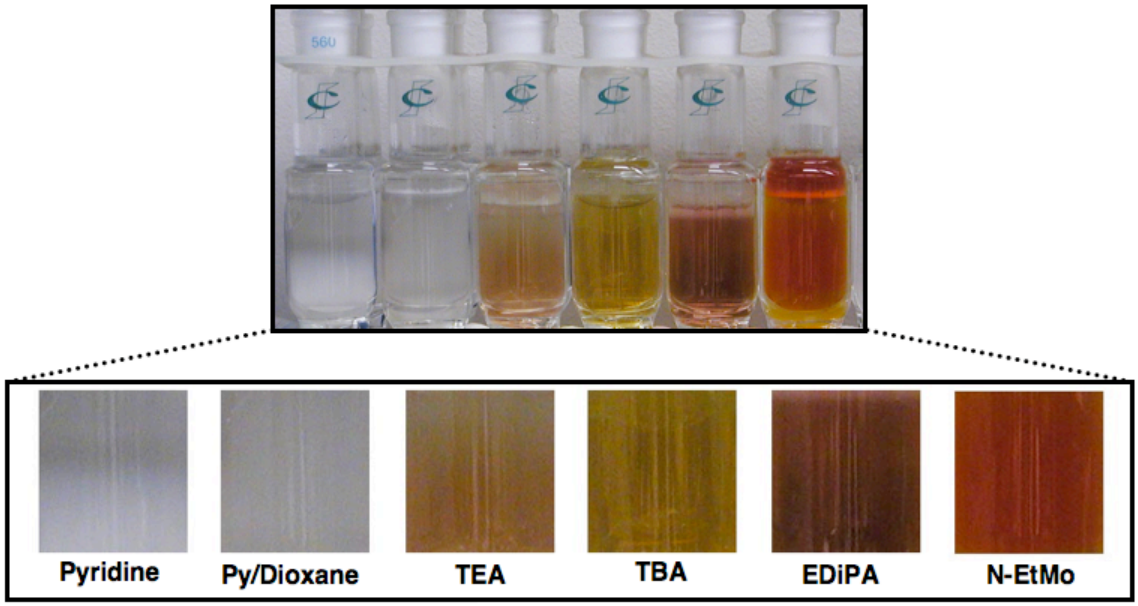

Figure 4.8 Detail of solutions inside reactors showing product with different color

The side reaction that must have occurred during polycondensation is the addition of the base to the end of the polymer chain, resulting in a low molecular weight product due to the end capping of the growing chain. The difference in the chemical properties of the bases then caused the difference in colors. A side reaction with aliphatic amines in which *N,N*-diethylcarbamate end-groups result from the acylation of –OH groups with diethylcarbamoyl chloride has been reported by Kricheldorf and colleagues.[165] The diethylcarbamoyl chloride was formed by the decomposition of a phosgene-TEA complex, similar to the reaction in Figure 4.9.

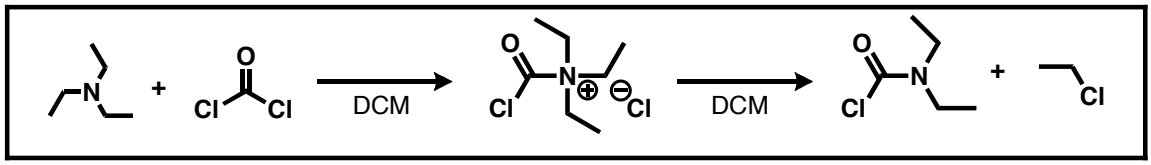

Figure 4.9 Side reaction for tertiary amines and phosgene derivatives

The assumption is that this intermediate can grow the polymer chain or break it, thus causing the low molecular weights obtained when using TEA, TBA, and DiPEA as catalysts. In the case of *N*-EtMo, the same side reaction may be occurring – however, and due to the fact that the intermediate is much more hydrophilic than the other tertiary amine complexes, it is possible that chloroformate hydrolysis is also taking place, causing the molecular weight to be lower than that obtained when using other catalysts.

The use of pyridine as an acid acceptor and as a catalyst proves to be more efficient than the use of other tertiary amines, even when these are hindered, as in the case of DiPEA, or are more hydrophobic, as in the case of TBA. It is important to observe that, when the reactors were rendered inert prior to reagent addition, the molecular weights obtained are high and consistent throughout the various repetitions. Therefore, the next step was to investigate other variables that can be important during the polymerization process, e.g., vortexing speed and concentration.

4.2.3 Advanced Design of Experiments and Multiple Variable Analysis

A design of experiments (DoE) was developed in order to investigate different variables during the automated parallel synthesis of polycarbonates. Using different bases

as catalysts made it clear that pyridine is the best possible catalyst for the process. Moreover, rendering reactors inert before reagent transfers constitutes an important step in obtaining high and consistent molecular weight polymers. Therefore, revisiting the use of aliquots of triphosgene solution during polymerization as a means to add a delay to the reaction, and analyzing the corresponding effects, is a worthwhile step. The DoE involves 14 different methods that use 3 factors, with 3 levels per factor, and is shown in Table 4.1 below.

Table 4.1 Factorial design of experiments for polycondensation reactions

Method	Factors		
	Reaction time, min	**Total volume, mL[a]**	**Cycles for triphosgene addition, #[b]**
A	50	4.75	2
B	50	4.75	3
C	45	5.00	3
D	45	4.50	1
E	55	5.00	1
F	55	4.50	3
G	55	4.50	2
H	45	5.00	1
I	55	4.50	1
J	55	5.00	2
K	55	5.00	3
L	45	4.50	2
M	50	4.75	1
N	45	5.00	3

[a]The final concentrations, starting with 300 mg of monomer (w/v), are 6.67, 6.32%, and 6.0%.
[b]The total volume of triphosgene solution is 900 μL.

The polycondensation of a DTE monomer and triphosgene was selected again as the model reaction. The results shown in Figure 4.10 include the highest molecular weights obtained in the automated synthesizer.

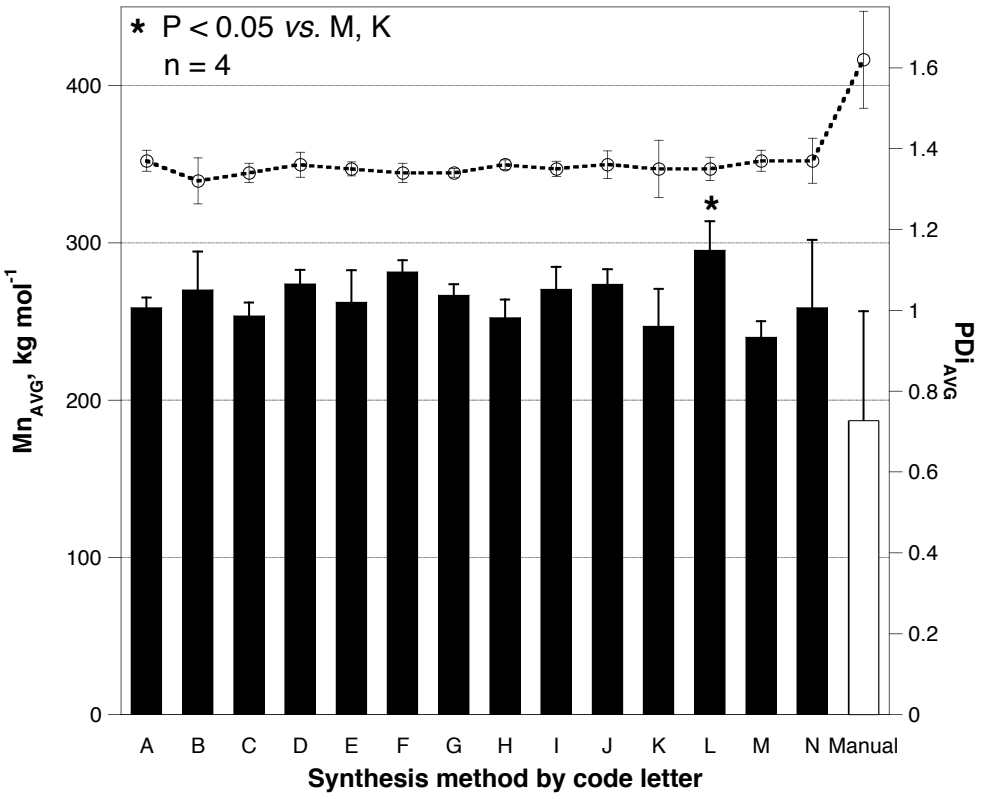

Figure 4.10 Synthesis results from factorial design of experiments

In general, the molecular weights that were obtained were consistent within each method. The polydispersities were constant, independently of the synthesis method used. In order to select the appropriate synthetic methods for further validation (i.e., the ones yielding the highest and most consistent molecular weights), further statistical analysis is required. When comparing each mean's pairs with Student's *t* ($\alpha = 0.05$) for both Mn and PDi by factor (i.e., reaction time, total volume, and cycles of triphosgene addition), no significant differences were found between the levels used per factor, except for the Total volume = 5.0 mL. This was done by looking at the Least Significant Different (LSD) threshold, which is the difference between the absolute difference in the means and the

LSD that would be significantly different. If the values are positive, then the difference between means is significant. As a result, the methods that used 5.0 mL as the total volume were discarded, since they yielded the lowest molecular weights, generally speaking. Out of the remaining methods, "M" yielded the lowest molecular weights among all methods, so it was eliminated from further validation. Regarding the methods remaining after this elimination, it was possible to rank them by their variance as Low (0-99), Medium (100-499), or High (500 >), as shown in Table 4.2, and to discard those featuring a high variance.

Table 4.2 Methods ranked by the variance of their average molecular weights

Method	Variance
A	41.46
G	49.19
F	55.05
D	80.28
I	199.69
L	341.06
B	588.67

Out of the six remaining methods, it was possible to discard the ones with longer reaction times (i.e., 55 minutes) in order to minimize side reactions, like the one previously suggested by Piotrowska and Bolikal[166] and shown in Figure 4.11.

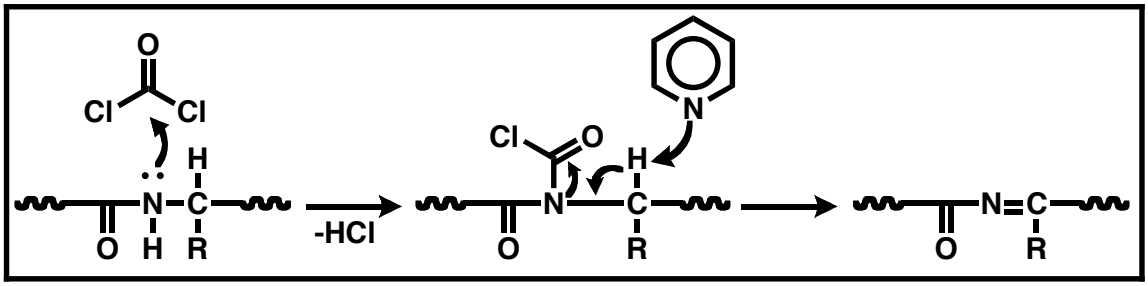

Figure 4.11 Side-reaction occurring at long reaction times and excess triphosgene

Of the three methods left for validation (i.e., A, D, and L), an arbitrary number of two were selected in order to further validate them and determine the best choice for other reactions. The methods with the highest molecular weights were D and L, and they were validated in an additional experiment in the automated parallel synthesizer. The results presented in Table 4.3 come from an automated procedure in which fourteen polymers were synthesized per method.

Table 4.3 Validation of methods D and L

Method	Reaction time, min	Total volume, mL	Cycles for triphosgene addition, #[a]	Mn[b]	PDi[b]
D	45	4.50	1	275±24	1.37±0.03
L	45	4.50	2	265±17	1.37±0.03

[a]The total volume of triphosgene solution is 900 mL.

[b]n = 14, P > 0.05

The only difference between the methods was the number of cycles involved in the triphosgene addition process. In the case of method D, the triphosgene solution (900 µL) was added in one step at a rate of 50 µL /min. In the meantime, the triphosgene was added in two aliquots of 450 µL for method L, in order to add a delay during the

triphosgene addition process and to emulate manual synthetic procedures time wise. The results achieved with n = 14 resulted in no significant differences between molecular weights or polydispersity indices. Therefore, in order to save time for other reactions, method D was chosen as a reasonable procedure for obtaining high and consistent molecular weights for polycarbonate synthesis. The next step was to apply this protocol to different reactions including homo-, co-, and terpolymer synthesis in order to evaluate the method's reliability with different monomers and compositions.

4.2.4 Synthesis of Diverse Compositions of Homo-, Co- and Terpolymers

In order to synthesize several different polymers, the compositions were randomly selected from a pool of 15 diphenols and three different mol% (3.0, 6.0, and 9.0 mol%) for the monomer incorporating the free-carboxylate into the polymer (via DT*t*B), as well as for the PEG_{1k}. The compositions for this experiment are shown in Table 4.4. The total number of moles of the diphenol monomer per reaction vessel was fixed at 0.75 mmol, independently of the composition.

Table 4.4 Random compositions by polymer code

Polymer code	Name
1	poly(DTD carbonate)
2	poly(DTH carbonate)
3	poly(HTH-co-6%PEG_{1k} carbonate)
4	poly(PTD-co-3%PEG_{1k} carbonate)
5	poly(DTE-co-3%PEG_{1k} carbonate)
6	poly(CTD-co-3%DT*t*B-co-3%PEG_{1k} carbonate)
7	poly(HTD-co-10%DT*t*B-co-3%PEG_{1k} carbonate)
8	poly(CTE-co-10%DT*t*B-co-6%PEG_{1k} carbonate)

The monomers were dissolved in CH_2Cl_2, using pyridine as a co-solvent, and were then placed in 8-mL sealed vials inside the automated synthesizer for automated dispensing. Four reactions (i.e., two pairs) were performed per composition, and a comparison is shown in Figure 4.12. In the case of Polymer 1, poly(DTD carbonate), there was an error during the triphosgene transfer, so the polymerization did not go through, resulting only in the formation of oligomers.

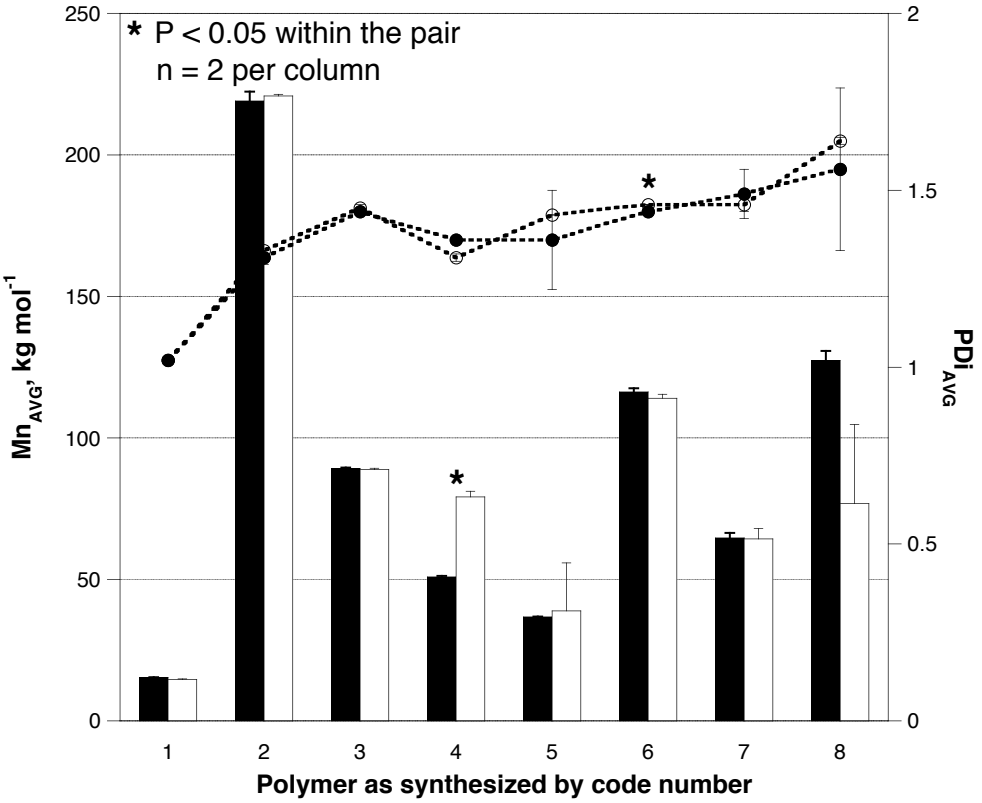

Figure 4.12 Random polymer compositions including homo-, co- and terpolymers

Despite the fact that there is a high level of variability in molecular weight between composition and composition (excluding Polymer 1), it is possible to see that polydispersity remains almost constant in all the polymers that were synthesized (1.42±0.17). However, polydispersity in polymers containing PEG was higher than that in polymers with no PEG, generally speaking. This is of particular importance, since PEG_{1k} often carries water, which might be difficult to remove by just using molecular sieves, as was the case for this set of reactions. As previously mentioned, small amounts of water can lead to the triphosgene hydrolysis, eventually resulting in low molecular weight polymers. Other reasons for the low performance of this set of reactions were the purity of the reagents and the time of reaction. It is possible that longer reaction times are

needed for co- and terpolymers in order to obtain high molecular weights, in particular if macromers (i.e., PEG) are introduced into the reaction system, since the aliphatic –OH groups may have a different reactivity than that of their aromatic counterparts. In general, the method used to synthesize homo-, co-, and terpolymers works, but it might be necessary to optimize specific compositions depending on the base monomer used for copolymers and terpolymers. Based on this information, a library of 162 individual polycarbonate compositions was synthesized in the automated synthesizer with minimum modifications to the synthesis methods previously described. The expected result is for the synthesis of 162 individual polymers with one repetition, i.e., a total of 324 individual polymers, to be performed in a much shorter period of time than that required for the corresponding manual procedure.

4.2.5 Design and Synthesis of a Polymer Library of 162 Tyrosine-Derived Polycarbonates

The design of a library of 162 tyrosine-derived polycarbonates comes from the idea of expanding a small-library of polycarbonates studied *in vivo* by Kohn and colleagues.[97, 98, 167] In this study, a library of four structurally-related polymers extruded as pins were implanted transcortically in the proximal tibia and the distal femur of New Zealand white rabbits. The tissue response at the bone-implant interface was characterized as featuring a minimally fibrous or non-fibrous capsule (i.e., direct bone apposition). Although this study identified poly(DTE carbonate) as a promising polymer for orthopedic applications, all four polymers in general showed a very slow (i.e., years)

rate of degradation and limited processability due to their high T_g and relatively low decomposition temperatures. The idea behind this chapter is to expand this library as an example for the rational exploration of polymer space. The objective is to use an automated parallel synthesis method in order to create structurally related polymer libraries that can be used for a specific application. The purpose of this specific example is not to study a large library of polycarbonates *in vivo*, but rather to expand on the idea of tailoring a polymer for a specific application instead of exploring polymer space through "trial and error" approaches that simply cannot keep up with the demand for innovative technologies. Based on promising results seen *in vivo,*[97] a library of more processable, fine-tuned materials with potentially increased osteoconductive properties is suggested. The corresponding synthesis is performed by using automated parallel synthesis as a way to reduce the workload associated with the creation of a library with more than 100 individual compositions. The possibility of using combinatorial and high-throughput approaches in order to eventually accelerate the discovery of novel biomaterials for specific applications is discussed. Since the chemical structures and compositions of the suggested library have been designed with the objective of yielding high-strength materials, their complexity is higher in comparison to that of traditional biomaterials such as polylactides and polyglycolides. It is important to note that it would be very difficult to discover an ideal composition by randomly exploring polymer design space. The use of automated procedures as a powerful tool in the synthesis of screening materials with optimized methods that can be incorporated into the workflow of multiple polymer compositions is emphasized.

The strategy for the library design is to use the monomers described in Chapter 3 and to fine-tune the corresponding composition with the incorporation of "free-acid" into the pendent chain and of PEG_{1k} into the backbone, as explained in Table 4.5 below.

Table 4.5 Design of library of 162 unique polymer compositions

Variable	Levels	Detail of change	Expected change
Backbone	6	DTR, HTR, BTR, CTR, PTR, GTR	Physical and chemical changes
Pendent chain	3	Ethyl (short) Hexyl (medium) Dodecyl (long)	Hydrophobicity, cell-material interactions, processability, degradation profiles
Free carboxylate	3	0, 15, 30 mol%	Tune degradation, mechanical properties, cell-material interactions
PEG_{1k}	3	0, 3, 7 mol%	Processability, can create water-rich regions in the polymer

The monomers used for this experiment were house-synthesized and used without further purification. The 162 polymers were synthesized with one repetition, for a total of 324 polymers. The library was synthesized in six different sessions on the automated parallel synthesizer, for a total of 54 unique polymers per session, or 27 unique polymer compositions with one repetition each, as shown in Table 4.6

Table 4.6 Monomers used per session and compositions synthesized per monomer

Session	Monomers	Unique compositions
1	DTE, DTH, DTD	poly(ATR carbonate)
2	HTE, HTH, HTD	poly(ATR-co-3%PEG_{1k} carbonate)
3	BTE, CTH, CTD	poly(ATR-co-7%PEG_{1k} carbonate)
4	PTE, PTH, PTD	poly(ATR-co-15%DT*t*B carbonate)
5	Z-GTE, Z-GTH, Z-GTD	poly(ATR-co-30%DT*t*B carbonate)
6	CTE, BTH, BTD	poly(ATR-co-15% DT*t*B -co-3%PEG_{1k} carbonate)
A = D, H, B, C, P, Z-G R = Ethyl, Hexyl, Dodecyl		poly(ATR-co-15% DT*t*B -co-7%PEG_{1k} carbonate)
		poly(ATR-co-30% DT*t*B -co-3%PEG_{1k} carbonate)
		poly(ATR-co-30% DT*t*B -co-7%PEG_{1k} carbonate)

The polymers were synthesized and worked-up in a record-time of nine days (within a six week period) without an optimized automated workflow. The work-up of each polymer was done manually, and the corresponding deprotection reactions were carried out with dry polymer samples. All the reported molecular weights are before deprotection and a result of the use of crude samples (i.e., after synthesis and before work-up). An attempt to analyze the molecular weights and explain the results obtained is based on the degree of polymerization (DP) of each polymer. This makes it necessary to divide the Mn obtained by the molecular weight of the repeating unit. The results for the unified library are presented in Figure 4.13.

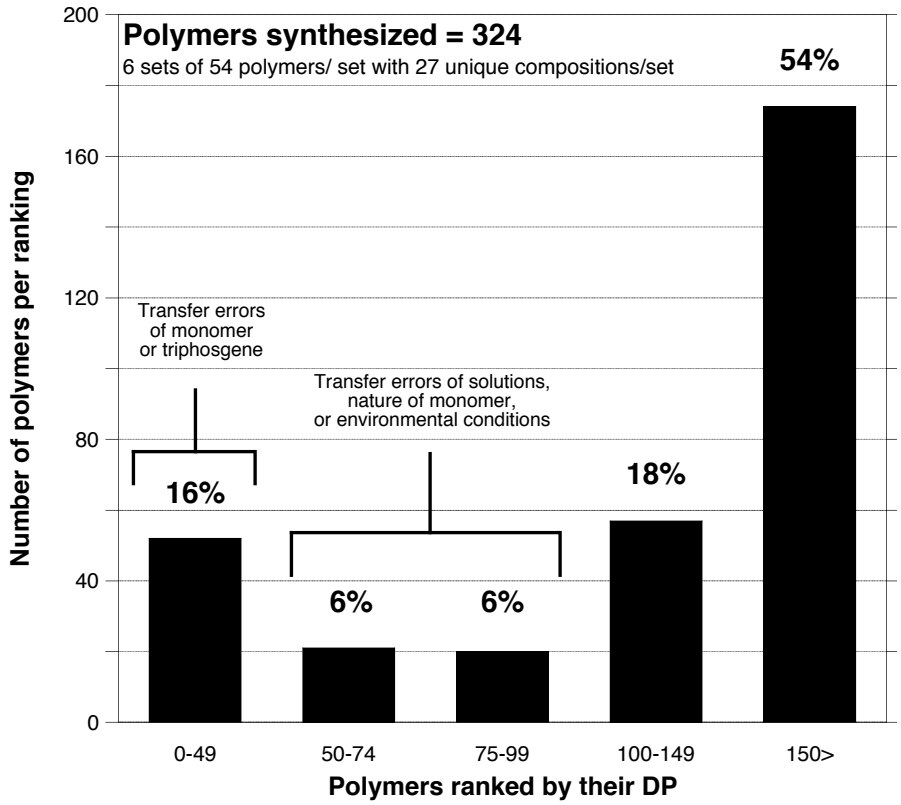

Figure 4.13 Library of polymers ranked by their degree of polymerization

Out of the 324 polymers that were synthesized, 28% (91 polymers) were ranked below a DP of 100. These polymers were not used for further analysis, since their relatively low degree of polymerization could have compromised their physical properties, e.g., T_g or modulus. Of these 91 polymers, 52 were the result of monomer or triphosgene transfer errors, as indicated by a DP lower than 50. During a reaction, transfer errors, especially those involving the triphosgene solution, are bound to happen due to the aspiration of the solution, since a backflow can be generated and in turn lead to the formation of air bubbles inside the Teflon tube. When such errors occur, the molecular weight is affected by the fact that only part of the reagent is transferred. This is minimized by adding a certain amount of equilibrium time before the needle is retracted

from the stock solution vial. Also, performing a pre-cut in the septa helps ameliorate the backflow. Another important aspect to note is the fact that while the aspiration of triphosgene solution happens, the whole system vibrates due to reactor vortexing. These vibrations can cause tubing connections to become loose over time, making it possible for air bubbles or air pockets to form inside the Teflon lines during reactions.

The rest of the polymers with a low degree of polymerization ($DP \geq 50 < 100$) were caused by solution or solvent transfer errors (i.e., monomer, co-monomer, triphosgene, or CH_2Cl_2 to complete the volume), by the nature of the monomer (i.e., purity), by environmental conditions (i.e., high relative humidity) or by method-dependent effects (i.e., reaction time, vortexing speed). It is estimated that, in the case of manual procedures, six out of ten different reactions will reach completion, making automated parallel synthesis the preferred method for synthesizing polymers intended for screening experiments and thus for the exploration of polymer design space.

Although an exhaustive statistical analysis is impossible due to an $n = 2$ per composition, a qualitative series of observations can be made in order to draw some conclusions about the effect of compositions, side chains, and backbone modifications on the degrees of polymerization obtained. In order to do this, the polymers are ranked by their DP and are then divided by a different parameter, as noted in Tables 4.7–4.9.

Table 4.7 Ranked polymers by DP divided in groups by their monomer composition

Rank by DP	Divided by composition[a]			
	homo	**co-PEG**	**co-DT*t*B**	**co-DT*t*B-co-PEG**
0 – 49	4	9	7	32
50 – 74	3	5	4	9
75 – 99	2	6	1	11
100 - 149	12	21	8	16
150 >	15	31	52	76

[a]Homopolymer:Copolymer-PEG:Copolymer-DT*t*B:Terpolymer = 1:2:2:4

When dividing polymers by their composition, some important observations can be made. For DP 0–49, the number of polymers expected follows the ratio of compositions, except for the case of terpolymers. As is logical, one would expect a higher number of failed reactions the more transfers that are performed per reactor. For DP 50–99, the ratio of polymers is maintained as the original ratio, except for copolymers with DT*t*B, since fewer polymers with this composition are observed. Polymers with DP>100, obey the 1:2:2:4 ratio of polymers synthesized, since 27:52:60:92 polymers were obtained. In general, when looking at the compositions, the trend that can be observed is that copolymers with DT*t*B constitute the type of polymer with the smallest number of low-DP-ranked samples, while terpolymers constitute the type of polymer with the highest number. This can be visualized by taking the polymers with DP<99 (9:20:**12**:**52**) and the polymers with DP>100 (27:52:60:92) and looking at their ratio on the basis of the corresponding compositions.

Table 4.8 Ranked polymers by DP divided in groups by their side chain

Rank by DP	Divided by side chain			
	Ethyl	Hexyl	Dodecyl	Mean
0 – 49	19	8	25	17
50 – 74	5	11	5	7
75 – 99	2	6	12	7
100 - 149	14	14	29	19
150 >	68	69	37	58

By looking at the polymers ranked by DP and grouped on the basis of their side chain, it is possible to see that, for the polymers with DP<100, the total amount of samples bearing an ethyl side chain was equal to the number of samples with a hexyl side chain. In general, this trend is correct, as the ratio is 1:1:1. However, for the dodecyl side chain containing polymers, the amount of polymers is almost twice as much as that found in ethyl and hexyl side chains. This means that it is possible for the dodecyl side chains to simply require much more time to react. The viscosity of the solutions is likely to be higher for dodecyl containing polymer solutions, and the polymerization process might be affected by this phenomenon. For polymers with DP>100, the ethyl and hexyl side chains containing polymers are once again the same, while, for the dodecyl side chain containing polymers, there are roughly 20 % less polymers, meaning that, under the conditions used, monomers with dodecyl esters do not reach high molecular weights as frequently as monomers with ethyl or hexyl esters in polycondensation reactions.

Table 4.9 Ranked polymers by DP divided in groups by their backbone modification

Rank by DP	Divided by backbone modification						
	D	H	B	C	P	Z-G	Mean
0 - 49	11	4	16	9	5	7	9
50 - 74	5	1	2	7	4	2	4
75 - 99	5	0	0	1	0	14	3
100 - 149	3	13	2	13	7	19	10
150 >	30	36	34	24	38	12	29

Looking at the backbone modification makes it possible to evidence the fact that the polymers derived from 4-hydroxyphenoxyacetic acid (P acid) and 4-hydroxyphenylacetic acid (H acid) yielded the highest DP among the polymers synthesized (roughly 35% more). However, it is important to note the fact that all the other sub-families yielded roughly the same numbers of high DP polymers (30 polymers in average). In the case of polymers derived from Z-*N*-(4-hydroxyphenyl)glycine, more polymers fell within a range of 100–149 DP, and fewer above 150, suggesting reactivity issues for those materials, e.g., steric hindrance. For polymers with DP<100, the numbers were very similar in general, with no obvious relationship between the type of backbone and the DP obtained.

By comparing the polymers' Mn and PDi, it is possible to see that polydispersity varies among the groups divided by their degree of polymerization, as seen in Figure 4.14.

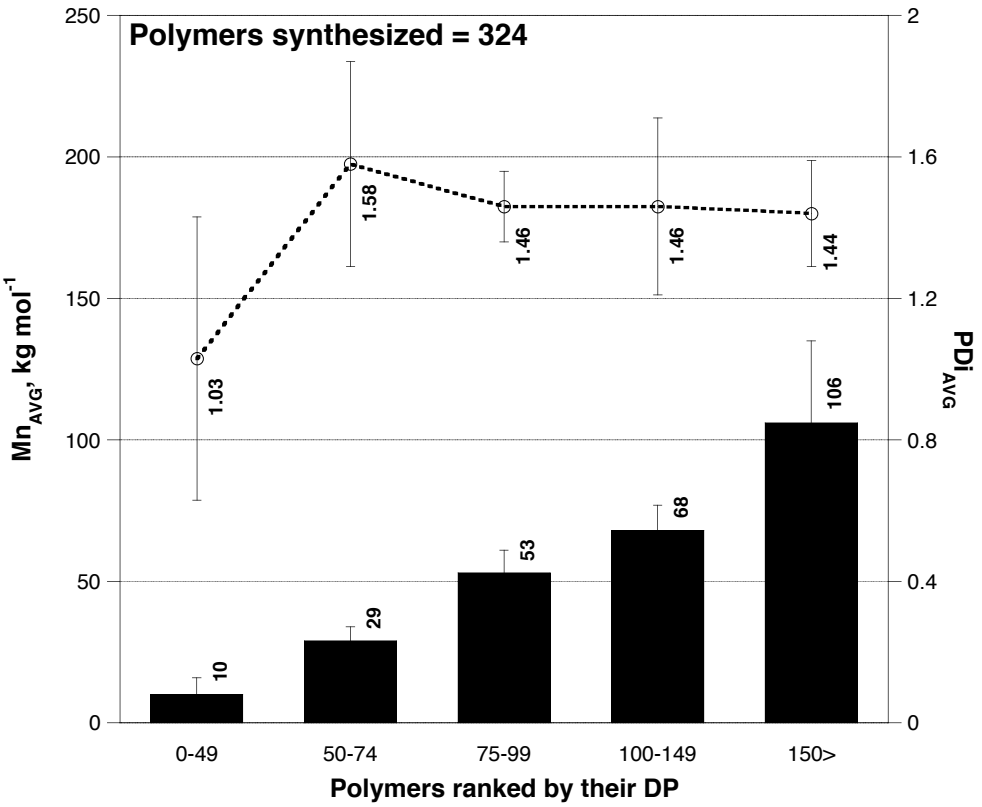

Figure 4.14 Molecular weights and degree of polymerization by ranking of DP

Starting with a DP of 75 the PDi is the same on average. However, it varies widely at lower DPs, as the chain is still growing and there are more variations in chain lengths and, therefore, compositions. It is important to note that, although the success rate, measured on the basis of a DP ≥ 100, is 72%, it is still higher than that obtained with manual procedures, where the estimated success rate would range from 50 – 65 % for a target molecular weight or composition. Based on these results, it is possible to conclude that the use of automated synthetic procedures is preferable to the use of manual synthesis during reaction optimization, during the initial screening of synthetic procedures, and for the synthesis of multiple samples with different compositions. In comparison to manual procedures, the automated synthesis method constitutes a

convenient way to accelerate the throughput for multiple samples, therefore making it possible to explore materials design space more effectively, as explained below.

4.2.6 Automated Parallel Synthesis *Vs.* Manual Synthetic Procedures

When performing automated synthesis, just as with manual procedures, preparing a large number of individual or repetitive experiments requires a significantly larger amount of time for planning and preparation than just running a single experiment. The optimization of reaction conditions constitutes a critical step in this process, regardless of whether manual or automated procedures are used. The only additional step involved in automated synthesis, when compared to manual procedures, is the creation of an automated workflow that emulates a manual procedure. The automated workflow includes the sequence of tasks that must be performed on the automated synthesizer, e.g., heating, cooling, transferring solutions, and vortexing. Switching from a manual protocol to an automated workflow usually takes a long time, but the effort required can be minimized with the use of Macro-tasks, which are individual instructions with a number of sequences embedded within them. For instance, the following steps: transfer of triphosgene solution, waiting time (i.e., reaction time), and quenching of the reaction after the reaction time, can be programmed as a single Macro-task rather than as individual steps. In order to minimize programming errors, a simulation of the automated workflow, as well as a dry run, might be needed before using expensive or limited reagents.

Therefore, the critical question is as follows: When are the efforts and time involved in automating the procedure and generating the workflow compensated for by savings in time, throughput, quality, etc.? As a specific example, the time required for the synthesis of various different quantities of polycarbonates (assuming several unique compositions) is estimated for both automated and manual synthesis in Table 4.10.

Table 4.10 Estimated time for the synthesis of 1 – 96 polycarbonates

No. Reactions	Unique compositions	Manual synthesis, h[a]	Operator time (manual), h[b]	Automated synthesis, h[c]	Operator time (automated), h[d]
1	1	3	2	7	4
2	1	4	2	6	3
4	1	8	4	6	3
8	2	15	7	8	3
16	4	30	15	11	4
32	8	60	29	18	5
48	12	90	44	25	7
64	16	120	59	33	9
80	20	150	73	40	10
96	24	180	88	48	13

[c]Includes: Calculations, set-up of synthesis apparatus, reagent preparation, reaction time, and clean-up.
[d]Includes: Calculations, set-up of synthesis apparatus, reagent preparation, and clean-up.
[c]Includes: Calculations, programming & simulation, set-up of reactors and equipment, reagent preparation, degassing of reactors or reagents, reaction time, and clean-up.
[d]Includes: Calculations, programming & simulation, set-up of reactors and equipment, reagent preparation, and clean-up.

For a single reaction, the total time required from start to finish for the automated synthesis method is several hours longer than that involved in manual synthesis. Furthermore, the total operator time (i.e., the time a person is engaged in performing the synthesis, excluding waiting and idle times) is two hours longer for automated synthesis than for manual synthesis. As should be expected, the use of an automated parallel synthesizer becomes significantly more efficient than the use of manual synthesis when a

larger number of reactions are involved, as seen in Figure 4.15. When 96 reactions or more are performed, the time saved remains the same. More importantly, the turnover rate for reactions performed in the automated synthesizer is faster, meaning that, by the time 96 reactions are completed manually, nearly 900 reactions will have been completed with an automated workflow (assuming non-supervised experiments).

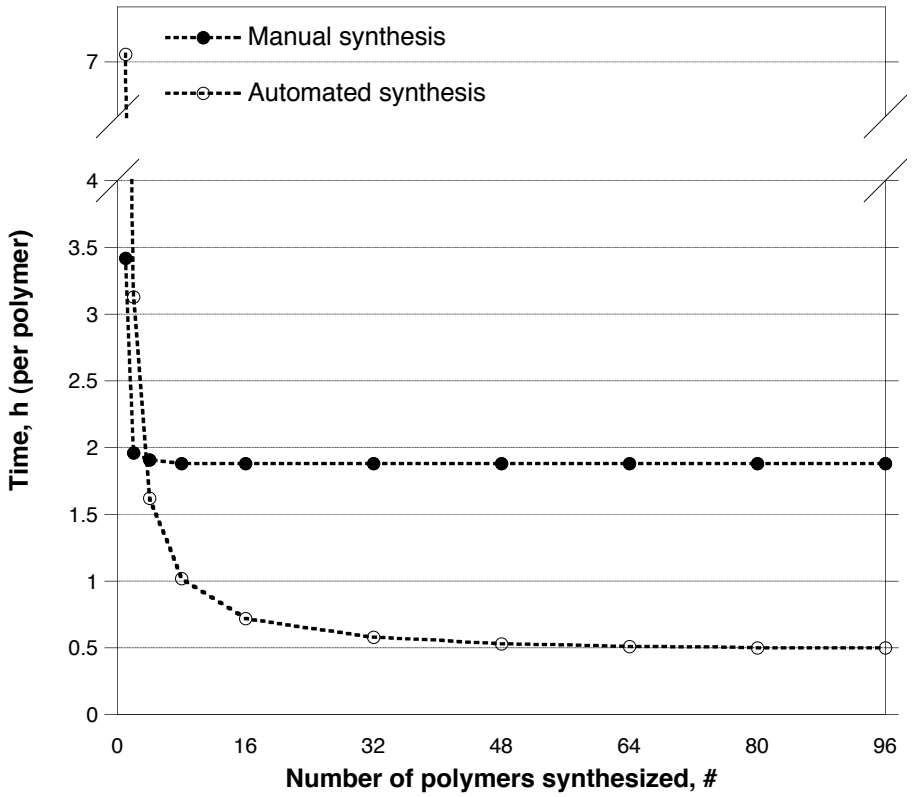

Figure 4.15 Time required per reaction as a function of the number of polymers synthesized

In the case of manual polycarbonate synthesis, triphosgene reactions require a significant amount of operator time. Even an experienced operator can only synthesize an average of four polymers a day by performing two reactions in parallel at a time. With an

optimized workflow, an automated synthesizer is able to reduce the time required to synthesize 96 polycarbonates (n = 4 for 24 unique compositions) from over a month to around 48 hours.

4.3 CONCLUSIONS

Automated parallel synthesis not only has the potential of improving many of the parameters that characterize existing manual procedures, but also of contributing a number of new benefits to this field. To further these advantages, this chapter has been used to describe a number of successful solutions to the synthetic challenges involved in automated synthesis methods, including drop-wise addition and toxic chemical handling.

Since one of the advantages of using an automated synthesizer is the fact that it enables scientists to explore different reaction conditions in parallel, the optimization of reaction conditions is very fast and reliable. In regard to these advantages, this chapter has been used to describe and validate procedures for the automated synthesis of tyrosine-based polycarbonates.

More specifically, the information shown in this chapter makes it possible to conclude that humidity control is essential when performing polycondensation reactions involving triphosgene, as hydrolysis can occur even with trace amounts of water. Various different bases were used in order to correct this situation, with pyridine being the best catalyst and acid scavenger for diphenol phosgenation. These results established the fact that using automated reagent dispensers with a precise control of volumes that can lead to specific compositions is feasible.

Continuing with the previous findings, a test library of random compositions was synthesized, which led to even more information regarding the optimization of reaction conditions. For a unified library of 162 polymers, automated synthetic procedures were generally more successful than manual methods, making automated synthesis a preferable method when preparing several screening compounds. Furthermore, comparing automated and manual synthesis methods for 1-96 polycarbonates demonstrated that automated synthesis provides substantial advantages by optimizing reactions, providing faster throughputs, and improving reproducibility. Moreover, it is also important to note that the ability of automated synthesis to significantly accelerate project timelines becomes more pronounced when a larger number of polymers are synthesized.

Finally, one of the most important advantages of automated synthesis is the preservation of "know-how:" Once a workflow has been optimized and archived, any trained chemist can reproduce the synthetic results initially obtained by highly trained chemists, thus providing a benefit that not only extends across different processes, but also across different individuals.

5. CHARACTERIZATION OF SELECTED POLYCARBONATES

5.1 INTRODUCTION

The creation of large libraries of materials not only depends on the synthetic aspect behind the process, but also on the characterization required. Since numerous different polymers are generated during automated parallel synthesis, a wide range of physical properties and applications has to be measured for the corresponding materials. While it is true that tens, not to mention hundreds or thousands, of materials cannot be fully characterized in a short period of time (due to the limited availability of high-throughput characterization methods), the methods selected can be such that they make it possible to obtain the best possible results by correlating properties or trends within a structurally-related family of polymers. As Campbell, Pethrick, and White conclude, "being able to identify and characterize materials is not just of academic interest but also of commercial and environmental concern" when referring to the actual application in which a material would be involved.[168]

One of the disadvantages of synthesizing degradable polymer libraries on a very small (e.g., microgram to milligram) scale is the availability of material for performing traditional polymer analyses and determining the corresponding fundamental properties (e.g., absolute molecular weights, mechanical properties, degradation profiles, solubility indices, surface properties). In the case of polymeric materials intended for biomedical applications, the number of polymer analyses is increased significantly due to the fact that cell-material interactions must be studied according to multiple aspects (e.g.,

biocompatibility, cytotoxicity, degradation). This major disadvantage has been addressed by several groups by adapting high-throughput characterization techniques available in the drug, protein, and chemical discovery industries to different types of materials.[8, 18, 21, 69, 81, 83, 169-176] Other research groups rely more on traditional characterization techniques of several structurally-related polymers, making it possible to obtain enough data to perform computational data modeling and predict the physical or biological behaviors of different uncharacterized materials.[11, 173, 177-180]

This chapter contains an analysis of the library of polymer synthesized in Chapter 4. The analysis is based on thermal characterization, or, more specifically, Differential Scanning Calorimetry (DSC). The main purpose is to determine trends related to the physical behavior of polymers and to group polymers on the basis of potential applications. Moreover, the molecular compositions of different polymers are calculated from ^{1}H-NMR data and simultaneously assessing the synthetic capabilities of automated parallel procedures. Finally, a few selected polymers are evaluated in regard to their surface energy properties, making it possible to explain how, on certain occasions, basic characterization (i.e., air-water contact angle) is not adequate for explaining more complicated phenomena, such as cell-material interactions, in a straightforward manner.

Since a material's properties can change depending on the corresponding shape and processing, this chapter deals exclusively with "as synthesized" materials and 2-D spin-coated films. The data obtained has been carefully interpreted in order to avoid any generalizations regarding the polymer's physical properties, and the interpretations included have focused mostly on the field of polymeric biomaterials.

5.2 RESULTS AND DISCUSSION

5.2.1 Acidolysis of *tert*-Butyl Esters Prior to the Characterization of Tyrosine-Derived Polycarbonates

A deprotection step via means of an acidolysis mechanism to remove the *tert*-Butyl ester was needed prior to the characterization of the DT*t*B containing polycarbonates. Kohn and colleagues have investigated different ways of obtaining a free-carboxylate as the pendent chain without compromising the molecular weight of a high polymer.[181] To accomplish the deprotection of *tert*-Butyl esters, the DT*t*Bs containing polymers were dissolved in CH_2Cl_2, and TFA was added in order to cleave the *tert*-Butyl ester, as shown in Figure 5.1. The procedure is described in Chapter 2.

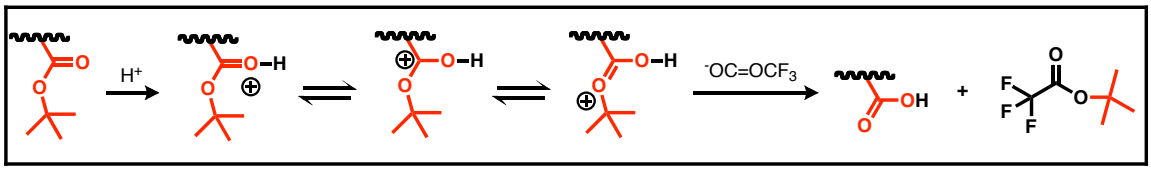

Figure 5.1 Acidolysis mechanism occurring during the deprotection step of DT*t*B-containing polymers

This reaction, used for the purpose of obtaining a free-carboxylate, is preferable to other methods, e.g., the cleavage of the Cbz group through hydrogenolysis, since these methods often use heavy metals (e.g., Pd, Pt) that cannot be totally removed after purification.[181] This is of particular concern if the material is intended for use in the manufacture of an implant for biomedical applications. Hydrolytic *tert*-Butyl ester

cleavage can be performed, but can affect the molecular weight of the polycarbonate, since the carbonate bonds can be hydrolytically cleaved (as shown in Figure 5.2).

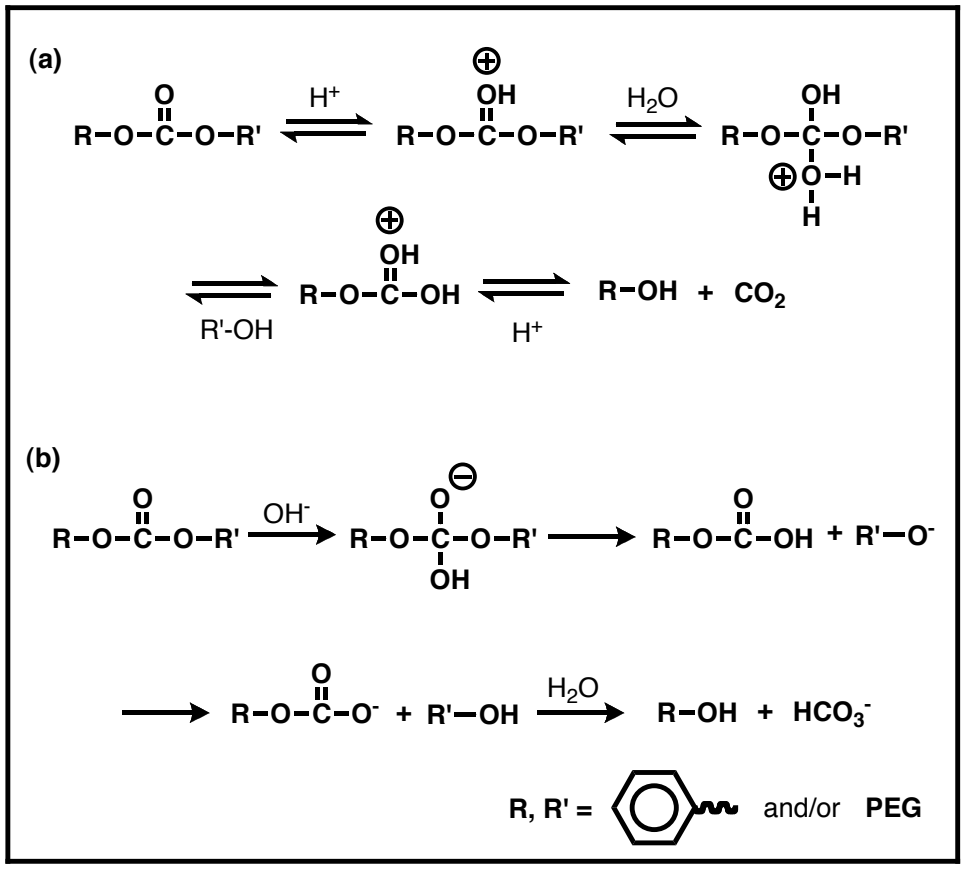

Figure 5.2 Acid and base-catalyzed hydrolysis of carbonate bonds

A potential issue involved in deprotection via the acidolysis mechanism is carbonate hydrolysis, which may occur if any moisture is present. Because of this, the deprotection of *tert*-Butyl esters in tyrosine-derived polycarbonates should be performed in worked-up and dried polymers. When performing the deprotection process under anhydrous conditions, Kohn and colleagues have obtained > 99.9% free carboxylate while keeping the loss of molecular weight at a maximum of 10%.[181] DT*t*B-containing

polymers were deprotected in 20-mL scintillation vials as an additional procedure after the work-up. The resulting polymers were precipitated in water and lyophilized for at least 48 hours before their characterization. Because there is no parallel method available for deprotecting the Cbz or Z group from the L-Tyrosine-N-[2-((benzyloxycarbonyl)(4-hydroxyphenyl)amino)-1-oxoethyl]-Alkyl Ester containing polymers, these materials were not tested for any of the physical properties described in this chapter.

5.2.2 Mass-Per-Flexible-Bond Analysis of Polymer Library

Since analyzing the entire library with regular polymer characterization techniques is not efficient when using traditional methods, an attempt was made to characterize several polymers and identify trends thereafter. While most polymers within the functional range of DP yielded 150-220 mg after work-up and purification, others were difficult to isolate, especially following *tert*-Butyl ester deprotection. An analysis of utmost importance, regardless of the type of polymer analyzed, is that concerning the polymer's glass transition temperature, or T_g. The T_g is the critical temperature at which a polymer changes its physical behavior and transitions from being glassy (hard and brittle) to being rubbery (soft and flexible).[182, 183] The T_g is used to define a physical "pseudo" second-order thermodynamic transition, meaning that this transition does not occur under thermodynamic equilibrium.[184] This physical transition is extremely important in terms of the processing and end-use of any polymer. For instance, in the case of biomaterial applications, the T_g can be an extremely useful indicator when determining whether a polymer should be used in hard or soft tissue applications. To

continue with this example, it would be possible to use a polymeric biomaterial with a T_g lower than the temperature of the human body (37 °C) to create a drug delivery device or a ligament graft. However, this same biomaterial might prove deficient when used for bone grafts or spine fusion devices.

It has been shown that there is a correlation between the T_g and the ratio of mass to the number of flexible bonds of the repeating unit in polymers.[183, 184] This parameter is known as the "mass-per-flexible-bond" (*M*/*f*), and is a simplified representation of the polymer's conformational entropy.[184, 185] This assumes that conformational changes in a polymer chain are controlled by the bonds of the repeating unit that are flexible.[182, 184] Because the correlation between the T_g and the *M*/*f* is linear, polymer class-specific constants A and C can be observed in Equation 5.1 and should reflect similar interactions and non-interactions within a given class of polymers:

$$T_g = A\left(\frac{M}{f}\right)_P + C \tag{5.1}$$

By using this simple correlation, which can be compared to other, more complicated semi-empirical methods, Kohn and colleagues have effectively predicted the T_g of tyrosine-derived co-and terpolymers with a high degree of correspondence with experimental data.[185] When dealing with the creation of a new library of materials, the "mass-per-flexible-bond" principle provides a good way of finding polymer property trends with simple information obtained from Differential Scanning Calorimetry experiments.

The first step involved in applying this method to the synthesized library of polymers was to assign the flexibility of the bonds in the repeating units. Covalent bonds are considered to be flexible ($f > 0$) if rotation around them causes a conformational change in the polymer chain. For the tyrosine-derived polycarbonates, some bonds were assumed to be non-flexible ($f = 0$), i.e., C-OH and C-CH_3, due to the small size of the hydrogen atom. Also, the amide bond is not flexible ($f = 0$) either, due to its double-bond character. The phenyl ring was assigned a flexibility of 1.5 because of its planar conformation, which does not change significantly in the event of rotation. The flexibility of the repeating units in the library is shown in Figure 5.3, below.

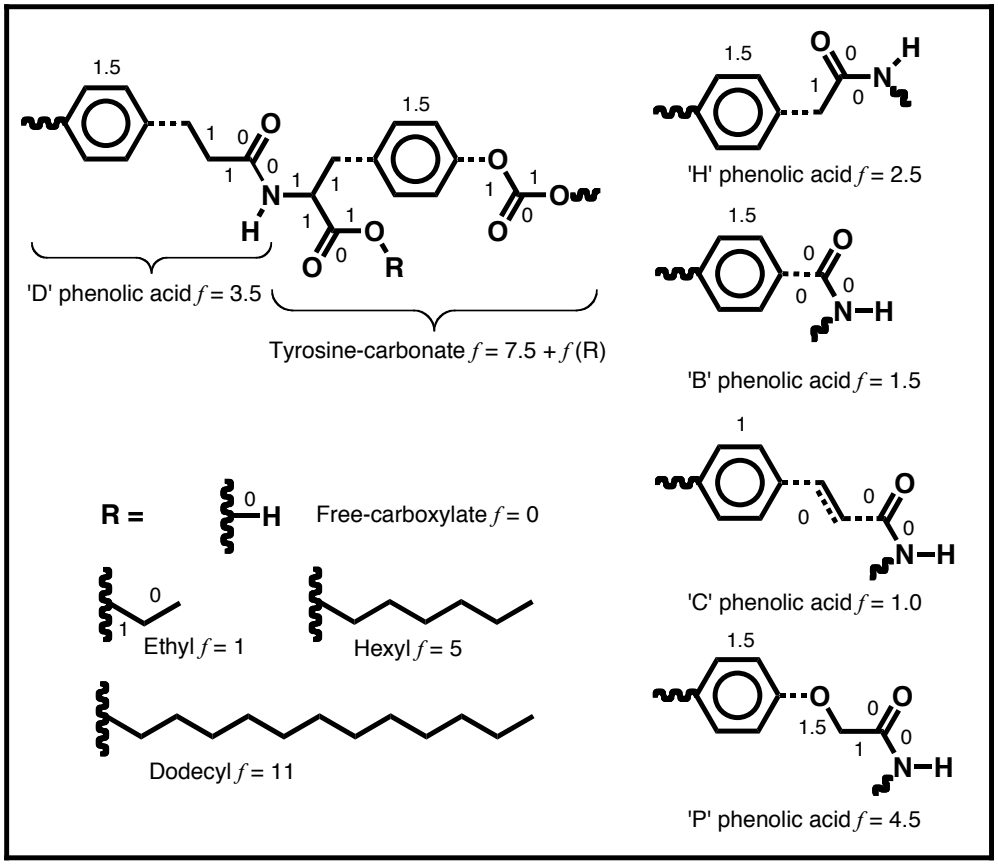

Figure 5.3 Assignment of flexible bonds for diphenol-carbonate repeating units

The tyrosine-carbonate has 7.5 flexible bonds (f = 7.5), without taking into account the ester pendent chain or functional group. In regard to the "parent" repeating unit, the DTE-carbonate, the total number of flexible bonds is 12 (f = 12). For the HTRs and BTRs, the assignment of the bonds consists of one and two less than the DTRs respectively, since the number of carbons in the backbone decreases. For the CTRs, there is an exception to the counting rule due to the resonance effect of the ring, the double bond, and the amide functional group, making the number of flexible bonds decrease to f = 9.5. In the case of the PTRs, yet another exception to the counting rule is made, since the oxygen in the backbone provides extra flexibility to the –O–C– bond.

For different classes of polymers, Schneider described a "crankshaft-like" motion in polymers with *n*-alkylic side chains that effectively increased the T_g when the number of methylenes was higher than four, which was supposedly caused by the interactions of the methylene units, which could even allow side-chain crystallization in different polymers.[183] The polymer systems described in this thesis are amorphous in nature and do not show a melting temperature transition, which is why the side chain's "crankshaft-like" motion was not considered for these systems.

The polymers' mass-per-flexible-bond for co- and terpolymers was calculated as the weighed average of the mass-per-flexible-bond of each constituent repeating unit, as shown in equation 5.2, where M_i is the molecular weight of the corresponding repeating unit, "i" in $gmol^{-1}$; f_i is the number of flexible bonds in the repeating unit, as explained above; and n is the total number of repeating units (i.e., from the number of monomers) in the polymer. In every instance, the composition of a polymer is expressed as the mass fraction of its repeating units. Equation 5.3 was used to convert the mole percent to mass

fractions. In this equation, x_i is the mass fraction of the repeating unit "*i*"; m_i is the mole fraction of said repeating unit; M_i is the molecular weight of the corresponding repeating unit, "*i*" in $gmol^{-1}$; and *n* is the total number of repeating units in the polymer.

$$\left(\frac{M}{f}\right)_{\mathrm{P}} = x_1\left(\frac{M_1}{f_1}\right) + x_2\left(\frac{M_2}{f_2}\right) + x_3\left(\frac{M_3}{f_3}\right) + \ldots + x_n\left(\frac{M_n}{f_n}\right) = \sum_{i=1}^{n}\left(\frac{M_i}{f_i}\right) \tag{5.2}$$

$$x_i = \frac{m_i M_i}{\sum_{i=1}^{n}(m_i M_i)} \tag{5.3}$$

An important observation is that the "mass-per-flexible-bond" approach does not take into account the effect of chain ends, and thus is only valid for infinite molecular weights. However, based on this information, applying this method can result in data noise when working with low molecular weights before a T_g plateau is reached.[186]

Table 5.1 summarizes the calculated number of flexible bonds and the "mass-per-flexible-bond index" for the repeating units of the polymers synthesized in this thesis. The repeating unit for PEG_{1k} (i.e., PEG_{1k}-carbonate) has 71 flexible bonds, calculated as follows: The molecular weight of a PEG_{1k} repeating unit is 44 $gmol^{-1}$, or 23 effective repeating units (1000 $gmol^{-1}$/44 $gmol^{-1}$). The number of flexible bonds in a PEG_{1k} repeating unit is three ($f = 3$), based on the increased flexibility of the backbone due to the oxygen linked to an aliphatic carbon. This means that PEG_{1k} has 69 effective flexible bonds, plus two ($f = 2$) from the carbonate, resulting in a total of 71 flexible bonds ($f = 71$).

Table 5.1 Summary of calculated flexibility and "mass-per-flexible-bond" ratios

Repeating unit	M[a] (gmol^{-1})	f[b]	M/f[c]
DTE-carbonate	383.39	12	31.95
DTH-carbonate	439.50	16	27.47
DTD-carbonate	523.66	22	23.80
HTE-carbonate	369.36	11	33.58
HTH-carbonate	425.47	15	28.36
HTD-carbonate	509.63	21	24.27
BTE-carbonate	355.34	10	35.53
BTH-carbonate	411.44	14	29.39
BTD-carbonate	495.60	20	24.78
CTE-carbonate	381.37	9.5	40.14
CTH-carbonate	437.48	13.5	32.41
CTD-carbonate	521.64	19.5	26.75
PTE-carbonate	385.36	13	29.64
PTH-carbonate	441.47	17	25.97
PTD-carbonate	525.63	23	22.85
DT-carbonate	355.34	10	35.53
PEG_{1k}-carbonate	1025.99	71[d]	14.45

[a] Molecular weight of repeating unit.
[b] Number of flexible bonds of repeating unit.
[c] Mass-per-flexible-bond of repeating unit.
[d] $3 \times 23 = 69$ flexible bonds in PEG_{1k} + 2 for carbonate = 71.

The library synthesized contains different variables: six different backbones (of which only five are analyzed), three different pendent chains, the incorporation of free carboxylate, and the incorporation of PEG_{1k}. An attempt was made to understand the interactions present in the different polymer sub-families by plotting the experimental T_g values against the calculated *M/f* values. In most cases, two different samples were obtained from the synthesis, in which case the average T_g was plotted. On the other hand, some of the polymers samples were difficult to isolate (i.e., low molecular weights), and their T_g was not measured as a result. Every sample that was present in solid form was measured, regardless of the corresponding degree of polymerization (as discussed in Chapter 4). Some of the graphs obtained seem to feature a considerable amount of noise, which is due to the difference between the molecular weights of some of the samples.

However, and for the purpose of verifying the model, every sample that was measurable was included in the graphs. At the end, out of 135 different polymer compositions, 112 were effectively measured for T_g (~80% of the planned measurements).

Figure 5.4 shows a graph of T_g versus calculated $(M/f)_P$ by polymer type (i.e., homopolymers, coplymers, terpolymers). In general, the addition of free carboxylate results in a pronounced increase in T_g when compared to homopolymers. In the case of tyrosine-derived copolymers with PEG_{1k}, and even with low PEG_{1k} concentrations (<7%), the effect of adding a flexible long chain, PEG, overcomes the addition of free carboxylate, as observed by comparing the curves corresponding to copolymers with PEG_{1k} and terpolymers.

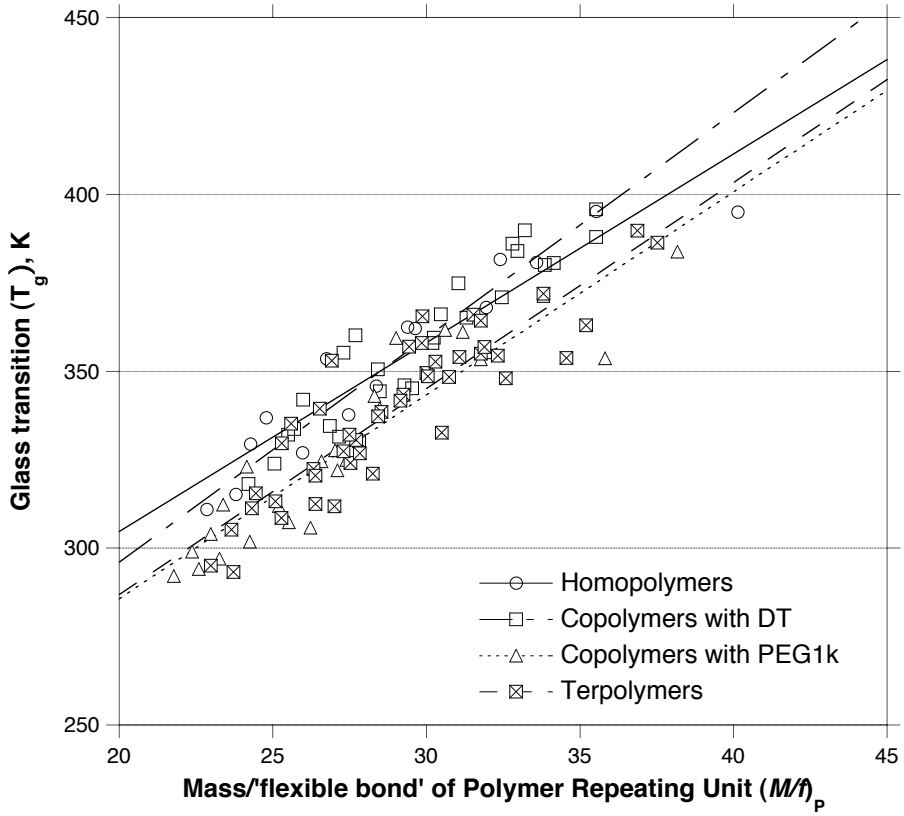

Figure 5.4 Experimental glass transition temperature plotted against the calculated mass-per-flexible bond of the library, arranged by type of polymer

When comparing the polymers on the basis of their backbone composition, Figure 5.5 shows that there are some disparities between the polymers' predicted behavior and the actual one. With an average $(M/f)_P$~28, the polymers derived from DTR, HTR, and PTR have a very similar T_g as expected, but as the $(M/f)_P$ increases (flexibility decreases), the polymers containing DTRs and PTRs seem to feature a higher T_g, while the ones containing HTRs seem to feature a lower one, leading to the assumption that the backbone effect is not as specific as the effect due to the polymers' composition.

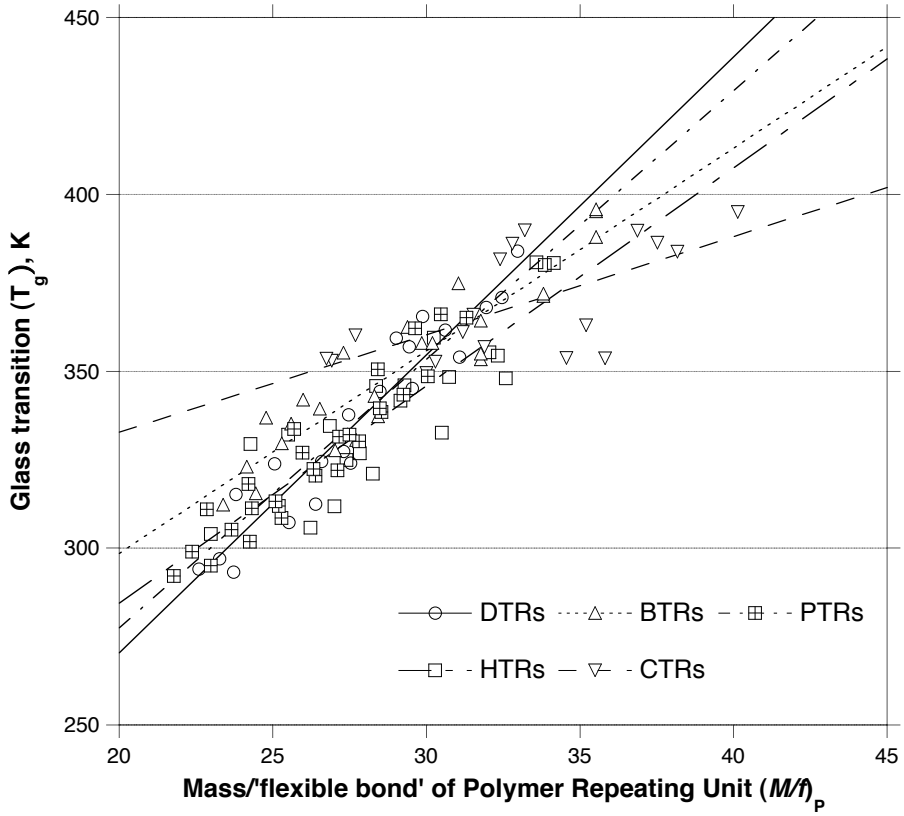

Figure 5.5 Experimental glass transition temperature plotted against the calculated mass-per-flexible bond of the library, arranged by type of backbone

Plotting the same data according to pendent chains results in Figure 5.6, which shows that there is less scatter for long pendent chains (dodecyl) and greater scatter for shorter pendent chains (ethyl). This can be a reflection of the side chain interactions that are common in long hydrocarbon chains (hydrophobic-hydrophobic). It is also possible to observe that the resulting flexibility index $(M/f)_P$–based order is as follows: Dodecyl<Hexyl<Ethyl side chains. As the length of the side chain increases, the pendent chain becomes the determining factor in regard to the flexibility index. On the other hand, when the side chains are shorter, the flexibility index is more dependent on the type of

polymer, reflecting other types of interactions, such as hydrogen bonding between amide and carbonyls and carboxylates and PEG.

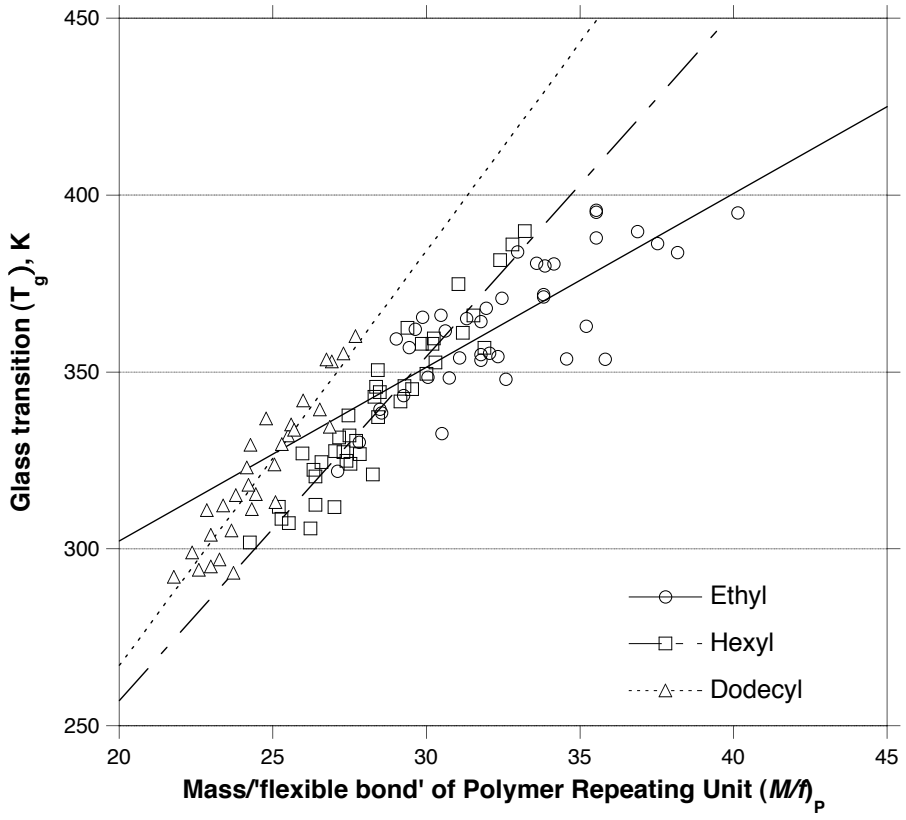

Figure 5.6 Experimental glass transition temperature plotted against the calculated mass-per-flexible bond of the library, arranged by type of side chain

Table 5.2, below, provides a summary of the fit parameters for the graphs presented in this section, based on the linear correlations resulting from Equation 5.1.

Table 5.2 Linear fit MPFB parameters for the library of polymers grouped according to classes

Class	A	C	R^2
DTRs	8.418	102.170	0.915
HTRs	6.153	161.480	0.751
BTRs	5.729	183.970	0.870
CTRs	2.770	277.430	0.441
PTRs	7.587	125.830	0.898
Ethyl	4.910	204.130	0.625
Hexyl	9.732	62.504	0.901
Dodecyl	11.734	32.540	0.863
Homopolymers	5.333	198.150	0.894
DT-copolymers	6.344	169.250	0.896
PEG-copolymers	5.745	170.830	0.866
Terpolymers	5.824	170.520	0.802
All polymers	6.246	163.580	0.805

As mentioned earlier, an important benefit of evaluating the flexibility of polymers is that this evaluation makes it possible to determine which materials to choose for a specific application. Figures 5.7 and 5.8 show the T_g of all the polymers measured plotted against the corresponding flexibility index, $(M/f)_P$, in order to describe how the flexibility index of a material can be used in order to classify polymers according to the end-use to which they are best suited. As a specific example, Figure 5.7 is used as an attempt to draw limits based on the thermal processing (i.e., compression molding) that polymers will undergo. The lower limit for a polymer that is intended for use in structural applications is 325 K. The reason for this temperature is that polymers will usually adsorb water and that water can penetrate into the device, effectively decreasing the T_g due to polymer chain plasticization. In the case of structural applications (e.g., spinal fusion), it is desirable for the polymer used for the device to always be below its T_g in order to prevent failures due to the transition from a hard and brittle state to a soft and

rubbery state. A margin of ~5% between the body temperature and the T_g of the material is necessary in order to account for water plasticization effects. The higher limit is set on 400 K, based on the average decomposition temperature of tyrosine-derived polymers: ~250 °C (523 K).[95, 96, 98] For thermal processing procedures such as pressing and extrusion, polymers are traditionally worked at 50 to 75 °C above their T_g. Therefore, using a temperature ~50 °C below the corresponding decomposition temperature is desirable in order to avoid thermal degradation and other side reactions that can occur at high temperatures (e.g., crosslinking, oxidation). Based on this information, it can be suggested for polymers with a flexibility index, $(M/f)_P$, of 26 to 38 to be used for structural applications. Based on the calculated flexibility indices, out of the 135 polymers synthesized, 92 could theoretically be used for this purpose. This makes it possible for researchers to make deductions regarding a material's design and synthesis on the basis of calculated data from a test library.

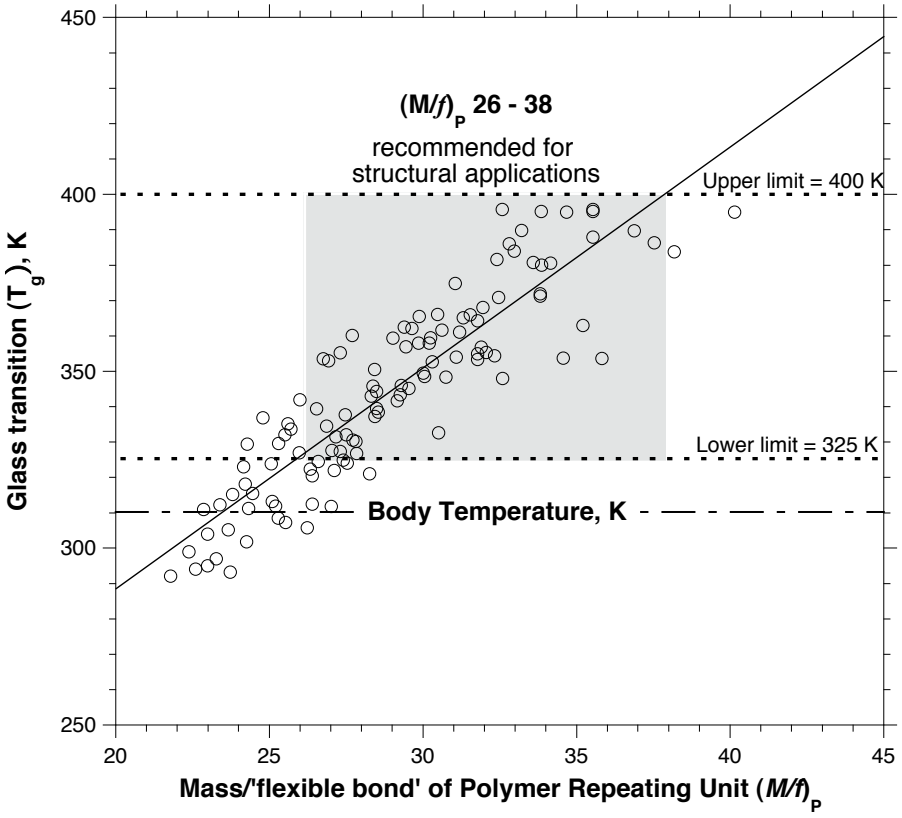

Figure 5.7 Experimental glass transition temperature plotted against the calculated mass-per-flexible bond of the library, suggesting a flexibility index range for biomaterials with structural applications

One can go as far as to suggest several device applications based on this information. Figure 5.8 shows how, for a library of tyrosine-derived terpolymers, a researcher can start his/her exploration of polymer space by using a simple parameter, such as the flexibility index. Even considering the fact that the R^2 value for the library of polymers synthesized is 0.805, being able to approximate a physical property as important as the T_g is an invaluable tool for any materials scientist.

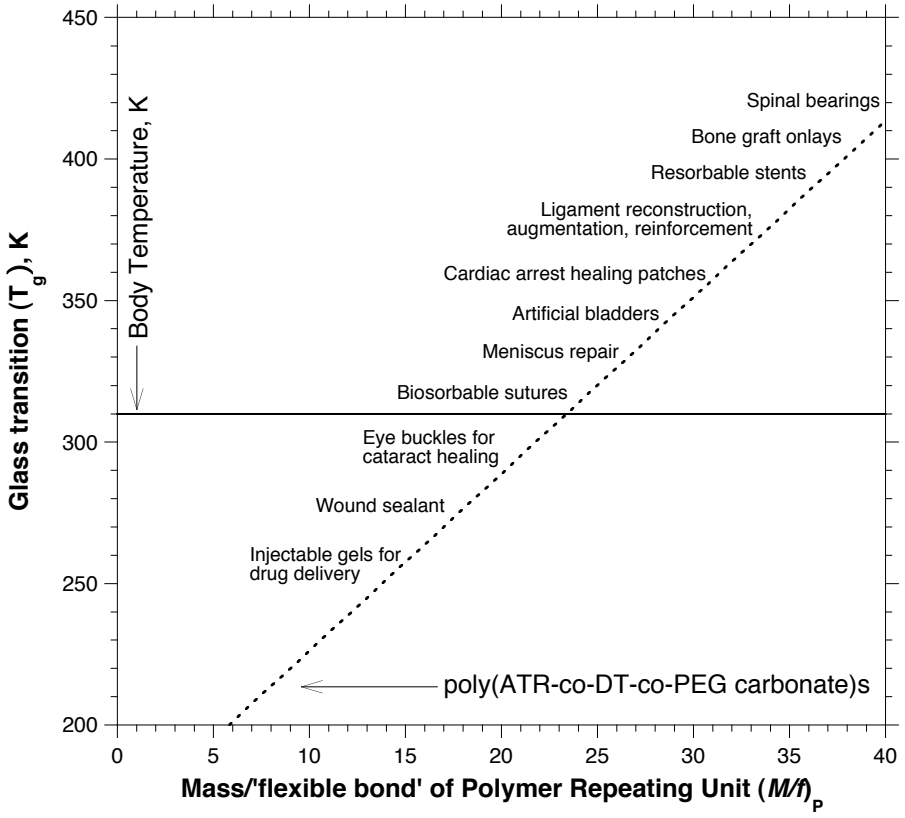

Figure 5.8 Flexibility index as a parameter used to make inferences regarding the design and selection of biomaterials intended for a specific application

By having this type of data readily available, the "mass-per-flexible- bond" principle can then be used to "calculate" a polymer structure (i.e., predict the polymer structure) based on a target T_g, since coefficients A and C are known, as described previously.[185] This is particularly important if a set of monomers is preferred to another one, since it provides scientists with the flexibility of having control over polymer compositions on the basis of a desired physical property. Complementary data can be gathered from the mechanical properties measurements conducted for three poly(CTR carbonate)s, as shown in Figure 5.9 (ethyl, hexyl, and dodecyl), where it is

obvious that the mechanical properties of a material can be associated to the material's thermal properties in order to serve as a basis for comparisons.

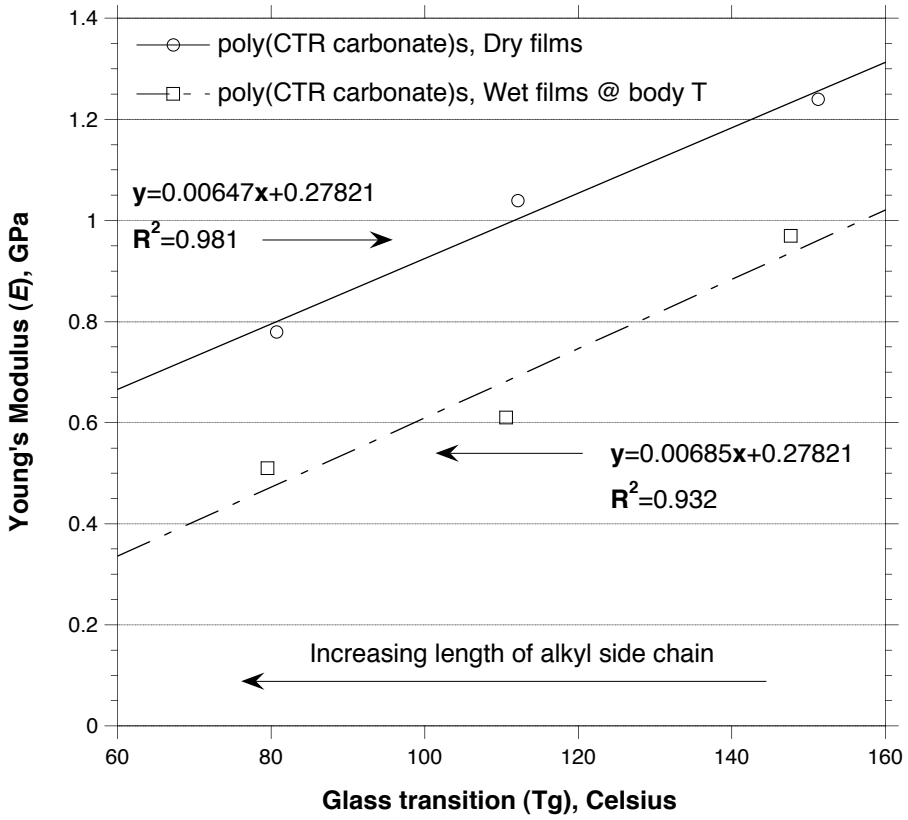

Figure 5.9 Relationship between tensile modulus and glass transition temperature for dry and wet polymer films of poly(CTR carbonate)s with ethyl, hexyl, and dodecyl side chains

5.2.3 ^{1}H-NMR Characterization of Randomly Selected Polycarbonates

Traditional ^{1}H-NMR is a useful tool for studying co- and terpolymer compositions in a semi-quantitative manner. This can result in an accurate analysis of compositions based on the areas under the curve (i.e., integration) of the peaks from

NMR spectra. However, due to the fact that these analyses are not performed under rigorous quantitative conditions, the molar compositions obtained are only approximations, making them adequate for screening purposes only.[187] In this section, the ^{1}H-NMR analyses of 18 randomly selected polymers (two homopolymers, four copolymers with DT, four copolymers with PEG, and eight terpolymers) are interpreted on the basis of polymer composition and molecular structure. The list of polymers analyzed, as well as the peaks used for this analysis, is given in Table 5.3, below.

Table 5.3 Randomly selected polymers for ^{1}H-NMR analysis

Polymer by code number	Polymer name	Peaks used
1	poly(HTH carbonate)	
2	poly(BTE carbonate)	
3	poly(DTE-co-15%DT carbonate)	7.23-6.79 (8.92H, aryl), 4.09 (1.89H, -O-CH2-)
4	poly(DTH-co-30%DT carbonate)	7.25-6.95 (9.03H, aryl), 4.26-3.88 (1.89H, -O-CH2-)
5	poly(HTH-co-30%DT carbonate)	8.61 (0.94H, amide), 8.24 (0.44H, amide)
6	poly(PTE-co-15%DT carbonate)	7.22-6.60 (9.34H, aryl+amide), 5.86 (0.03H, amide), 1.25-1.10 (2.65H, -CH3)
7	poly(DTH-co-3%PEG_{1k} carbonate)	4.35 (0.94H, α-proton), 3.33 (1.59H, PEG)
8	poly(CTE-co-3%PEG_{1k} carbonate)	4.62 (1.12H, α -proton), 3.66-3.44 (3.65H, PEG)
9	poly(BTE-co-3%PEG_{1k} carbonate)	5.01 (0.78H, α -proton), 3.82-3.35 (2.69H, PEG)
10	poly(PTE-co-3%PEG_{1k} carbonate)	4.90 (0.90H, α -proton), 3.80-3.53 (2.56H, PEG)
11	poly(HTE-co-15%DT-co-3%PEG_{1k} carbonate)	7.23-6.76 (8.68H, aryl), 4.10 (1.80H, -O-CH2-), 3.69-3.54 (3.11H, PEG)
12	poly(HTE-co-30%DT-co-7%PEG_{1k} carbonate)	8.61 (0.86H, amide), 8.25 (0.31H, amide), 3.62-3.39 (7.81H, PEG)
13	poly(BTE-co-15%DT-co-3%PEG_{1k} carbonate)	8.95 (0.79H, amide), 8.57 (0.15H, amide), 3.62-3.41 (3.19H, PEG)
14	poly(BTH-co-30%DT-co-7%PEG_{1k} carbonate)	8.94 (0.92H, amide), 8.24 (0.51H, amide), 3.77-3.44 (8.03H, PEG)
15	poly(CTE-co-15%DT-co-3%PEG_{1k} carbonate)	8.61 (0.84H, amide), 8.25 (0.14H, amide), 3.63-3.31 (3.14H, PEG)
16	poly(DTE-co-15%DT-co-3%PEG_{1k} carbonate)	7.22-6.84 (9.00H, aryl), 4.10 (1.94H, -O-CH2-), 3.65 (2.07H, PEG)
17	poly(PTD-co-15%DT-co-3%PEG_{1k} carbonate)	7.23-7.10 (7.18H, aryl), 6.99 (1.13H, amide), 6.86 (2.09H, aryl), 5.87 (0.54H, amide), 4.92 (0.90H, α -proton), 3.62 (1.95H, PEG)
18	poly(PTD-co-30%DT-co-3%PEG_{1k} carbonate)	7.23-7.04 (8.53H, aryl), 6.99 (1.23H, amide), 6.86 (2.09H, aryl), 5.92 (0.49H, amide), 4.92 (0.87H, α -proton), 3.62 (1.85H, PEG)

The reason why the peaks used in the analyses are indicated is the fact that DMSO-d_6 was used for some polymers, while $CDCl_3$ was used for others. Moreover, in certain instances, the spectrum obtained was rather noisy due to shimming or to the nature of the sample. Finally, certain polymer spectra were difficult to phase evenly, resulting in a natural error when performing manual integrations.

The NMR analyses were performed as explained in Chapter 2. Once the spectra were recorded, the curves were integrated with MestRe Nova software (Mestrelab Research SL, Spain). Following the integration of the area under the curve, a number of different peaks were selected on the basis of the repeating unit so as to obtain the corresponding composition. The process for poly(CTE-co-3%PEG_{1k} carbonate) is included here as an example:

1) Take the signal for the α-proton at δ = 4.62, which integrates for 1.12 protons. Calculate the relative moles of CTE:

$$\text{Relative moles of CTE monomer} = \frac{\text{Integral for } \alpha\text{ - protons}}{\#\text{ of } \alpha\text{ - protons}} = \frac{1.12}{1} = 1.12$$

2) Take the signal for PEG_{1k} at δ = 3.66-3.44, which integrates for 3.65 protons. Calculate the relative moles of PEG_{1k}:

$$\text{Relative moles of } PEG_{1k}\text{ co - monomer} = \frac{\text{Integral for } PEG_{1k}}{\#\text{ of } PEG_{1k}\text{ group protons}} = \frac{3.65}{88} = 0.0415$$

There are a total of 23 repeating units $–CH_2\text{-}CH_2\text{-}O-$ for PEG_{1k}, meaning that there are 92 protons (rounded-up) in the molecule. However, only about 88 are part of the NMR signal, since the end-groups have a slightly different shift (PEG-carbonate-PEG, PEG-carbonate-phenol) that can be blocked by tyrosine-derived diphenol signals.

3) Calculate the mol% of PEG_{1k} in the polymer:

$$\text{mol\% of } PEG_{1k} = \frac{\text{Rel. moles of } PEG_{1k}}{\text{Rel. moles of } PEG_{1k} + \text{Rel. moles of CTE}} \times 100 = 3.57\%$$

The results for the composition analyses are given in Table 5.4, along with the percent difference for DT, PEG_{1k}, or both.

Table 5.4 Calculated mol percentages of co- and terpolymers by ^{1}H-NMR

Polymer by code number	DT mol% by NMR	Percent difference, DT composition	PEG mol% by NMR	Percent difference, PEG_{1k} composition
1				
2				
3	15.24	-2%		
4	19.82	34%		
5	31.88	-6%		
6	15.25	-2%		
7			1.89	37%
8			3.57	-19%
9			3.77	-26%
10			3.13	-4%
11	16.51	-10%	3.15	-5%
12	24.63	18%	7.05	-1%
13	15.36	-2%	3.71	-24%
14	33.53	-12%	6.00	14%
15	13.78	8%	3.54	-18%
16	13.49	10%	2.09	30%
17	17.38	-16%	1.99	34%
18	29.00	3%	1.67	44%

The percent difference is provided in order to make possible an in-depth analysis of the results. By taking the absolute percent difference, it is possible to see that, in the case of DT-containing polymers, eight out of 12 polymers had a composition within 10% of the target mol%. However, in the case of PEG-containing polymers, only three out of 12 had a composition within 10% of the target mol%. This is the reason why the absolute percent difference is not adequate *per se* for the analysis, but rather has to be analyzed based on the sign of the corresponding value. A negative percent difference means that the target value has been exceeded. In the case of DT-containing polymers, 10 out of 12 polymers exceeded the target composition or were within 10% of this composition, meaning that only two polymers fell short regarding the expected mol%. In the case of PEG-containing polymers, seven out of 12 polymers exceeded the target composition or

were within 10% of said composition, meaning that only five polymers fell short in terms of the expected mol%. There is a number of possibilities that could have influenced this outcome: a) For small amounts of solution dispensing (50-200 μL) with the robot, the dispensing amount is subject to errors, especially when using volatile solvents such as CH_2Cl_2; b) For ^{1}H-NMR broad peaks that tend to hydrogen-bond with other molecules (e.g., water, same polymer chain), e.g., PEG or amides (when using $CDCl_3$ as solvent), a greater amount of errors should be expected when relative mol compositions are calculated; c) For some supra- and macromolecules, ^{1}H-NMR sensitivity can affect baselines, phases, and integration, even when these are performed with extreme care; d) Impurities (e.g., solvents, by-products, monomers, oligomers) can have an enormous impact when calculating relative mol compositions.

All ^{1}H-NMR shifts were analyzed, identified, and recorded for the 18 polymers studied. The results are shown below, and include the peaks for the co-monomers for the case of co- and terpolymers.

poly(HTH carbonate)

^{1}H-NMR (500 MHz, $CDCl_3$) δ 7.19 (d, J = 3.2, 4H, aryl), 7.10 (dd, J = 6.2, 2.2, 2H, aryl), 7.03 – 6.86 (m, 2H, aryl), 6.09 (s, 1H, amide), 4.80 (d, J = 6.4, 1H, α-proton), 4.17 – 3.94 (m, 2H, -O-CH_2-), 3.47 (s, 2H, -CH_2-), 3.17 – 2.87 (m, 2H, -CH_2-), 1.70 – 1.48 (m, 2H, -CH_2-), 1.26 (d, J = 10.9, 6H, -CH_2-), 0.86 (t, J = 6.7, 3H, -CH_3).

poly(BTE carbonate)

^{1}H-NMR (500 MHz, $CDCl_3$) δ 7.73 (dd, *J* = 17.2, 8.3, 2H, aryl), 7.29 (d, *J* = 7.5, 2H, aryl), 7.15 (dd, *J* = 10.4, 5.7, 4H, aryl), 6.78 (dd, *J* = 24.6, 16.0, 1H, amide), 5.00 (d, *J* = 5.3, 1H, α-proton), 4.33 – 4.11 (m, 2H, -O-CH_2-), 3.46 – 3.11 (m, 2H, -CH_2-), 1.28 (dt, *J* = 13.6, 6.7, 3H, -CH_3).

poly(DTE-co-15%DT carbonate)

^{1}H-NMR (500 MHz, $CDCl_3$) δ 7.23 – 6.79 (m, 8H, aryl), 6.10 (s, 1H, amide), 4.79 (s, 1H, α-proton), 4.09 (s, 2H, -O-CH_2-), 2.95 (d, *J* = 62.9, 4H, -CH_2-), 2.43 (s, 2H, -CH_2-), 1.17 (s, 3H, -CH_3).

poly(DTH-co-30%DT carbonate)

^{1}H-NMR (500 MHz, $CDCl_3$) δ 7.23 – 6.60 (m, 8H, aryl), 6.03 (s, 1H, amide), 4.82 (s, 1H, α-proton), 4.26 – 3.88 (m, 2H, -O-CH_2-), 2.97 (dd, *J* = 70.5, 6.0, 4H, -CH_2-), 2.63 – 2.04 (m, 2H, -CH_2-), 1.55 (d, *J* = 6.1, 2H, -CH_2-), 1.25 (s, 6H, -CH_2-), 0.86 (t, *J* = 6.3, 3H, -CH_3).

poly(HTH-co-30%DT carbonate)

^{1}H-NMR (500 MHz, DMSO-d_6) δ 8.61 (d, *J* = 7.5, 1H, amide), 7.23 (t, *J* = 9.4, 8H, aryl), 4.56 – 4.27 (m, 1H, α-proton), 3.96 (t, *J* = 6.1, 2H, -O-CH_2-), 3.13 – 2.82 (m, 2H, -CH_2-), 2.75 (s, 1H -CH_2-), 2.38 (t, *J* = 7.5, 1H -CH_2-) 1.43 (s, 2H, -CH_2-), 1.21 (d, *J* = 18.8, 6H, -CH_2-), 0.83 (t, *J* = 6.2, 3H, -CH_3).

Resolved DT peaks: 8.24 (d, *J* = 8.0, amide).

poly(PTE-co-15%DT carbonate)

^{1}H-NMR (500 MHz, $CDCl_3$) δ 7.22 – 6.74 (m, 9H, aryl + amide), 4.90 (d, *J* = 6.9, 1H, α-proton), 4.58 – 4.30 (m, 2H, -CH_2-), 4.13 (dd, *J* = 13.8, 6.8, 2H, -O-CH_2-), 3.12 (d, *J* = 5.4, 2H, -CH_2-), 1.30 – 1.13 (m, 3H, -CH_3).

Resolved DT peaks: 5.86 (s, amide, broad), 4.80 (s, α-proton), 3.71 (dd, *J* = 16.7, 10.5, -O-CH_2-), 2.95 (d, *J* = 37.7, -CH_2-), 2.45 (s, -CH_2-).

poly(DTH-co-3%PEG_{1k} carbonate)

^{1}H-NMR (300 MHz, DMSO-d_6) δ 9.20 (s, 1H, phenol, end group), 9.11 (s, 1H, phenol, end group), 8.21 (d, *J* = 7.7, 1H, amide), 6.95 (dd, *J* = 8.3, 7.3, 4H, aryl), 6.73 – 6.58 (m, 4H, aryl), 4.35 (d, *J* = 6.1, 1H, α-proton), 3.97 (t, *J* = 6.5, 2H, -O-CH_2-), 3.33 (s, -CH_2-, PEG), 2.80 (dd, *J* = 14.9, 7.4, 2H, -CH_2-), 2.62 (t, *J* = 7.8, 2H, -CH_2-), 2.31 (dd, *J* = 9.0, 6.7, 2H, -CH_2-), 1.62 – 1.37 (m, 2H, -CH_2-), 1.25 (d, *J* = 14.8, 6H, -CH_2-), 0.85 (t, *J* = 6.7, 3H, -CH_3).

poly(CTE-co-3%PEG_{1k} carbonate)

^{1}H-NMR (500 MHz, DMSO-d_6) δ 8.62 (s, 1H, amide), 7.65 (dd, *J* = 19.2, 11.0, 2H, aryl), 7.57 – 7.20 (m, 7H, aryl + alkene), 6.74 – 6.60 (m, 1H, alkene), 4.62 (d, *J* = 6.2, 1H, α-proton), 4.07 (s, 2H, -O-CH_2-), 3.63 – 3.44 (m, PEG), 3.20 – 2.81 (m, 2H, -CH_2-), 1.15 (t, *J* = 31.3, 3H, -CH_3).

poly(BTE-co-3%PEG$_{1k}$ carbonate)

^{1}H-NMR (500 MHz, $CDCl_3$) δ 7.76 (s, 2H, aryl), 7.29 (s, 2H, aryl), 7.14 (t, *J* = 19.4, 4H, aryl), 6.78 (dd, *J* = 25.1, 16.3, 1H, amide), 5.01 (s, 1H, α-proton), 4.24 (t, *J* = 51.5, 2H, -O-CH_2-), 3.82 – 3.52 (m, PEG), 3.23 (d, *J* = 12.9, 2H, -CH_2-), 1.38 – 1.11 (m, 3H, -CH_3).

poly(PTE-co-3%PEG$_{1k}$ carbonate)

^{1}H-NMR (500 MHz, $CDCl_3$) δ 7.21 – 6.91 (m, 7H, aryl + amide), 6.84 (t, *J* = 11.7, 2H, aryl), 4.90 (dd, *J* = 13.6, 6.5, 1H, α-proton), 4.52 – 4.38 (m, 2H, -CH_2-), 4.13 (q, J = 7.1, 2H, -O-CH_2-), 3.80 – 3.53 (m, PEG), 3.27 – 2.95 (m, 2H, -CH_2-), 1.21 (dt, *J* = 24.6, 7.1, 3H, -CH_3).

poly(HTE-co-15%DT-co-3%PEG$_{1k}$ carbonate)

^{1}H-NMR (500 MHz, $CDCl_3$) δ 7.23 – 6.76 (m, 8H), 6.21 (s, 1H, amide), 4.77 (s, 1H, α-proton), 4.10 (s, 2H, -O-CH_2-), 3.69 – 3.54 (m, PEG), 3.45 (s, 2H, -CH_2-), 2.99 (d, *J* = 40.5, 2H, -CH_2-), 1.17 (s, 3H, -CH_3).

poly(HTE-co-30%DT-co-7%PEG$_{1k}$ carbonate)

^{1}H-NMR (500 MHz, DMSO-d_6) δ 8.61 (d, *J* = 7.4, 1H, amide), 7.49 – 7.04 (m, 8H, aryl), 4.47 (dd, *J* = 14.1, 7.6, 1H, α-proton), 4.02 (d, *J* = 6.7, 2H, -O-CH_2-), 3.62 – 3.39 (m, PEG), 3.31 (d, *J* = 20.8, 2H, -CH_2-), 3.13 – 2.83 (m, 2H, -CH_2-), 1.29 – 0.88 (m, 3H, -CH_3).

Resolved DT peaks: 12.72 (s, free acid), 8.25 (d, *J* = 7.7, amide), 6.96 (dd, *J* = 16.5, 8.3, aryl), 6.65 (dd, *J* = 7.6, 4.3, aryl), 4.30 (s, α-proton), 3.68 (s, -O-CH_2-), 2.82 – 2.67 (m, -CH_2-), 2.40 (d, *J* = 7.5, -CH_2-).

poly(BTE-co-15%DT-co-3%PEG_{1k} carbonate)

^{1}H-NMR (500 MHz, DMSO-d_6) δ 8.95 (d, *J* = 4.6, 1H, amide), 7.91 (dd, *J* = 13.3, 5.8, 2H, aryl), 7.37 (dddd, *J* = 36.6, 33.6, 14.3, 12.1, 6H, aryl), 4.63 (dd, *J* = 20.6, 12.7, 1H, α-proton), 4.08 (d, *J* = 5.0, 2H, -O-CH_2-), 3.62 – 3.41 (m, PEG), 3.16 (dd, *J* = 12.6, 6.0, 2H, -CH_2-), 1.13 (s, 3H, -CH_3).

Resolved DT peaks: 8.57 (dd, *J* = 7.5, 4.5, amide), 7.70 (dd, *J* = 8.7, 2.6, aryl), 6.86 – 6.72 (m, aryl), 4.47 (s, α-proton), 2.90 (d, *J* = 6.6, -CH_2-), 2.76 (s, -CH_2-), 2.41 (s, -CH_2-).

poly(BTH-co-30%DT-co-7%PEG_{1k} carbonate)

^{1}H-NMR (500 MHz, DMSO-d_6) δ 8.94 (s, 1H, amide), 7.89 (d, *J* = 8.5, 2H, aryl), 7.64 – 7.18 (m, 6H, aryl), 4.65 (s, 1H, α-proton), 4.03 (s, 2H, -O-CH_2-), 3.77 – 3.44 (m, PEG), 3.27 – 3.00 (m, 2H, -CH_2-), 1.49 (s, 2H, -CH_2-), 1.20 (s, 6H, -CH_2-), 0.80 (s, 3H, -CH_3).

Resolved DT peaks: 12.72 (s, free acid), 8.24 (s, amide), 7.69 (d, *J* = 8.5, aryl), 6.77 (t, *J* = 10.5, aryl), 4.46 (s, α-proton), 2.81 (d, *J* = 62.1, -CH_2-), 2.39 (s, -CH_2-), 2.18 (s, -CH_2-).

poly(CTE-co-15%DT-co-3%PEG_{1k} carbonate)

^{1}H-NMR (500 MHz, DMSO-d_6) δ 8.61 (s, 1H, amide), 7.66 (t, *J* = 7.4, 2H, aryl), 7.33 (dddd, *J* = 33.1, 25.3, 13.1, 9.8, 7H, aryl + alkene), 6.70 (dd, *J* = 15.8, 2.9, 1H, alkene),

4.62 (d, J = 6.4, 1H, α-proton), 4.06 (d, J = 6.3, 2H, -O-CH_2-), 3.63 – 3.31 (m, PEG), 3.07 (dd, J = 33.4, 10.7, 2H, -CH_2-), 1.09 (t, J = 18.0, 3H, -CH_3).

Resolved DT peaks: 8.25 (s, amide), 7.03 (d, J = 6.9, aryl), 6.79 (d, J = 8.1, aryl), 4.55 – 4.41 (m, α-proton), 2.88 (d, J = 7.0, -CH_2-), 2.76 (s, -CH_2-), 2.40 (s, -CH_2-).

poly(DTE-co-15%DT-co-3%PEG_{1k} carbonate)

^{1}H-NMR (500 MHz, $CDCl_3$) δ 7.22 – 6.84 (m, 8H, aryl), 6.08 (s, 1H, amide), 4.80 (s, 1H, α-proton), 4.10 (s, 2H, -O-CH_2-), 3.65 (d, J = 34.2, PEG), 2.95 (d, J = 62.5, 4H, -CH_2-), 2.45 (s, 2H, -CH_2-), 1.17 (s, 3H, -CH_3).

poly(PTD-co-15%DT-co-3%PEG_{1k} carbonate)

^{1}H-NMR (500 MHz, $CDCl_3$) δ 7.23 – 7.04 (m, 6H, aryl), 6.99 (s, 1H, amide), 6.86 (d, J = 7.6, 2H, aryl), 4.92 (d, J = 7.3, 1H, α-proton), 4.44 (s, 2H, -CH_2-), 4.14 – 4.00 (m, 2H, -O-CH_2-), 3.62 (d, J = 7.5, PEG), 3.12 (t, J = 6.5, 2H, -CH_2-), 1.56 (s, 2H, -CH_2-), 1.23 (s, 18H, -CH_2-), 0.85 (t, J = 6.6, 3H, -CH_3).

Resolved DT peaks: 5.87 (d, J = 129.6, amide), 4.77 (s, α-proton), 3.02 – 2.87 (m, -CH_2-).

poly(PTD-co-30%DT-co-3%PEG_{1k} carbonate)

^{1}H-NMR (500 MHz, $CDCl_3$) δ 7.23 – 7.04 (m, 6H, aryl), 6.99 (s, 1H, amide), 6.86 (d, J = 7.2, 2H, aryl), 4.92 (d, J = 7.2, 1H, α-proton), 4.44 (s, 2H, -CH_2-), 4.19 – 3.96 (m, 2H, -O-CH_2-), 3.62 (d, J = 7.5, PEG), 3.13 (d, J = 6.3, 2H, -CH_2-), 1.56 (s, 2H, -CH_2-), 1.23 (s, 18H, -CH_2-), 0.85 (t, J = 6.8, 3H, -CH_3).

Resolved DT peaks: 5.92 (d, J = 92.4, amide), 4.70 (dd, J = 15.4, 8.9, α-proton), 3.05 – 2.84 (m, -CH_2-).

5.2.4 Surface Energy Characterization of Selected Polycarbonates

The wettability of a surface is a parameter that is frequently studied during biomaterial characterization.[49, 169, 174, 188, 189] In most cases, this parameter is characterized by looking at the contact angle (θ) of a liquid on a surface. There is generally an inverse proportion between the contact angle and the spreading of the drop, therefore providing an inverse measure of wettability.[190] While contact angle data makes it possible to predict surface characteristics by differentiating between hydrophobic and hydrophilic surfaces, it does not provide further information regarding the nature of such characteristics. This additional information is particularly important for materials with similar contact angles but different biological responses. In order to understand cell-material interactions "quantitatively", it is necessary to explain surfaces in terms of energy. To do this, it is necessary to look at the surface energy of the corresponding materials.

Surface free energy, also known as the surface energy of a solid (γ_s), is defined as the amount of energy per square meter required to change the surface area of a material, and its SI unit is mJ/m^2.[191, 192] Fowkes suggested that this free energy could be considered as the sum of the attraction forces on a solid surface,[192] e.g., dispersive (d) and polar (p):

$$\gamma = \gamma^d + \gamma^p \tag{5.4}$$

Since it is known that dispersive forces are due primarily to electrostatic interactions (Lifshitz-Van der Waals) and that polar forces can be explained through the acid-base components of a surface,[193, 194] Equation 5.4 can be rewritten as follows:

$$\gamma = \gamma^{LW} + \gamma^{AB} \tag{5.5}$$

The Lewis theory is the best option for further explaining acid-base components in this case. Sites on the surface are acidic in nature if they can act as electron acceptors (e.g., carbon atoms linked to electronegative groups). On the other hand, basic components are identified as those that can donate electrons (e.g., oxygens, double bonds).[195] Furthermore, the polar forces, or acid-base components of the surface energy, can be represented by Equation 5.6, according to van Oss.[194, 196] This equation includes hydrogen bonding, electron donor-acceptors, and organic nucleophile-electrophile interactions.

$$\gamma^{AB} = 2\sqrt{\gamma^+\gamma^-} \tag{5.6}$$

In order to describe the surface free energy of solids or liquids, Equation 5.6 is rewritten as Equation 5.7, shown below:

$$\gamma_{s,l} = \gamma_{s,l}^{LW} + 2\sqrt{\gamma_{s,l}^{+}\gamma_{s,l}^{-}} \tag{5.7}$$

Young's equation (Equation 5.8) is used to estimate the solid surface tension on the basis of contact angle data.[195] Subscripts s, l, and sl refer to solid, liquid, and solid-liquid energies respectively.

$$\gamma_l \cos\theta = \gamma_s - \gamma_{sl} \tag{5.8}$$

By combining Young's equation with the equation that describes the work of adhesion between a liquid and a solid (Equation 5.9), it is possible to find the relationship between the work of adhesion and the contact angle formed between a solid substrate and a probe liquid,[178, 189] as shown in Equation 5.10:

$$W_{sl} = \gamma_l + \gamma_s - \gamma_{sl} \tag{5.9}$$

$$W_{sl} = \gamma_l(1 + \cos\theta) \tag{5.10}$$

The fact that the work of adhesion between a solid and a liquid is given by Equation 5.11 in the acid-basic approach makes it possible to obtain Equation 5.12, which is the Good and van Oss equation that requires the use of three probe liquids in order to solve the resulting system of three equations with three unknowns (i.e., the surface energy components of the solid). The energy components for the probe liquids are available in relevant literature.[178, 192]

$$W_{sl} = 2(\sqrt{\gamma_s^{LW}\gamma_l^{LW}} + \sqrt{\gamma_s^{+}\gamma_l^{-}} + \sqrt{\gamma_s^{-}\gamma_l^{+}}) \quad (5.11)$$

$$\gamma_l(1+\cos\theta) = 2(\sqrt{\gamma_s^{LW}\gamma_l^{LW}} + \sqrt{\gamma_s^{+}\gamma_l^{-}} + \sqrt{\gamma_s^{-}\gamma_l^{+}}) \quad (5.12)$$

An alternative way of calculating the surface energy of a solid is to use the same contact angle information from at least three probe liquids and the solid of interest and following the Fowkes approach,[192] represented by Equation 5.13:

$$\left[\frac{1+\cos\theta}{2}\right] \times \left[\frac{\gamma_l}{\sqrt{\gamma_l^d}}\right] = \sqrt{\gamma_s^p} \times \frac{\sqrt{\gamma_l^p}}{\sqrt{\gamma_l^d}} + \sqrt{\gamma_s^d} \quad (5.13)$$

Equation 5.13 is a linear $y = mx + b$ equation, and results from approximating the surface energy with a geometric mean.[192, 195, 197] The disadvantage of using this approach, in comparison to the Good and van Oss equation, is that the individual components of the acid-base term (i.e., γ^+, γ^-) for the surface energy cannot be obtained.

For this section, the surface energy of various different polymers was calculated by using contact angle data from different probe liquids. The polymers analyzed were poly(DTE carbonate), poly(CTE carbonate), and poly(PTE carbonate) compared to poly(L-lactide) (PLLA). The probe liquids used were H_2O_c, ethylene glycol, and chlorobenzene, and their surface energy parameters are summarized in Table 5.5.[178, 193, 197] Although the experiments were not performed with a high-throughput method, this characterization study made it possible to obtain a general idea of the effect of the backbone component on the polymer (i.e., -CH_2-CH_2-, -CH=CH-, -O-CH_2-). The contact

angle data measurements were conducted, as described in Chapter 2, at 20±2 °C and 45-50 %RH.

Table 5.5 Surface tension of probe liquids parameters at 20 °C in mJ/m^2

Probe Liquid	γ_l	γ^{LW} (γ^d)	γ^{AB} (γ^p)	γ^+	γ^-
Water	72.80	21.80	51.00	25.50	25.50
Ethylene glycol	48.00	29.00	19.00	2.28	39.60
Chlorobenzene	33.60	32.10	1.50	0.90	0.61

Using the Fowkes method resulted in four curves. Linear fits were applied to the results in order to obtain the corresponding slope and intercept. Figure 5.10 shows the linear fits for poly(PTE carbonate) and poly(L-lactide). The other polymers were left out of the graph in order to ensure visual clarity, since the data points belonging to tyrosine-derived polycarbonates were very close to each other.

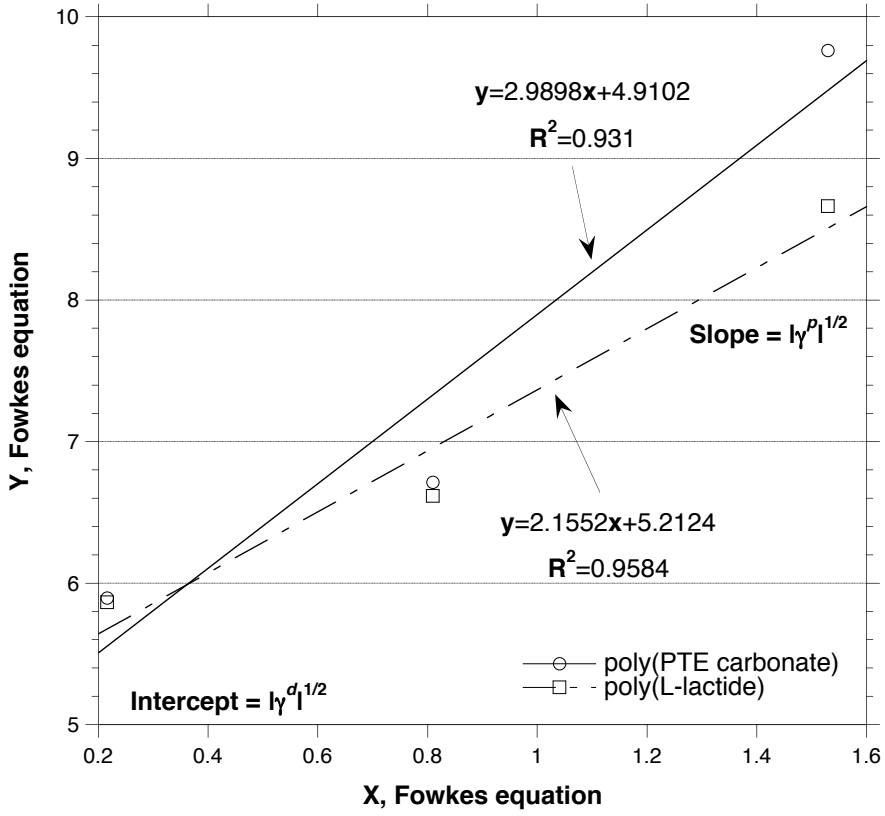

Figure 5.10 Linear fits for two polymers using the Fowkes approach

The contact angles measured and the linear fit parameters for the polymers analyzed are summarized in Table 5.6.

Table 5.6 Average contact angles and Fowke's linear fit parameters of test substrates

Polymer	θ, H_2O_c	θ, Ethylene glycol	θ, Chlorobenzene	M	b	R^2
poly(DTE carbonate)	81.97±1.67	62.41±1.97	9.35±0.64	2.315	5.127	0.930
poly(CTE carbonate)	82.99±4.62	65.81±3.04	9.30±0.66	2.219	5.085	0.888
poly(PTE carbonate)	75.39±7.96	59.58±5.83	8.88±0.56	2.990	4.910	0.931
poly(L-lactide)	83.63±3.23	61.02±1.80	12.05±0.64	2.155	5.212	0.958

These results confirm that contact angle data alone is not sufficient for a partial surface characterization assessment. The air-water contact angles corresponding to the different polymers were very similar and could be grouped as belonging to "hydrophobic" surfaces. However, this qualitative data resulting from water-air contact angle data is not adequate for explaining differences in cell-material interaction responses in the event that said phenomena were to be studied. The corresponding total surface energy and dispersion and polar parameters are shown in Table 5.7.

Using the Good and van Oss equation makes it possible to obtain more information regarding the polar component of the surface energy by dividing the polar component into acidic and basic terms (as per the Lewis Acid-Base theory). The solution for the system of three equations with three unknowns is summarized in Table 5.7, below.

Table 5.7 Surface energy calculations using two different approaches

Polymer	Fowkes approach, mJ/m^2			Good and van Oss approach, mJ/m^2			
	γ_s	γ^{LW}	γ^{AB}	γ_s	γ^{LW}	γ^{+}	γ^{-}
poly(DTE carbonate)	31.65	26.29	5.36	30.34	28.65	0.08	8.89
poly(CTE carbonate)	30.77	25.85	4.92	29.09	28.83	0.00	9.49
poly(PTE carbonate)	33.05	24.11	8.94	29.90	27.03	0.14	14.80
poly(L-lactide)	31.81	27.17	4.65	31.13	28.82	0.20	6.77

Although the contact angle is very similar for all four polymers, the corresponding surface energy is not, implying that small changes can have a significant impact on cellular response.[97, 198] The results obtained by using the Fowkes approach for total surface energy differ little from those obtained with the Good and van Oss

approach. However, the dispersion and polar forces are different, as the estimated polar component of the tyrosine-derived polycarbonates is higher when using the Good van Oss approach. This is a direct result of the data used, since a trend line is drawn when using the Fowkes approach, whereas the Good and van Oss approach does not account for this error. While this can certainly affect the surface energy obtained, the difference is minimal when comparing both methods. However, the fact that the acidic and basic components of the polar force are obtained with the Good and van Oss approach represents an important advantage. Although the surface energy is similar for all polymers, there are large differences in their "electron donating" or "basic" components. The corresponding data suggests that the polymer order, based on "electron donating" components, is as follows:

poly(PTE carbonate) > poly(CTE carbonate) > poly(DTE carbonate) > PLLA

The information obtained during the surface energy measurements opens up yet another method that can be used to quantify hydrophobicity. The relevant parameter in this additional method consists of the free energy of interaction between surface molecules (i) immersed in water (w), and is represented by ΔG_{iwi}.[191, 197, 199-201] The free energy of interaction can be calculated with Equation 5.14, shown below:

$$\Delta G_{iwi} = -2\gamma_{iw} \tag{5.14}$$

Where γ_{iw} is the interfacial tension between the surface and the water. Calculating this parameter on the basis of the surface tension components is possible, as explained by van Oss,[194, 196] with Equations 5.15 and 5.16:

$$\gamma_{iw}^{LW} = \left(\sqrt{\gamma_i^{LW}} - \sqrt{\gamma_w^{LW}}\right)^2 \tag{5.15}$$

$$\gamma_{iw}^{AB} = 2\left(\sqrt{\gamma_i^+\gamma_i^-} + \sqrt{\gamma_w^+\gamma_w^-} - \sqrt{\gamma_i^+\gamma_w^-} - \sqrt{\gamma_w^+\gamma_i^-}\right) \tag{5.16}$$

Combining Equations 5.15 and 5.16 makes it possible to obtain the corresponding total interfacial tension. Substituting the result in Equation 5.14 makes it possible to obtain the free energy of hydrophobic interaction, which can be used as a quantitative measure of the degree of hydrophobicity or hydrophilicity of a given substrate in SI units (mJ/m^2):

$$\Delta G_{iwi} = -2\left(\sqrt{\gamma_i^{LW}} - \sqrt{\gamma_w^{LW}}\right)^2 - 4\left(\sqrt{\gamma_i^+\gamma_i^-} + \sqrt{\gamma_w^+\gamma_w^-} - \sqrt{\gamma_i^+\gamma_w^-} - \sqrt{\gamma_w^+\gamma_i^-}\right) \tag{5.17}$$

By further defining the degree of hydrophobicity, it is possible to group compounds, cell particles, and surfaces as hydrophobic if $\Delta G_{iwi} < 0$, and as hydrophilic if $\Delta G_{iwi} > 0$.[194, 196] The interfacial energy between the aforementioned surfaces and water was calculated, with the results being shown in Table 5.8, below:

Table 5.8 Interfacial free energy of hydrophobic interactions of test substrates and water in mJ/m^2

Substrate	γ_s	γ^{LW}	γ^+	γ^-	ΔG_{iwi}
poly(DTE carbonate)	30.34	28.65	0.08	8.89	-40.37
poly(CTE carbonate)	29.09	28.83	0.00	9.49	-40.76
poly(PTE carbonate)	29.90	27.03	0.14	14.80	-23.05
Poly(L-Lactide)	31.13	28.82	0.20	6.77	-46.04
TCPS[b]	44.00	38.90	0.40	13.70	-28.74

[a]In mJ/m^2
[b]Values for surface parameters obtained from Wood *et al.*[193]

Even though the contact angle values were very similar, and all surfaces are hydrophobic in nature based on the corresponding interfacial energy, it is possible to observe that poly(PTE carbonate) seems to has a similar interfacial energy to that of tissue culture polystyrene (TCPS). If, in fact, interfacial energy controls how proteins adsorb on the surface and has an effect on cell adhesion and proliferation, then similar results should be observed for poly(PTE carbonate) and TCPS in cell-material interactions.

5.2.5 Interaction of Human Mesenchymal Stem Cells with Selected Substrates

Spin-coated polymer films on glass were seeded with human mesenchymal stem cells (hMSCs) for 14 days with non-inducing media (basal). As a control, tissue culture polystyrene (TCPS) was seeded with hMSCs with basal and osteogenic-inducing media, as well as with PLLA with basal media only. On days 3, 7, and 14, the cells were fixed and actin and nuclei-stained for microscopy analysis. Figure 5.11 shows the results of this preliminary study. Figure 5.12 shows the morphology of the cells at different points in

time. Generally speaking, there was a decrease in terms of the normalized seeding density of 5,000 cells/cm^2 for all substrates on Day 3. This was probably due to the use of vacuum to aspirate non-attached cells at different points in time. There was a further drop in the number of cells for some substrates on Day 7, but, in general, the cells appeared to reach some sort of "quiescent" state, except for the cells growing on TCPS (with both basal and osteogenic-inducing media) and poly(PTE carbonate). Between Day 7 and Day 14, various different substrates allowed regular cell growth, except for poly(DTE carbonate) and poly(CTE carbonate).

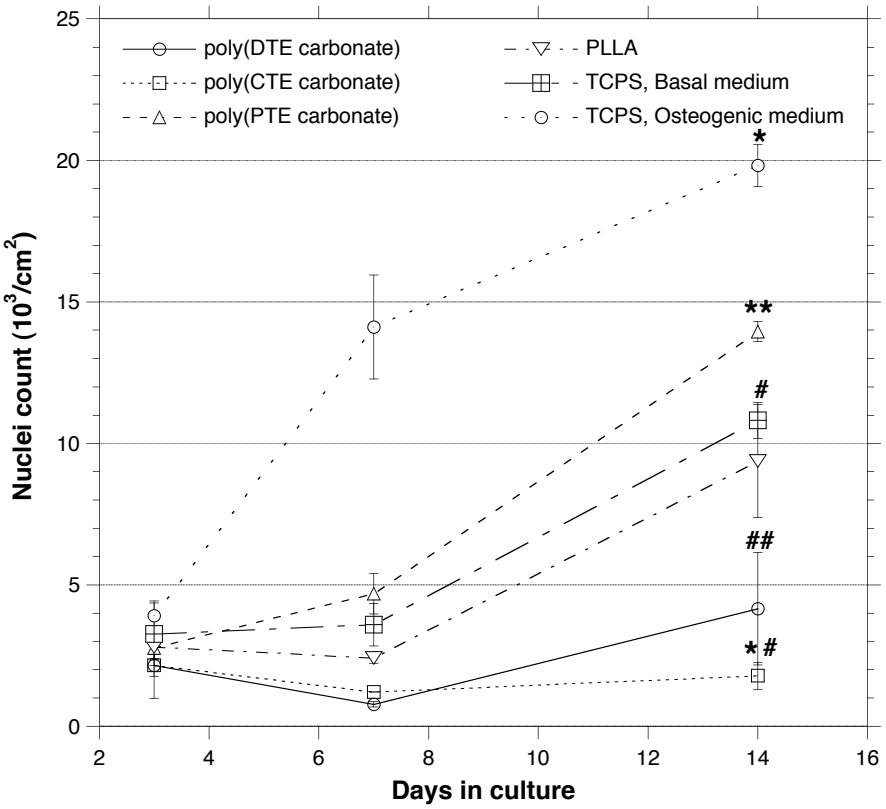

Figure 5.11 Nuclei count of hMSC with Hoescht staining. The number of nuclei was significantly different ($p<0.05$) in various cases *vs.*: *All substrates; **All substrates except TCPS with osteogenic-inducing media; #poly(DTE carbonate), poly(CTE carbonate), and PLLA; ##poly(CTE carbonate); *#PLLA.

The cells that grew on the TCPS with osteogenic-inducing media appeared to have reached a plateau by Day 14, but this was due to the cells reaching confluency inside the well plate. On the other hand, the cells that grew on poly(DTE carbonate) and poly(CTE carbonate) appeared to remain in a "quiescent" state in which no growth was apparent. Moreover, the cells that were growing on TCPS, basal media, poly(PTE carbonate), and PLLA grew almost in parallel. Both TCPS and poly(PTE carbonate) had the same degree of hydrophobicity in mJ/m^2, as per the calculations in Chapter 5.2.4, suggesting a similar protein arrangement that contributed to the homologous hMSC growth observed. The PLLA featured surface energy characteristics similar to those of poly(DTE carbonate) and poly(CTE carbonate), but cells grew better on this substrate. This can be explained by looking at the actin and nuclei stains under a fluorescence microscope, as shown in Figure 5.12. In the case of poly(DTE carbonate) and poly(CTE carbonate), cells do not appear to be as elongated as those for the other substrates on any given date. It is possible that a "quiescent" state was attained and then overcome after Day 14, when the cells look elongated and similar to those corresponding to the other substrates on Day 7, which suggests cell growth and proliferation after Day 14. As for the PLLA, there is no final explanation that elucidates why its cell growth was similar to that of TCPS. Perhaps its slightly higher hydrophobicity is sufficient to allow for good cell adhesion and proliferation. A more in-depth explanation would require analyzing additional phenomena, such as polymer crystallinity.[202, 203] Although it is clear that this preliminary data cannot be used to explain the behavior of cells on PLLA, similar polymers (i.e., the tyrosine-derived polymers) with similar surface energy properties have

a significant effect on cell-material interactions with a slightly different chemical composition in the backbone, while maintaining their overall dispersive forces the same.

For the specific case of TCPS with osteogenic media, the clear difference in cell morphology is self-evident even on Day 3, when the cells appear to be smaller, more cube-shaped, and not as elongated, which is typical of osteoblasts even when compared to TCPS with basal media.[204]

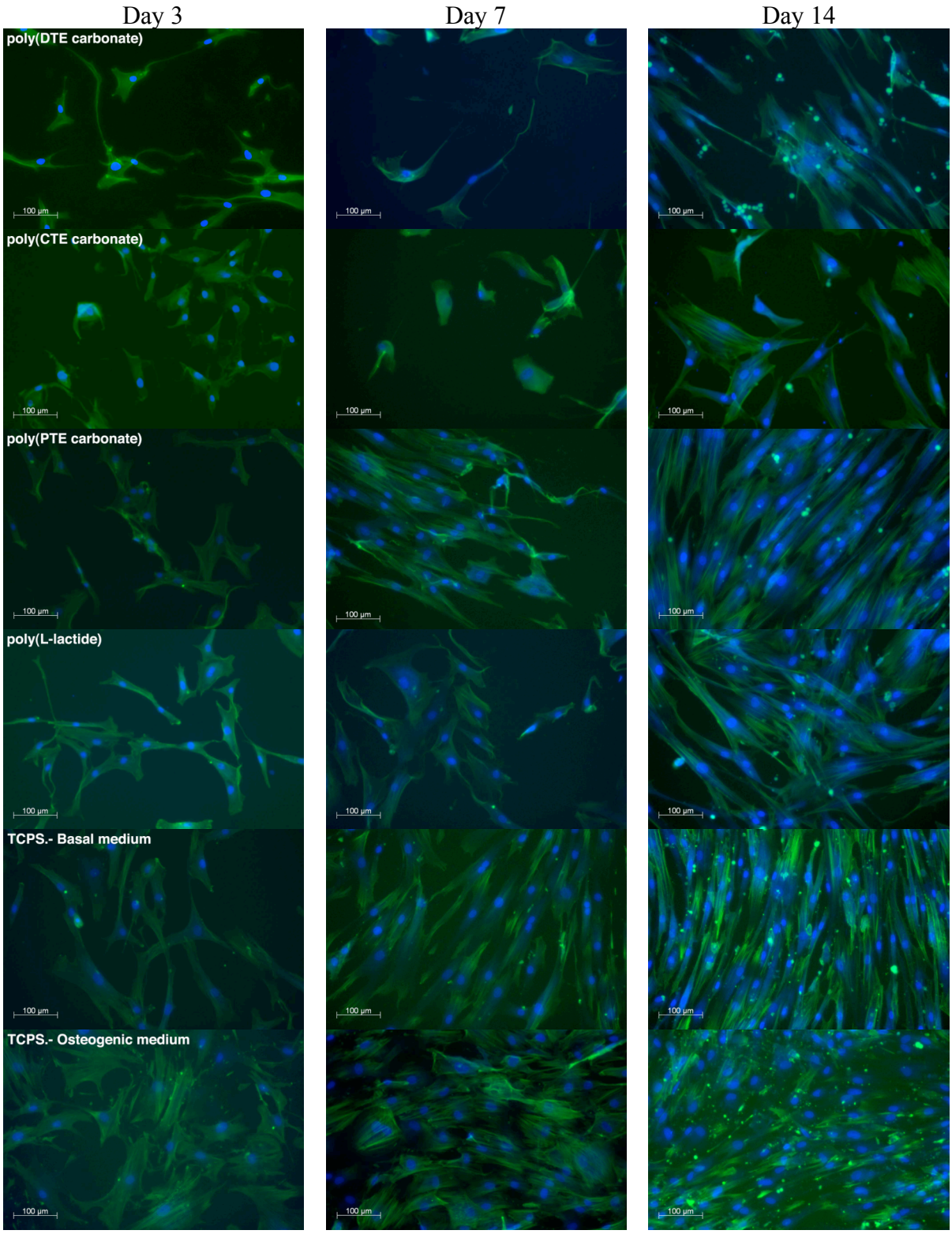

Figure 5.12 Representative images of actin and nuclei stains of hMSCs on different substrates at three different points in time

Overall, observing the cell morphology of cells seeded in basal media shows no apparent change in their phenotype, meaning that the substrates used were able to expand cells without differentiation into osteoblasts. However, more sophisticated cell biology tests can be performed in order to quantify the degree of differentiation of the cells.[21, 173, 177, 202, 205] On the other hand, the purpose of this experiment was to compare and contrast the cell-material interactions of three very similar tyrosine-derived polycarbonates qualitatively and to attempt to explain the results on the basis of their surface energy properties.

While studying human marrow stromal cells (same as hMSCs) and working with poly(ε-caprolactone) (PCL), Ciapetti and colleagues observed significant cell growth on He^{+}-irradiated PCL surfaces with γ = 40 mJ/m^2 with a γ^{LW} of 37 mJ/m^2 and a γ^{-} of 10 mJ/m^2 when compared to TCPS as a control.[206] They also observed that, after extended culture times (4–5 weeks), hMSCs differentiated into functional osteoblasts (i.e., formed a mineralized matrix). In another study, Curran and colleagues investigated the effect of growing hMSCs on a range of silane-modified surfaces with different surface functionalities: hydroxyl, carboxyl, amino, silane, and methyl with increasing surface energies between 35 and 53 mJ/m^2.[179, 205, 207] While all surfaces supported the same growth rate of hMSCs in a basal medium, only methyl, silane, and amino surfaces (with a higher surface energy) promoted the up-regulation of Collagen I, osteopontin, and osteonectin through 21 days in culture, and osteocalcin and core binding factor alpha 1 (CBFA1) from Day 14 onwards. A report by Wood and co-workers on the study of the surface energy of different biomaterials (e.g., TCPS, silicon, glass, and indium tin oxide) coated with adhesion molecules used in cell cultures stressed the importance of the

acid/base surface energy component and its effect on adhesion relative to the dispersion component.[193] The same was described by De Bartolo and colleagues for the adsorption of serum proteins to different polymeric membranes. As the serum proteins were adsorbed, the contact angle decreased and the basic element of the polar component of surface energy increased.[191, 201] After the culture of isolated rat hepatocytes on these modified surfaces, a significantly higher number of cells adhered to surfaces with a higher γ^- after 24 hours. In yet another study, Masters and colleagues described the haemocompatibility of polyurethane-hyaluronic acid copolymers by investigating platelet and red blood cell adhesion, as well as porcine aorta endothelial cell adhesion, on the surfaces. They found that a surface energy change from 38 to 58 mJ/m^2 caused by the incorporation of 0.33% (w/w) hyaluronic acid (HA) was enough to reduce platelet and red blood cell adhesion by almost 90 % when compared to regular polyurethane (PU). This however, did not change endothelial cell adhesion and viability at low HA percentages.[178] In two different reports, Redey and colleagues showed that, as the polar surface energy component of different types of apatites increased, the adhesion of osteoclasts and osteoblasts also increased.[208, 209] All these reports show the importance of determining both surface energy and its components in order to be able to explain cell-material interactions to a greater extent – particularly when very similar polymers (i.e., the tyrosine-derived polymers studied here) are analyzed.

5.3 CONCLUSIONS

A number of different characterization experiments were performed in order to study the physical behavior of a library of polymeric biomaterials. Specifically, thermal characterization through Differential Scanning Calorimetry proved useful in isolating a parameter unique to supra- and macromolecules, i.e., the glass transition temperature, and made it possible to use the values obtained in order to further classify the library of polymers. This is beneficial for further experiments, since the information revealed a linear relation between the glass transition temperature and the mass-per-flexible bond index of homo-, co-, terpolymers. In the long run, this information could also be used to systematically determine which polymers should be used in specific applications, as well as to approximate this important physical value even before synthesizing a polymer.

Selected polymers were also analyzed in order to determine the usefulness of automated parallel synthesis when obtaining polymers with defined molecular compositions. At the same time, a number of other polymers were evaluated in terms of their surface energy, and a number of preliminary biological studies were performed. It was concluded that, while some parameters can be used to predict polymer properties (i.e., T_g), others could not be used as freely (i.e., air-water contact angle) for correlating or approximating the response of cell-material interactions.

6. SUMMARY

It has been four decades since the approval of the first synthetic and degradable medical implant: a suture. This particular suture was fabricated from a polymeric biomaterial, poly(glycolic acid). Since then, the rate of discovery of new polymeric biomaterials intended for the production of temporary medical devices for various applications has been rather slow. Although a few polymeric biomaterials are currently in use in rather simple medical devices, the discovery of fundamentally new synthetic and degradable polymer systems has failed to meet the demands of the tissue engineering and medical device industries. A new biomaterials discovery paradigm, devised by Kohn, was taken into consideration in order to find alternative polymer systems that would make it possible to overcome the limitations of "traditional" biomaterials. Therefore, the work involved in this thesis revolved around the use of combinatorial and high-throughput approaches as a tool for the rational design and efficient exploration of the polymer design space of novel tyrosine-derived polycarbonates.

A family of structurally-related tyrosine-derived diphenols was synthesized and characterized. For the first time ever, the structural differences in the corresponding backbone were analyzed in a systematic manner in order to help with the design of innovative tyrosine-derived polycarbonates as biomaterials. The corresponding findings should help understand complex phenomena, such as cell-biomaterial interactions, in a top-bottom manner, that is, starting from the polymer itself, all the way down to the polymer's degradation products.

One of the fundamental hypotheses of this work involved creating libraries of materials that shared common features in order to provide meaningful cross-disciplinary correlations (e.g., chemistry-materials, chemistry-biology, materials-biology). To help achieve this goal, automated parallel synthesis procedures were created for the polycondensation reaction of tyrosine-derived diphenols and triphosgene. This allowed for faster, safe, and unattended polymerizations to be performed. At the same time, consistent high-molecular-weight polycarbonates were obtained in amounts that were sufficient for screening purposes.

Characterizing the library of polymers made it possible to observe a linear relationship between repeating unit "flexibility" and T_g on the basis of the "mass-per-flexible-bond" principle. By studying systematic variations in polymer structures, researchers will be able to develop a more detailed understanding of structure-property relationships that could eventually lead to polymers designed for specific medical device applications, even before any syntheses are undertaken.

This thesis focused on the use of combinatorial and high-throughput approaches as a way of tailoring macromolecular chemistry in order to systematically explore polymer design spaces that could include specific sets of physicochemical and biological specifications, which in turn could ultimately lead to unique biomaterial compositions for specific applications. Although a large portion of this work was dedicated to translating manual synthetic protocols into their automated equivalents, it is expected for these new workflows to help researchers accomplish the same synthetic goals that were attained in this thesis. One of the important goals achieved with this thesis was that of increasing the number of viable biomaterial candidates. However, it is important to mention that, even

though close to two hundred unique polymer compositions were synthesized, it is likely that not all of them will be suitable for medical device applications. However, it is hereby suggested that the rapid synthesis of materials could very well lead to a dramatic improvement in terms of the rate at which new biomaterials can be discovered.

REFERENCES

[1] E. S. Place, J. H. George, C. K. Williams, M. M. Stevens, *Chemical Society Reviews* **2009**, *38*, 1139.
[2] J. Kohn, W. J. Welsh, D. Knight, *Biomaterials* **2007**, *28*, 4171.
[3] S. I. Stupp, J. J. J. M. Donners, L. S. Li, A. Mata, *MRS Bulletin* **2005**, *30*, 864.
[4] J. Kohn, *Nature Materials* **2004**, *3*, 745.
[5] S. Brocchini, *Advanced Drug Delivery Reviews* **2001**, *53*, 123.
[6] N. Angelova, D. Hunkeler, *Trends in Biotechnology* **1999**, *17*, 409.
[7] F. Brandl, F. Sommer, A. Goepferich, *Biomaterials* **2007**, *28*, 134.
[8] J. R. Smith, A. Seyda, N. Weber, D. Knight, S. Abramson, J. Kohn, *Macromolecular Rapid Communications* **2004**, *25*, 127.
[9] S. D. Abramson, G. Alexe, P. L. Hammer, J. Kohn, *Journal of Biomedical Materials Research Part A* **2005**, *73A*, 116.
[10] A. J. Holder, K. V. Kilway, *Dental Materials* **2005**, *21*, 47.
[11] S. Brocchini, K. James, V. Tangpasuthadol, J. Kohn, *Journal of Biomedical Materials Research* **1998**, *42*, 66.
[12] S. Brocchini, K. James, V. Tangpasuthadol, J. Kohn, *Journal of the American Chemical Society* **1997**, *119*, 4553.
[13] A. Akinc, D. G. Anderson, D. M. Lynn, R. Langer, *Bioconjugate Chemistry* **2003**, *14*, 979.
[14] A. Akinc, D. M. Lynn, D. G. Anderson, R. Langer, *Journal of the American Chemical Society* **2003**, *125*, 5316.
[15] D. G. Anderson, D. M. Lynn, R. Langer, *Angewandte Chemie-International Edition* **2003**, *42*, 3153.
[16] J. F. Lutz, Z. Zarafshani, *Advanced Drug Delivery Reviews* **2008**, *60*, 958.
[17] C. P. McCoy, R. J. Morrow, C. R. Edwards, D. S. Jones, S. P. Gorman, *Bioconjugate Chemistry* **2007**, *18*, 209.
[18] M. Goldberg, K. Mahon, D. Anderson, *Advanced Drug Delivery Reviews* **2008**, *60*, 971.
[19] Y. Mei, M. Goldberg, D. Anderson, *Current Opinion in Chemical Biology* **2007**, *11*, 388.
[20] A. J. Urquhart, D. G. Anderson, M. Taylor, M. R. Alexander, R. Langer, M. C. Davies, *Advanced Materials* **2007**, *19*, 2486.
[21] M. Yliperttula, B. G. Chung, A. Navaladi, A. Manbachi, A. Urtti, *European Journal of Pharmaceutical Sciences* **2008**, *35*, 151.
[22] X. D. Xiang, X. D. Sun, G. Briceño, Y. L. Lou, K. A. Wang, H. Y. Chang, W. G. Wallacefreedman, S. W. Chen, P. G. Schultz, *Science* **1995**, *268*, 1738.
[23] R. Hoogenboom, U. S. Schubert, *Review of Scientific Instruments* **2005**, *76*.
[24] W. F. Maier, K. Stowe, S. Sieg, *Angewandte Chemie-International Edition* **2007**, *46*, 6016.
[25] M. A. R. Meier, R. Hoogenboom, U. S. Schubert, *Macromolecular Rapid Communications* **2004**, *25*, 21.
[26] M. A. R. Meier, U. S. Schubert, *Journal of Materials Chemistry* **2004**, *14*, 3289.

[27] U. S. Schubert, C. S. Kniep, *Macromolecular Rapid Communications* **2003**, *24*, 13.
[28] H. Q. Zhang, R. Hoogenboom, M. A. R. Meier, U. S. Schubert, *Measurement Science & Technology* **2005**, *16*, 203.
[29] J. N. Cawse, D. Olson, B. J. Chisholm, M. Brennan, T. Sun, W. Flanagan, J. Akhave, A. Mehrabi, D. Saunders, *Progress in Organic Coatings* **2003**, *47*, 128.
[30] R. A. Potyrailo, *Angewandte Chemie-International Edition* **2006**, *45*, 702.
[31] R. A. Potyrailo, V. M. Mirsky, *Chemical Reviews* **2008**, *108*, 770.
[32] D. C. Webster, *Macromolecular Chemistry and Physics* **2008**, *209*, 237.
[33] P. Brooking, A. Doran, P. Grimsey, N. W. Hird, W. S. MacLachlan, M. Vimal, *Tetrahedron Letters* **1999**, *40*, 1405.
[34] F. M. Menger, A. V. Eliseev, V. A. Migulin, *Journal of Organic Chemistry* **1995**, *60*, 6666.
[35] K. Lewandowski, P. Murer, F. Svec, J. M. J. Fréchet, *Journal of Combinatorial Chemistry* **1999**, *1*, 105.
[36] A. Nefzi, J. M. Ostresh, R. A. Houghten, *Chemical Reviews* **1997**, *97*, 449.
[37] C. R. Becer, R. M. Paulus, R. Hoogenboom, U. S. Schubert, *Journal of Polymer Science: Part A: Polymer Chemistry* **2006**, *44*, 6202.
[38] E. Danielson, J. H. Golden, E. W. McFarland, C. M. Reaves, W. H. Weinberg, X. D. Wu, *Nature* **1997**, *389*, 944.
[39] X. G. Li, Y. Kang, M. R. Huang, *Journal of Combinatorial Chemistry* **2006**, *8*, 670.
[40] R. Rojas, N. K. Harris, K. Piotrowska, J. Kohn, *Journal of Polymer Science: Part A: Polymer Chemistry* **2009**, *47*, 49.
[41] P. Vandezande, L. E. M. Gevers, N. Weyens, I. F. J. Vankelecom, *Journal of Combinatorial Chemistry* **2009**, *11*, 243.
[42] D. C. Webster, B. J. Chisholm, S. J. Stafslien, *Biofouling* **2007**, *23*, 179.
[43] J. J. Hanak, *Applied Surface Science* **2004**, *223*, 1.
[44] M. Bulut, L. E. M. Gevers, J. S. Paul, N. F. J. Vankelecom, P. A. Jacobs, *Journal of Combinatorial Chemistry* **2006**, *8*, 168.
[45] E. W. McFarland, W. H. Weinberg, *Trends in Biotechnology* **1999**, *17*, 107.
[46] J. R. Nowers, S. R. Broderick, K. Rajan, B. Narasimhan, *Macromolecular Rapid Communications* **2007**, *28*, 972.
[47] C. H. Reynolds, *Journal of Combinatorial Chemistry* **1999**, *1*, 297.
[48] B. M. Vogel, J. T. Cabral, N. Eidelman, B. Narasimhan, S. K. Mallapragada, *Journal of Combinatorial Chemistry* **2005**, *7*, 921.
[49] J. F. O. Thaburet, H. Mizomoto, M. Bradley, *Macromolecular Rapid Communications* **2004**, *25*, 366.
[50] S. D. Kamau, P. Hodge, R. T. Williams, P. Stagnaro, L. Conzatti, *Journal of Combinatorial Chemistry* **2008**, *10*, 644.
[51] A. Ekin, D. C. Webster, *Journal of Combinatorial Chemistry* **2007**, *9*, 178.
[52] C. Guerrero-Sanchez, R. M. Paulus, M. W. M. Fijten, M. J. de la Mar, R. Hoogenboom, U. S. Schubert, *Applied Surface Science* **2006**, *252*, 2555.
[53] M. W. M. Fijten, J. M. Kranenburg, H. M. L. Thijs, R. M. Paulus, B. M. van Lankvelt, J. de Hullu, M. Springintveld, D. J. G. Thielen, C. A. Tweedie, R. Hoogenboom, K. J. Van Vliet, U. S. Schubert, *Macromolecules* **2007**, *40*, 5879.

[54] C. Guerrero-Sanchez, C. Abeln, U. S. Schubert, *Journal of Polymer Science: Part A: Polymer Chemistry* **2005**, *43*, 4151.
[55] J. M. Kranenburg, C. A. Tweedie, R. Hoogenboom, F. Wiesbrock, H. M. L. Thijs, C. E. Hendriks, K. J. Van Vliet, U. S. Schubert, *Journal of Materials Chemistry* **2007**, *17*, 2713.
[56] R. Hoogenboom, M. W. M. Fijten, S. Wijnans, A. M. J. van den Berg, H. M. L. Thijs, U. S. Schubert, *Journal of Combinatorial Chemistry* **2006**, *8*, 145.
[57] C. Weber, C. R. Becer, A. Baumgaertel, R. Hoogenboom, U. S. Schubert, *Designed Monomers and Polymers* **2009**, *12*, 149.
[58] H. Q. Zhang, V. Marin, M. W. M. Fijten, U. S. Schubert, *Journal of Polymer Science: Part A: Polymer Chemistry* **2004**, *42*, 1876.
[59] M. W. M. Fijten, M. A. R. Meier, R. Hoogenboom, U. S. Schubert, *Journal of Polymer Science: Part A: Polymer Chemistry* **2004**, *42*, 5775.
[60] T. M. Eggenhuisen, C. R. Becer, M. W. M. Fijten, R. Eckardt, R. Hoogenboom, U. S. Schubert, *Macromolecules* **2008**, *41*, 5132.
[61] C. R. Becer, A. M. Groth, R. Hoogenboom, R. M. Paulus, U. S. Schubert, *QSAR & Combinatorial Science* **2008**, *27*, 977.
[62] M. W. M. Fitjen, R. M. Paulus, U. S. Schubert, *Journal of Polymer Science: Part A: Polymer Chemistry* **2005**, *43*, 3831.
[63] J. M. Kranenburg, H. M. L. Thijs, C. A. Tweedie, S. Hoeppener, F. Wiesbrock, R. Hoogenboom, K. J. Van Vliet, U. S. Schubert, *Journal of Materials Chemistry* **2009**, *19*, 222.
[64] M. A. R. Meier, D. Wouters, C. Ott, P. Guillet, C. A. Fustin, J. F. Gohy, U. S. Schubert, *Macromolecules* **2006**, *39*, 1569.
[65] M. A. R. Meier, J. F. Gohy, C. A. Fustin, U. S. Schubert, *Journal of the American Chemical Society* **2004**, *126*, 11517.
[66] R. J. Pieper, A. Ekin, D. C. Webster, F. Casse, J. A. Callow, M. E. Callow, *Journal of Coatings Technology and Research* **2007**, *4*, 453.
[67] A. Ekin, D. C. Webster, J. W. Daniels, S. J. Stafslien, F. Casse, J. A. Callow, M. E. Callow, *Journal of Coatings Technology and Research* **2007**, *4*, 435.
[68] A. Ekin, D. C. Webster, *Journal of Polymer Science: Part A: Polymer Chemistry* **2006**, *44*, 4880.
[69] A. J. Kugel, L. E. Jarabek, J. W. Daniels, L. J. V. Wal, S. M. Ebert, M. J. Jepperson, S. J. Stafslien, R. J. Pieper, D. C. Webster, J. Bahr, B. J. Chisholm, *Journal of Coatings Technology and Research* **2009**, *6*, 107.
[70] M. J. Nasrullah, J. A. Bahr, C. Gallagher-Lein, D. C. Webster, R. R. Roesler, P. Schmitt, *Journal of Coatings Technology and Research* **2009**, *6*, 1.
[71] M. J. Nasrullah, D. C. Webster, *Macromolecular Chemistry and Physics* **2009**, *210*, 640.
[72] R. A. Potyrailo, R. J. Wroczynski, J. E. Pickett, M. Rubinsztajn, *Macromolecular Rapid Communications* **2003**, *24*, 124.
[73] R. A. Potyrailo, B. J. Chisholm, W. G. Morris, J. N. Cawse, W. P. Flanagan, L. Hassib, C. A. Molaison, K. Ezbiansky, G. Medford, H. Reitz, *Journal of Combinatorial Chemistry* **2003**, *5*, 472.
[74] R. A. Potyrailo, R. J. Wroczynski, J. P. Lemmon, W. P. Flanagan, O. P. Siclovan, *Journal of Combinatorial Chemistry* **2003**, *5*, 8.

[75] R. A. Potyrailo, L. Hassib, *Review of Scientific Instruments* **2005**, *76*.
[76] O. Lavastre, I. Illitchev, G. Jegou, P. H. Dixneuf, *Journal of the American Chemical Society* **2002**, *124*, 5278.
[77] P. Vandezande, X. F. Li, L. E. M. Gevers, I. F. J. Vankelecom, *Journal of Membrane Science* **2009**, *330*, 307.
[78] M. Petro, S. H. Nguyen, M. J. Liu, O. Kolosov, *Macromolecular Rapid Communications* **2004**, *25*, 178.
[79] D. M. Lynn, D. G. Anderson, D. Putnam, R. Langer, *Journal of the American Chemical Society* **2001**, *123*, 8155.
[80] G. Tourniaire, J. Collins, S. Campbell, H. Mizomoto, S. Ogawa, J. F. Thaburet, M. Bradley, *Chemical Communications* **2006**, 2118.
[81] S. Pernagallo, A. Unciti-Broceta, J. J. Diaz-Mochon, M. Bradley, *Biomedical Materials* **2008**, *3*.
[82] C. G. Simon, J. S. Stephens, S. M. Dorsey, M. L. Becker, *Review of Scientific Instruments* **2007**, *78*.
[83] J. C. Meredith, A. Karim, E. J. Amis, *MRS Bulletin* **2002**, *27*, 330.
[84] C. Xu, T. Wu, C. M. Drain, J. D. Batteas, M. J. Fasolka, K. L. Beers, *Macromolecules* **2006**, *39*, 3359.
[85] J. L. Sormana, J. C. Meredith, *Macromolecular Rapid Communications* **2003**, *24*, 118.
[86] C. G. Simon, N. Eidelman, Y. Deng, N. R. Washburn, *Macromolecular Rapid Communications* **2004**, *25*, 2003.
[87] B. J. de Gans, C. Sanchez, D. Kozodaev, D. Wouters, A. Alexeev, M. J. Escuti, C. W. M. Bastiaansen, D. J. Broer, U. S. Schubert, *Journal of Combinatorial Chemistry* **2006**, *8*, 228.
[88] K. A. Hooper, J. Kohn, *Journal of Bioactive and Compatible Polymers* **1995**, *10*, 327.
[89] M. Vert, *Progress in Polymer Science* **2007**, *32*, 755.
[90] M. Vert, *Biomacromolecules* **2005**, *6*, 538.
[91] M. Vert, *E-Polymers* **2005**.
[92] M. Vert, *Journal of Materials Science-Materials in Medicine* **2009**, *20*, 437.
[93] K. Marcincinova-Benabdillah, M. Boustta, J. Coudane, M. Vert, *Biomacromolecules* **2001**, *2*, 1279.
[94] D. Domurado, M. Vert, *Journal of Biomaterials Science-Polymer Edition* **2007**, *18*, 287.
[95] S. Pulapura, J. Kohn, *Biopolymers* **1992**, *32*, 411.
[96] S. L. Bourke, J. Kohn, *Advanced Drug Delivery Reviews* **2003**, *55*, 447.
[97] K. James, H. Levene, J. R. Parsons, J. Kohn, *Biomaterials* **1999**, *20*, 2203.
[98] K. James, J. Kohn, *Trends in Polymer Science* **1996**, *4*, 394.
[99] J. Choueka, J. L. Charvet, K. J. Koval, H. Alexander, K. S. James, K. A. Hooper, J. Kohn, *Journal of Biomedical Materials Research* **1996**, *31*, 35.
[100] S. I. Ertel, J. Kohn, M. C. Zimmerman, J. R. Parsons, *Journal of Biomedical Materials Research* **1995**, *29*, 1337.
[101] J. Fiordeliso, S. Bron, J. Kohn, *Journal of Biomaterials Science-Polymer Edition* **1994**, *5*, 497.
[102] D. G. Sprous, F. R. Salemme, *Food and Chemical Toxicology* **2007**, *45*, 1419.

[103] G. A. Burdock, I. G. Carabin, J. C. Griffiths, *Toxicology* **2006**, *221*, 17.
[104] G. A. Burdock, I. G. Carabin, *Toxicology Letters* **2004**, *150*, 3.
[105] R. D. Benz, H. Irausquin, *Environmental Health Perspectives* **1991**, *96*, 85.
[106] K. M. Herrmann, L. M. Weaver, *Annual Review of Plant Physiology and Plant Molecular Biology* **1999**, *50*, 473.
[107] L. M. Weaver, K. M. Herrmann, *Trends in Plant Science* **1997**, *2*, 346.
[108] C. A. Rice-Evans, J. Miller, G. Paganga, *Trends in Plant Science* **1997**, *2*, 152.
[109] J. B. Harborne, *Phytochemical Methods. A Guide to Modern Techniques of Plant Analysis. 2nd Ed*, **1984**.
[110] C. A. Rice-Evans, N. J. Miller, G. Paganga, *Free Radical Biology and Medicine* **1996**, *20*, 933.
[111] C. Proestos, N. Chorianopoulos, G. J. E. Nychas, M. Komaitis, *Journal of Agricultural and Food Chemistry* **2005**, *53*, 1190.
[112] V. Viswanath, A. Urooj, N. G. Malleshi, *Food Chemistry* **2009**, *114*, 340.
[113] M. Arlorio, M. Locatelli, F. Travaglia, J. D. Coisson, E. Del Grosso, A. Minassi, G. Appendino, A. Martelli, *Food Chemistry* **2008**, *106*, 967.
[114] A. R. Proteggente, A. S. Pannala, G. Paganga, L. Van Buren, E. Wagner, S. Wiseman, F. Van De Put, C. Dacombe, C. A. Rice-Evans, *Free Radical Research* **2002**, *36*, 217.
[115] C. Sanbongi, N. Osakabe, M. Natsume, T. Takizawa, S. Gomi, T. Osawa, *Journal of Agricultural and Food Chemistry* **1998**, *46*, 454.
[116] N. Osakabe, M. Yamagishi, C. Sanbongi, M. Natsume, T. Takizawa, T. Osawa, *Journal of Nutritional Science and Vitaminology* **1998**, *44*, 313.
[117] Y. Goda, F. Kiuchi, M. Shibuya, U. Sankawa, *Chemical & Pharmaceutical Bulletin* **1992**, *40*, 2452.
[118] W. R. Russell, A. Labat, L. Scobbie, S. H. Duncan, *Molecular Nutrition & Food Research* **2007**, *51*, 726.
[119] M. Yamaguchi, Y. L. Lai, S. Uchiyama, T. Nakagawa, *Molecular and Cellular Biochemistry* **2008**, *311*, 31.
[120] M. Yamaguchi, S. Uchiyama, Y. L. Lai, *International Journal of Molecular Medicine* **2007**, *19*, 803.
[121] H. J. P. Marvin, C. F. Krechting, E. N. van Loo, C. H. A. Snijders, L. N. I. H. Nelissen, O. Dolstra, *Journal of Agricultural and Food Chemistry* **1996**, *44*, 3467.
[122] H. J. P. Marvin, C. F. Krechting, E. N. van Loo, C. H. A. Snijders, A. Lommen, O. Dolstra, *Journal of the Science of Food and Agriculture* **1996**, *71*, 111.
[123] R. Zadernowski, S. Czaplicki, M. Naczk, *Food Chemistry* **2009**, *112*, 685.
[124] R. D. Hatfield, J. M. Marita, K. Frost, *Journal of the Science of Food and Agriculture* **2008**, *88*, 2529.
[125] M. N. Clifford, *Journal of the Science of Food and Agriculture* **2000**, *80*, 1033.
[126] M. N. Clifford, *Journal of the Science of Food and Agriculture* **1999**, *79*, 362.
[127] Y. Goda, M. Shibuya, U. Sankawa, *Chemical & Pharmaceutical Bulletin* **1987**, *35*, 2668.
[128] J. C. Cheng, F. Dai, B. Zhou, L. Yang, Z. L. Liu, *Food Chemistry* **2007**, *104*, 132.
[129] G. K. Yoya, F. Bedos-Belval, P. Constant, H. Duran, M. Daffe, M. Baltas, *Bioorganic & Medicinal Chemistry Letters* **2009**, *19*, 341.

[130] M. Yamaguchi, Y. L. Lai, S. Uchiyama, T. Nakagawa, *International Journal of Molecular Medicine* **2008**, *22*, 287.
[131] Y. L. Lai, M. Yamaguchi, *International Journal of Molecular Medicine* **2007**, *19*, 123.
[132] Y. L. Lai, M. Yamaguchi, *Journal of Health Science* **2006**, *52*, 308.
[133] Y. L. Lai, M. Yamaguchi, *Molecular and Cellular Biochemistry* **2006**, *292*, 45.
[134] F. Laurent, R. Scalla, *Journal of Agricultural and Food Chemistry* **2000**, *48*, 4389.
[135] F. M. G. Laurent, R. Scalla, *Pesticide Science* **1999**, *55*, 3.
[136] D. Mascagna, G. Ghanem, R. Morandini, M. Dischia, G. Misuraca, F. Lejeune, G. Prota, *Melanoma Research* **1992**, *2*, 25.
[137] E. W. Barrett, M. V. B. Phelps, R. J. Silva, R. P. Gaumond, H. R. Allcock, *Biomacromolecules* **2005**, *6*, 1689.
[138] S. I. Ertel, J. Kohn, *Journal of Biomedical Materials Research* **1994**, *28*, 919.
[139] F. G. Bordwell, D. J. Algrim, *Journal of the American Chemical Society* **1988**, *110*, 2964.
[140] F. G. Bordwell, *Accounts of Chemical Research* **1988**, *21*, 456.
[141] T. W. Greene, P. G. M. Wuts, *Protective Groups in Organic Synthesis. 2nd Ed*, **1991**.
[142] A. Heydari, S. E. Hosseini, *Advanced Synthesis & Catalysis* **2005**, *347*, 1929.
[143] T. Vilaivan, *Tetrahedron Letters* **2006**, *47*, 6739.
[144] R. Barbe, J. Hasserodt, *Tetrahedron* **2007**, *63*, 2199.
[145] L. A. Carpino, B. J. Cohen, K. E. Stephens, S. Y. Sadataalaee, J. H. Tien, D. C. Langridge, *Journal of Organic Chemistry* **1986**, *51*, 3732.
[146] M. Frankel, D. Ladkany, C. Gilon, Y. Wolman, *Tetrahedron Letters* **1966**, *7*, 4765.
[147] A. G. Myers, J. L. Gleason, T. Yoon, D. W. Kung, *Journal of the American Chemical Society* **1997**, *119*, 656.
[148] H. M. Konig, R. Abbel, D. Schollmeyer, A. F. M. Kilbinger, *Organic Letters* **2006**, *8*, 1819.
[149] A. Ollbert-Majkut, M. Wierzejewska, *Journal of Physical Chemistry A* **2008**, *112*, 5691.
[150] V. Tangpasuthadol, S. M. Pendharkar, R. C. Peterson, J. Kohn, *Biomaterials* **2000**, *21*, 2379.
[151] V. Tangpasuthadol, S. M. Pendharkar, J. Kohn, *Biomaterials* **2000**, *21*, 2371.
[152] C. Hansch, J. E. Quinlan, G. L. Lawrence, *The Journal of Organic Chemistry* **1968**, *33*, 347.
[153] L. B. Lockwood, D. E. Yoder, M. Zienty, *Annals of the New York Academy of Sciences* **1965**, *119*, 854.
[154] W. L. Jorgensen, E. M. Duffy, *Advanced Drug Delivery Reviews* **2002**, *54*, 355.
[155] N. Jain, S. H. Yalkowsky, *Journal of Pharmaceutical Sciences* **2001**, *90*, 234.
[156] S. Gao, C. Z. Cao, *International Journal of Molecular Sciences* **2008**, *9*, 962.
[157] J. S. Delaney, *Drug Discovery Today* **2005**, *10*, 289.
[158] J. S. Delaney, *Journal of Chemical Information and Computer Sciences* **2004**, *44*, 1000.

[159] P. Chapon, C. Mignaud, G. Lizarraga, M. Destarac, *Macromolecular Rapid Communications* **2003**, *24*, 87.
[160] J. C. Meredith, *Journal of Materials Science* **2003**, *38*, 4427.
[161] R. Hoogenboom, M. A. R. Meier, U. S. Schubert, *Macromolecular Rapid Communications* **2003**, *24*, 16.
[162] H. R. Kricheldorf, S. Bohme, G. Schwarz, C. L. Schultz, *Macromolecules* **2004**, *37*, 1742.
[163] H. R. Kricheldorf, S. Bohme, G. Schwarz, C. L. Schultz, *Macromolecular Chemistry and Physics* **2003**, *204*, 1539.
[164] H. R. Kricheldorf, S. Bohme, G. Schwarz, *Macromolecules* **2001**, *34*, 8879.
[165] H. R. Kricheldorf, S. Bohme, G. Schwarz, *Macromolecular Chemistry and Physics* **2005**, *206*, 432.
[166] D. Bolikal, K. Piotrowska, *Side reaction in poly(DTE carbonate) synthesis, NJCBM (Internal report)*, **2006**.
[167] K. James, J. Kohn, *MRS Bulletin* **1996**, *21*, 22.
[168] D. Campbell, R. A. Pethrick, J. R. White, *Polymer characterization: Physical techniques. 2nd edition.*, **2000**.
[169] J. Yang, F. R. A. J. Rose, N. Gadegaard, M. R. Alexander, *Advanced Materials* **2009**, *21*, 300.
[170] M. Taylor, A. J. Urquhart, D. G. Anderson, R. Langer, M. C. Davies, M. R. Alexander, *Surface and Interface Analysis* **2009**, *41*, 127.
[171] J. C. Meredith, *Journal of Materials Chemistry* **2009**, *19*, 34.
[172] S. Kim, J. H. Kim, O. Jeon, I. C. Kwon, K. Park, *European Journal of Pharmaceutics and Biopharmaceutics* **2009**, *71*, 420.
[173] Y. Yang, D. Bolikal, M. L. Becker, J. Kohn, D. N. Zeiger, C. G. Simon, *Advanced Materials* **2008**, *20*, 2037.
[174] M. Taylor, A. J. Urquhart, D. G. Anderson, P. M. Williams, R. Langer, M. R. Alexander, M. C. Davies, *Macromolecular Rapid Communications* **2008**, *29*, 1298.
[175] J. J. Green, R. Langer, D. G. Anderson, *Accounts of Chemical Research* **2008**, *41*, 749.
[176] J. C. Meredith, J. L. Sormana, B. G. Keselowsky, A. J. Garcia, A. Tona, A. Karim, E. J. Amis, *Journal of Biomedical Materials Research Part A* **2003**, *66A*, 483.
[177] A. K. Kundu, C. B. Khatiwala, A. J. Putnam, *Tissue Engineering Part A* **2009**, *15*, 273.
[178] F. Xu, J. C. Nacker, W. C. Crone, K. S. Masters, *Biomaterials* **2008**, *29*, 150.
[179] R. Chen, J. M. Curran, J. A. Hunt, *Tissue Engineering Part A* **2008**, *14*, 782.
[180] E. Pedone, X. W. Li, N. Koseva, O. Alpar, S. Brocchini, *Journal of Materials Chemistry* **2003**, *13*, 2825.
[181] A. Pesnell, S. Abramson, D. Bolikal, J. Kohn, *In preparation* **2009**.
[182] H. A. Schneider, *Journal of Applied Polymer Science* **2003**, *88*, 1590.
[183] H. A. Schneider, *Polymer* **2005**, *46*, 2230.
[184] H. A. Schneider, *Journal of Research of the National Institute of Standards and Technology* **1997**, *102*, 229.

[185] J. Schut, D. Bolikal, I. J. Khan, A. Pesnell, A. Rege, R. Rojas, L. Sheihet, N. S. Murthy, J. Kohn, *Polymer* **2007**, *48*, 6115.
[186] B. Stuart, *Polymer analysis. 1st edition.*, **2002**.
[187] V. Rizzo, V. Pinciroli, *Journal of Pharmaceutical and Biomedical Analysis* **2005**, *38*, 851.
[188] A. J. Urquhart, M. Taylor, D. G. Anderson, R. Langer, M. C. Davies, M. R. Alexander, *Analytical Chemistry* **2008**, *80*, 135.
[189] C. Ozcan, N. Hasirci, *Journal of Biomaterials Science-Polymer Edition* **2007**, *18*, 759.
[190] E. G. Shafrin, W. A. Zisman, *The Journal of Physical Chemistry* **1960**, *64*, 519.
[191] L. De Bartolo, S. Morelli, A. Bader, E. Drioli, *Journal of Materials Science-Materials in Medicine* **2001**, *12*, 959.
[192] C. Ozcan, N. Hasirci, *Journal of Applied Polymer Science* **2008**, *108*, 438.
[193] E. M. Harnett, J. Alderman, T. Wood, *Colloids and Surfaces B-Biointerfaces* **2007**, *55*, 90.
[194] C. J. van Oss, *Current Opinion in Colloid & Interface Science* **1997**, *2*, 503.
[195] W. Vandervegt, H. C. Vandermei, H. J. Busscher, *Langmuir* **1994**, *10*, 1314.
[196] C. J. van Oss, *Colloids and Surfaces B-Biointerfaces* **1995**, *5*, 91.
[197] R. R. Deshmukh, A. R. Shetty, *Journal of Applied Polymer Science* **2008**, *107*, 3707.
[198] Y. H. Bae, P. A. Johnson, C. A. Florek, J. Kohn, P. V. Moghe, *Acta Biomaterialia* **2006**, *2*, 473.
[199] M. Morra, C. Cassinelli, *International Journal of Artificial Organs* **2006**, *29*, 824.
[200] M. Morra, C. Cassinelli, *Langmuir* **1999**, *15*, 4658.
[201] L. De Bartolo, S. Morelli, A. Bader, E. Drioli, *Biomaterials* **2002**, *23*, 2485.
[202] P. Zapata, J. Su, A. J. Garcia, J. C. Meredith, *Biomacromolecules* **2007**, *8*, 1907.
[203] F. J. Sung, J. Su, J. D. Berglund, B. V. Russ, J. C. Meredith, Z. S. Galis, *Biomaterials* **2005**, *26*, 4557.
[204] Z. G. Ge, S. Baguenard, L. Y. Lim, A. Wee, E. Khor, *Biomaterials* **2004**, *25*, 1049.
[205] J. M. Curran, R. Chen, J. A. Hunt, *Tissue Engineering Part A* **2008**, *14*, 715.
[206] G. Marletta, G. Ciapetti, C. Satriano, F. Perut, M. Salerno, N. Baldini, *Biomaterials* **2007**, *28*, 1132.
[207] J. M. Curran, R. Chen, J. A. Hunt, *Biomaterials* **2006**, *27*, 4783.
[208] S. A. Redey, M. Nardin, D. Bernache-Assolant, C. Rey, P. Delannoy, L. Sedel, P. J. Marie, *Journal of Biomedical Materials Research* **2000**, *50*, 353.
[209] S. A. Redey, S. Razzouk, C. Rey, D. Bernache-Assollant, G. Leroy, M. Nardin, G. Cournot, *Journal of Biomedical Materials Research* **1999**, *45*, 140.

CURRICULUM VITA

Ramiro Rojas Escontrillas

Education

2003	B.S. in Chemistry [Licenciado en Ciencias Químicas] Department of Chemistry Tecnológico de Monterrey [ITESM, Campus Monterrey]
2004-2005	Teaching Assistant Department of Chemistry and Chemical Biology Rutgers, The State University of New Jersey
2005-2009	Graduate Assistant Department of Chemistry and Chemical Biology Rutgers, The State University of New Jersey
2009	Ph.D. in Chemistry Department of Chemistry and Chemical Biology Rutgers, The State University of New Jersey

Professional Experience

2003	Research Assistant Tecnológico de Monterrey (Center of Biotechnology) Monterrey, Nuevo León 64849 MEX

Publications

Rojas, R; Rojas de Gante, C; Biodegradación por fermentación aerobia en bioenvases de sorgo por *Aspergillus Niger*, X Congreso Nacional de Biotecnología y Bioingeniería, Puerto Vallarta, Jal, MEX, (2003).

Schut, J; Khan, IJ; Pesnell, A; Rojas, R; Sheihet, L; Murthy, NS; Kohn, J; Glass transition temperature prediction of polymers through the mass-per-flexible-bond principle *Polymer,* 48 (20): 6115-6124, (2007).

Rojas, R; Harris, N; Kohn, J; Evaluation of automated synthesis for chain and step-growth polymerizations: Can robots replace the chemists? *PMSE Preprints*, New Orleans, LA, (2008).

Rojas, R; Kohn, J; Rational design and exploration of polymer space through combinatorial and high-throughput approaches with the application in mind, *POLYMER Preprints*, Philadelphia, PA, (2008).

Rojas, R; Harris, N; Piotrowska, K; Kohn, J; Evaluation of automated synthesis for chain and step-growth polymerizations: Can robots replace the chemists? *Journal of Polymer Science, Part A: Polymer Chemistry*, 47: 49-58, (2009).

Bolikal, D; Joy, A; Rojas, R; Kohn, J; Biocompatible, bioresorbable polymers synthesized from monomer analogs of natural metabolites, *In preparation as US Patent*, (2009).

Rojas, R; Kohn, J; Automated parallel synthesis of polymeric biomaterials as an effective tool for the exploration of materials design space. *In preparation for Macromolecular Rapid Communications*.

Luk, A; Murthy, S; Rojas, R; Kohn, J; Effects of nanoscale spatial features on protein adsorption and their implication on the design of polymeric biomaterials. *In preparation.*